Notch & NF-κB signals at the heart of development and disease

DISSERTATION

EMBL-UNIVERSITY OF CRETE
JOINT PhD PROGRAM

Paschalis Kratsios
Rome, Italy
2008

DISSERTATION
submitted to the
University of Crete, Greece
for the degree of
Doctor of Natural Sciences

Joint PhD Programme
EMBL - University of Crete

Presented by: Paschalis Kratsios
Diploma: Molecular Biology & Genetics
Born in: Kozani, Greece

Notch & NF- κB signals at the heart of development and disease

SUPERVISOR
Nadia Rosenthal, PhD
EMBL, Mouse Biology Program,
Monterotondo, Italy

THESIS DEFENSE COMMITTEE
Sifis Papamatheakis, Professor, University of Crete
Irene Athanassakis, Associate Prof., University of Crete
Chrestos Delidakis, Associate Prof., University of Crete
Giorgos Mavrothalassitis, Associate Prof., University of Crete
Giorgos Chalepakis, Associate Prof., University of Crete
Maria Grigoriou, Associate Prof., Democritus University of Thrace

EMBL ADVISORS
Anne Ephrussi, PhD
Walter Witke, PhD
Manolis Pasparakis, PhD

“How could you describe this heart
in words, without filling a whole book?”

Note written by Leonardo da Vinci beside
an anatomical drawing of the heart, 1513

“So close no matter how far
couldn't be much more from the heart
forever trusting who we are
and nothing else matters.

Never opened myself this way
life is ours we live it our way
all these words I don't just say
and nothing else matters.

Trust I seek and I find in you
every day for us something new
open mind for a different view
and nothing else matters”

James Alan Hetfield, 1991

Acknowledgements

First of all, I would like to thank my supervisor, Nadia Rosenthal, who provided me with the unique opportunity to be part of the EMBL family and enjoying her lab's friendly atmosphere. I am grateful to Nadia for her generosity, open-mindness, and scientific input; values that will always remind me the transformation of a naïve university student to a curious graduate student. Moreover, unforgettable lab dinners in the Eternal City and elsewhere, as well as hundreds of "destroyed" wine bottles (all organized by Nadia) taught me that science should be fun and a balance between work and entertainment is highly desirable. I learnt a lot from her and I will always be grateful.

Next, I would like to express my gratitude to my in-lab supervisor, Foteini Mourkioti, who supported me and believed in me during my Phd time. I would like to thank her for sharing scientific and technical knowledge with me, as well as for the long and relieving discussions that led to a true friendship and a fruitful collaboration. I also learnt a lot from her and I sincerely hope she enjoyed the journey of teaching her first student.

Moreover, I would like to thank former and present members of the Rosenthal lab for maintaining a healthy and friendly atmosphere, making enjoyable most of my moments in this lab. In particular, I would like to thank Esfir Slonimsky for her generosity, technical assistance and her warm every-day smile. Moreover, my gratitude goes to Pascal te Welscher for making me think also on an evo-devo axis, to Marion Huth for her excellent technical assistance, and to Ekaterina Salimova for our collaboration. Next, I am grateful to Catarina Catela for sharing every-day frustrations and being a patient desk-neighbor. In addition, Lieve Temmerman, Catarina Catela, Pascal te Welscher, Foteini Mourkioti, Nadine Winn, Tommaso Nastasi, Ekaterina Semenova, Marianne Hede, and Lars Bochman were always willing to discuss science and life matters over a warm cup of coffee and I specifically thank them for this. Also, I would like to thank Marco D'Ercole, Stefano Tatti and Giulia Zanin for taking care of the animals.

I especially thank the members of my Thesis Advisory Committee, Dr. Anne Ephrussi, Dr. Walter Witke, Dr. Manolis Pasparakis, Professor Joseph Papamatheakis and Associate Professor Irene Athanassakis for their valuable input and suggestions during the progression of my PhD thesis work. Moreover, I express my gratitude to the Associate Professors Chrestos Delidakis, Giorgos Mavrothalassitis, Giorgos Chalepakis, and Maria Grigoriou for accepting to participate in the Thesis Defence Committee.

Off the lab, I would like to thank Lieve and Pieter, Faye and Teo, Vaggelis, Gabriele, Emanuele, Tiago, Sylvia, Susana, Shin, Olivier, Elena, Stefanos, Nikos,

Alekos, Panos and many others for all their distraction attempts that keep me balanced and happy, allowing me to think that I have friends all over the world.

I would also like to thank my father Costas, my mother Eirini and my brother Panos for always being there, and apologize to them for not being able to respond successfully to their common question “what exactly are you doing still in the lab?”.

Last but not least, I am thankful to Catarina for making me see life from another perspective.

TABLE OF CONTENT

SUMMARY - 12 -

INTRODUCTION - 13 -

1. INTRODUCTION - 14 -

1. 1. EVOLUTION OF THE HEART AT A GLANCE - 14 -
1. 2 CARDIAC DEVELOPMENT IN MAMMALS - 16 -
First heart field - 17 -
Second heart field - 17 -
Cardiac neural crest - 18 -
Remodeling after looping - 18 -
Mutations affecting FHF, SHF and CNC contributions - 19 -
1.3 MODES OF CARDIAC GROWTH - 21 -
1.3.1 HYPERPLASIA - 21 -
1.3.2 HYPERTROPHY - 21 -
1.4 HEART DISEASE - 24 -
1.4 HEART DISEASE - 25 -
1.5 STRATEGIES FOR CARDIAC REPAIR - 27 -
Cell replacement - 27 -
Regulation of the cardiac cell cycle - 28 -
Resident cardiac stem cells (CSCs) - 28 -
Re-employment of embryonic signaling - 29 -
TRANSLATIONAL SCOPES OF THE THESIS - 31 -

CHAPTER 1 - 32 -

NOTCH-1 SIGNALING ACTIVATION IN CARDIAC DEVELOPMENT AND DISEASE - 32 -

1.1 BACKGROUND - 33 -

1.1.1 CELL FATE DETERMINATION & NOTCH SIGNALING - 34 -
1.1.2 NOTCH SIGNALING IN MAMMALS - CORE PATHWAY - 36 -
Notch receptor family - 36 -
Delta/Serrate/Jagged family of Notch ligands. - 36 -
γ-secretase complex - 37 -
Notch transcriptional machinery. - 38 -
Notch target genes. - 39 -
Processing and trafficking regulate Notch receptor activity - 39 -
1.1.3 NOTCH SIGNALING IN THE CARDIOVASCULAR SYSTEM - 41 -
1.1.3.1 Notch expression patterns - 41 -
1.1.3.2 Notch & cardiomyocyte differentiation - 42 -
1.1.3.3 Notch & valve formation - 43 -
1.1.3.4 Notch & outflow tract remodeling - 44 -
1.1.3.5 Notch signaling and vascular formation - 45 -
1.1.3.6 Notch target genes in cardiac development - 47 -
1.1.4 NOTCH SIGNALING & TISSUE REGENERATION - 50 -

1.2 RESULTS - 51 -

NOTCH-1 SIGNALING ACTIVATION RESULTS IN ABNORMAL CARDIAC MORPHOGENESIS - 51 -

1.2.1 RATIONALE - 52 -
1.2.2 NOTCH-1 IS EXPRESSED IN CARDIOMYOCYTES - 53 -
1.2.3 GENETIC APPROACH FOR CARDIOMYOCYTE-SPECIFIC NOTCH1-MEDIATED SIGNALING ACTIVATION - 54 -
1.2. 4 NICD1:TG MICE DISPLAY PERINATAL LETHALITY - 56 -
1.2. 5 ABNORMAL CARDIAC MORPHOGENESIS AND IMPAIRED FUNCTION IN NICD1:TG MICE - 56 -

1.2. 6 DIFFERENTIATION DELAY AND ENHANCED CARDIOMYOCYTE PROLIFERATION IN NICD1:TG HEARTS ..... - 59 -

1.3 DISCUSSION ..... - 63 -

NOTCH-1 SIGNALING ACTIVATION RESULTS IN ABNORMAL CARDIAC MORPHOGENESIS ..... - 63 -

1.3.1 DISCUSSION ..... - 64 -
1.3.2 FUTURE PERSPECTIVES ..... - 68 -
1.3.3 CONCLUSIONS ..... - 69 -

1.4 RESULTS ..... - 70 -

RE-ACTIVATION OF NOTCH-1 SIGNALING PROTECTS AGAINST MYOCARDIAL INFARCTION ..... - 70 -

1.4.1 RATIONALE ..... - 71 -
1.4. 2 NOTCH-1 IS EXPRESSED IN CARDIOMYOCYTES AND ENDOTHELIAL CELLS OF THE ADULT HEART - 71 -
1.4. 3 EXPRESSION LEVELS OF SEVERAL NOTCH PATHWAY COMPONENTS ARE UP-REGULATED AFTER MYOCARDIAL INFARCTION ..... - 72 -
1.4.4 INTRAMYOCARDIAL NOTCH-1 ANTIBODY (NOTCH1 AB) INJECTION ACTIVATES NOTCH SIGNALING, IMPROVES SURVIVAL AND CARDIAC FUNCTION ..... - 74 -
1.4.5 EARLY NOTCH-1 SIGNALING ACTIVATION PROTECTS AGAINST MYOCARDIAL INFARCTION ..... - 75 -
1.4. 6 ANGIOGENESIS AND/OR PROLIFERATION; POSSIBLE MECHANISMS FOR NOTCH-1 MEDIATED CARDIAC REPAIR ..... - 77 -

1.5 DISCUSSION ..... - 78 -

RE-ACTIVATION OF NOTCH-1 SIGNALING PROTECTS AGAINST MYOCARDIAL INFARCTION ..... - 78 -

1.5.1 DISCUSSION ..... - 79 -
1.5.2 FUTURE PERSPECTIVES ..... - 82 -
1.5.3 CONCLUSIONS ..... - 83 -

1.6 MATERIALS & METHODS ..... - 84 -

CHAPTER 1 ..... - 84 -

NOTCH-1 SIGNALING ACTIVATION IN CARDIAC DEVELOPMENT AND DISEASE ..... - 84 -

1.6.1 ANIMALS ..... - 85 -
1.6.1.1 Genotyping ..... - 85 -
1.6.1.2 Husbandry ..... - 86 -
1.6.1.3 Induction of myocardial ischemia (LAD operation) ..... - 86 -
1.6.1.4 In vivo Notch-1 activation ..... - 86 -
1.6.1.5 Echocardiography Analysis ..... - 86 -
1.6.2 HISTOLOGY ..... - 87 -
1.6.2.1 Cardiac morphology & morphometric analysis ..... - 87 -
1.6.2.2 Immunohistochemistry ..... - 87 -
1.6.2.2.1 Immunofluorescence ..... - 87 -
1.6.2.2.2 DAB staining ..... - 87 -
1.6.2.2.3 BrdU staining ..... - 88 -
1.6.3 MOLECULAR BIOLOGY ..... - 88 -
1.6.3.1 Western blot analysis ..... - 88 -
1.6.3.2 Quantitative Real Time PCR ..... - 89 -
1.6.4 STATISTICS ..... - 90 -

CHAPTER 2 ..... - 91 -

CARDIAC-RESTRICTED *NEMO* GENE INACTIVATION LEADS TO DILATED CARDIOMYOPATHY ..... - 91 -

2.1 BACKGROUND ..... - 92 -

2.1.1 DILATED CARDIOMYOPATHIES - INTRODUCTION ..... - 93 -
2.1.2 COMMON GENETIC MUTATIONS IN DILATED CARDIOMYOPATHY (DCM) ..... - 93 -
2.1.2.1 Cytoskeletal mutations in dilated cardiomyopathy ..... - 93 -
2.1.2.2 Impaired calcium-handling in dilated cardiomyopathy ..... - 96 -
2.1.2.3 Survival pathways in dilated cardiomyopathy ..... - 96 -
2.1.3 NF-κB SIGNALING PATHWAY ..... - 97 -
2.1.3.1 Introduction ..... - 97 -
2.1.3.2 NF-κB pathway components ..... - 98 -
(i) NF-κB/Rel family proteins ..... - 98 -
(ii) IκB family proteins. ..... - 98 -
(iii) IKK complex ..... - 99 -
(iv)Converging signals to IKK complex. ..... - 102 -
2.1.3.3 NF-κB target genes ..... - 105 -
2.1.4 NF-κB SIGNALING IN CARDIAC DEVELOPMENT ..... - 105 -
2.1.5 NF-κB SIGNALING IN CARDIAC HYPERTROPHY ..... - 106 -

2.2 RESULTS ..... - 108 -

2.2 RESULTS ..... - 109 -
2.2.1 RATIONALE ..... - 109 -
2.2.2 CONDITIONAL INACTIVATION OF THE NEMO GENE IN THE MYOCARDIUM ..... - 109 -
2.2.3 CHARACTERIZATION OF NEMO^{HKO} MICE ..... - 111 -
2.2.4 NEMO^{HKO} MICE DEVELOP DILATED CARDIOMYOPATHY ..... - 112 -
2.2.4.1 Assessment of cardiac morphology ..... - 112 -
2.2.4.2 Up-regulation of heart failure markers in Nemo^{hko} mice ..... - 114 -
2.2.5 INCREASED APOPTOSIS IN NEMO^{HKO} HEARTS ..... - 115 -
2.2.6 ADVANCED CARDIAC DYSFUNCTION IN NEMO^{HKO} MICE ..... - 116 -
2.2.7 RECAPITULATION OF THE DILATED CARDIOMYOPATHY PHENOTYPE IN YOUNG NEMO^{HKO} MICE AFTER TRANSVERSE AORTIC BANDING ..... - 117 -
2.2.8 ANTIOXIDANT TREATMENT AMELIORATES HEART FAILURE PHENOTYPE IN OLD NEMO^{HKO} HEARTS ..... - 119 -

2.3 DISCUSSION ..... - 121 -

2.3.1 DISCUSSION ..... - 122 -
2.3.2 FUTURE PERSPECTIVES ..... - 124 -
2.3.3 CONCLUSIONS ..... - 125 -

2.4. MATERIALS & METHODS ..... - 127 -

CHAPTER 2 ..... - 127 -

CARDIAC-RESTRICTED *NEMO* GENE INACTIVATION LEADS TO DILATED CARDIOMYOPATHY ..... - 127 -

2.4.1 ANIMALS ..... - 128 -
2.4.1.1 Generation of Nemo^{hko} mice ..... - 128 -
2.4.1.2 Genotyping ..... - 129 -
2.4.1.3 Husbandry ..... - 130 -
2.4.1.4 Aortic Banding ..... - 130 -
2.4.1.5 Echocardiography Analysis ..... - 130 -
2.4.1.6 Antioxidant Treatment ..... - 131 -
2.4.2 HISTOLOGY ..... - 131 -
2.4.2.1 Morphological and morphometrical analysis ..... - 131 -
2.4.2.2 TUNEL Assay ..... - 131 -
2.4.3 MOLECULAR BIOLOGY ..... - 132 -
2.4.3.1 Quantitative RT-PCR ..... - 132 -
2.4.3.2 Southern blot analysis ..... - 132 -

2.4.3.3 Immunoblot Analysis ..... *- 133 -*
2.4.3.4 Electromobility Assay ..... *- 133 -*
2.5 STATISTICS ..... - 134 -

3. BIBLIOGRAPHY ..... **- 135 -**

4. PUBLICATIONS ..... **- 151 -**

Περίληψη

Η συγγενής καρδιοπάθεια αποτελεί την πιο συχνή μορφή ανθρώπινων δυσπλασιών (1% του παγκόσμιου πληθυσμού), ενώ η επίκτητη καρδιοπάθεια είναι η κύρια αιτία θνησιμότητας στον δυτικό ηλικιωμένο πληθυσμό, υπογραμμίζοντας την σημαντικότητα ερευνητικών προσπαθειών εστιαζόμενων στην μελέτη μοριακών μονοπατιών που εμπλέκονται στην καρδιακή ανάπτυξη και ασθένεια. Το μοριακό μονοπάτι Notch είναι απαραίτητο για μορφές διακυτταρικής επικοινωνίας, οι οποίες επηρεάζουν τον σχηματισμό και ομοιοστασία ιστών κατά την διάρκεια της εμβρυικής και ενήλικης ζωής. Ωστόσο, δεν είναι σαφές σε ποιους κυτταρικούς πληθυσμούς της καρδιάς θηλαστικών το μοριακό μονοπάτι Notch είναι ενεργό. Εδώ αναφέρουμε ότι υπερ-έκφραση του ενδοκυτταρικού τμήματος του Notch1 υποδοχέα (NICD1) σε μυοκύτταρα της εμβρυικής καρδιάς οδηγεί σε αναπτυξιακές ανωμαλίες και πρόωρη θνησιμότητα. Αντιθέτως, ενίσχυση της ενδογενούς Notch ενεργοποίησης μετά από έμφραγμα του μυοκαρδίου με την χρήση ενός ψευδοπροσδέματος (pseudoligand) για τον υποδοχέα Notch1 μειώνει το ποσοστό θνησιμότητας, βελτιώνει την καρδιακή λειτουργία και ελαχιστοποιεί την εναπόθεση κολλαγόνου (ίνωση), προάγωντας μηχανισμούς κυτταρικού πολλαπλασιασμού και δημιουργία νέων αιμοφόρων αγγείων. Τα αποτελέσματα μας αποκαλύπτουν πως ο βαθμός ενεργότητας του Notch μοριακού μονοπατιού στα καρδιομυοκύτταρα επηρεάζει την καρδιακή ανάπτυξη και αποδεικνύουν πως το ίδιο μοριακό μονοπάτι το οποίο προκαλεί καρδιακές ανωμαλίες όταν επηρεαστεί κατά την εμβρυική ανάπτυξη, μπορεί να χρησιμοποιηθεί για θεραπεία ασθενών με έμφραγμα του μυοκαρδίου. Επίσης, μελετήσαμε τον ρόλο του μεταγραφικού παράγοντα nuclear factor κΒ (NF-κΒ) στο μυοκάρδιο στα πλαίσια της επίκτητης καρδιακής ασθένειας. Οι μοριακές δράσεις του NF-κΒ στην ενήλικη καρδιά παραμένουν άγνωστες διότι η καθολική απενεργοποίηση του NF-κΒ σε ποντίκια οδηγεί σε πρόωρη θνησιμότητα κατά την εμβρυική ανάπτυξη. Χρησιμοποιώντας τεχνολογία Cre/loxP, απενεργοποιήσαμε το γονίδιο *Nemo* (NF-κΒ essential modulator) ειδικά στα καρδιομυοκύτταρα ποντικών. Η συγκεκριμένη προσέγγιση οδήγησε σε ανάπτυξη καρδιακής φλεγμονής και αποπτώσης, οι οποίες οδήγησαν σε καρδιομυοπάθεια κατά το ενήλικο στάδιο ζωής. Επιπρόσθετα, πειράματα επαγωγής υπερτροφίας σε νεαρές καρδιές ποντικών με μεταλλαγμένο το *Nemo* γονίδιο οδήγησαν πρόωρα σε καρδιακή δυσλειτουργία, η οποία θυμίζει την σποραδική καρδιοπάθεια που παρατηρείται σε ενήλικα μεταλλαγμένα *Nemo* ποντίκια. Πιστεύουμε πως η απώλεια του *Nemo* γονιδίου στα καρδιομυοκύτταρα οδηγεί σε οξειδωτική δυσλειτουργία η οποία προκαλεί καρδιομυοπάθεια, διότι αντιοξειδωτική δίαιτα επέφερε βελτίωση της καρδιακής παθολογίας στα μεταλλαγμένα *Nemo* ποντίκια. Τα αποτελέσματα μας αποκαλύπτουν έναν απαραίτητο ρόλο για τον μεταγραφικό παράγοντα NF-κΒ στην ενήλικη καρδιά ώστε να διατηρεί την φυσιολογική της λειτουργία ανταποκρινόμενη σε μηχανικές επιβαρύνσεις ή γήρανση. Συνοψίζοντας, οι παρατηρήσεις μας συνεισφέρουν στην βαθύτερη κατανόηση του ρόλου των μοριακών μονοπατιών Notch1 και NF-κΒ στα καρδιομυοκύτταρα στα πλαίσια συγγενών και επίκτητων καρδιακών ανωμαλιών.

Summary

Congenital heart disease is the commonest human birth defect occurring in 1% of the population worldwide, whereas acquired heart disease is the main cause of mortality in the elderly western populations, highlighting the importance of research focus on signaling pathways involved in cardiac development and disease. Notch signaling pathway is important for cell-cell communication that controls tissue formation and homeostasis during embryonic and adult life, but the precise cell targets of Notch signaling in the mammalian heart remain poorly defined. Here, we report that conditional over-expression of Notch1 intracellular domain (NICD1) in the embryonic cardiomyocyte compartment results in developmental defects and perinatal lethality in mice. In contrast, augmentation of endogenous Notch reactivation after myocardial infarction in the adult by intramyocardial delivery of a Notch1 pseudoligand increases survival rate improves cardiac functional performance and minimizes fibrosis, promoting proliferative and angiogenic mechanisms. These results reveal a strict requirement for cell-autonomous modulation of Notch signaling during heart morphogenesis, and illustrate how the same signaling pathway that promotes congenital heart defects when perturbed in the embryo can be therapeutically redeployed for the treatment of adult myocardial damage. Additionally, we sought to determine the role of NF-κB pathway in the adult myocardium and acquired cardiac disease. Insight into the function of nuclear factor κB (NF-κB) in the adult heart has been hampered by the embryonic lethality of constitutive NF-κB inactivation in mice. Using Cre/loxP technology, we disrupted in a cardiac-specific manner the NF-κB essential modulator (NEMO) in the murine heart, which simulated the adaptive changes underlying human heart failure, causing adult-onset dilated cardiomyopathy accompanied by inflammation and apoptosis. Pressure overload challenges of NF-κB-deficient young hearts precociously induced the functional decrements that develop spontaneously in older knockout animals. Oxidative stress in NF-κB-deficient cardiomyocytes is a critical pathological component that can be attenuated with antioxidant diet *in vivo*. These results reveal an essential physiological role for NF-κB in the adult heart to maintain cardiac function in response to aging-related or mechanical challenges, in part through modulation of oxidative stress. Taken together, our observations provide valuable insights regarding the cardiomyocyte-autonomous role of Notch1 and NEMO/ NF-κB signaling in congenital and acquired heart disease.

INTRODUCTION

1. Introduction

1. 1. Evolution of the heart at a glance

Animals, throughout species, have developed micropumps and macropumps associated with circulatory systems in order to guarantee for their cells -through diffusion- access to oxygen and nutrients as well as elimination of carbon dioxide and excreta. Thinking on an evolutionary scale, heart can be defined as any organ that propels fluid through a circulatory system. In a more vertebrate-oriented approach, heart is a chambered pumping organ and the first to form and function during embryogenesis[1].

The first heart-like structure has possibly appeared 500 million years ago in an ancestral bilaterian and resembles the tubular vessel-like heart of tunicates (ascidians) and cephalochordates (amphioxus), characterized by a myoepithelial cell layer and no defined chambers or valves (fig.1.1)[2-4]. Interestingly, the arthropod (*Drosophila*) heart is also a vessel-like organ that functions as a linear peristaltic pump but contains a cardio-aortic valve that separates the posterior cardiac muscle compartment from the anterior aorta-like structure[5]. In addition, nematodes (*C.elegans*) possess a contractile pharynx instead of a heart, where pharyngeal muscle cells exhibit contractile properties reminiscent of mammalian cardiomyocytes[1]. The appearance of primordial cardiac muscle cells that resemble the myoepithelial layer in amphioxus possibly precedes the divergence of Cnideria (hydra, jellyfish, and corals) from the Bilateria (tunicates, cephalochordates, fish, amphibian, and amniotes), from which mammals descended[6]. It is believed that these primordial cardiac muscle cells in Cnideria and amphioxus (the closest living approximation of the invertebrate ancestor of vertebrates) existed in the gastrodermis and facilitated fluid movement during feeding[7, 8]. Similarly, cardiac muscle in Bilateria is derived from mesoderm that has probably arisen from the gastrodermis of a diploblastic ancestor.

During evolution, the single-layered vessel-like hearts evolved to more complex structures with thick muscular chambers programmed to receive (atria) or pump (ventricles) blood to the rest of the body through a closed circulatory system[2]. Moreover, the transition from aquatic to terrestrial environments had a huge impact on cardiac complexity since further adaptations were required for the separation

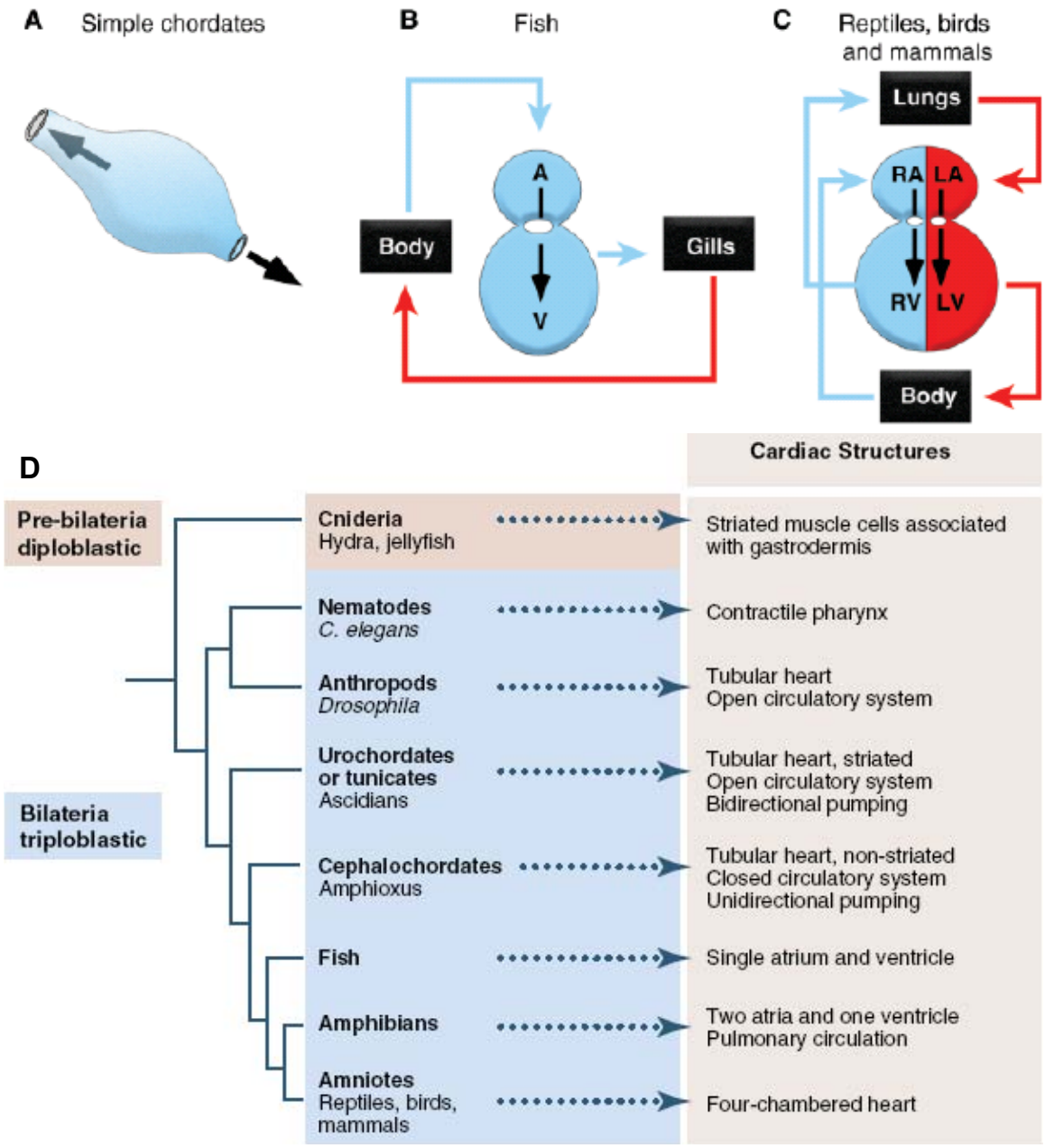

Figure 1.1 Evolution of the heart. Simplified depiction of the heart in chordates (**A**), fish (**B**), and terrestrial vertebrates (**C**). Arrows demonstrate the direction of the blood. Oxygenated blood is highlighted in red and deoxygenated blood in blue. Simple chordates have vessel-like hearts, some of which pump bidirectionally (**A**), whereas unidirectional blood flow is achieved in fish (**B**) (one atrium, one ventricle) and in terrestrial vertebrates (two atria, two ventricles) such as reptiles, birds and mammals **(C**). The evolution of cardiac structures of representative animals of certain taxa/phyla and their evolutionary relationships (**D**). *(Adapted from EN Olson, Science,2006).*

of the oxygenated and deoxygenated blood[4]. Hence, simple chordates have tubular hearts characterized sometimes by bidirectional blood pumping, whereas fish have a single atrium and ventricle from where the blood is pumped through the capillaries of the gills and on to the capillaries of the body tissues (fig.1.1). Amphibians possess two atria and a single ventricle, while terrestrial vertebrates have two atria and two ventricles divided by septae in order to guarantee separation of the deoxygenated and oxygenated blood within the pulmonary and systemic circulation, respectively. Furthermore, unidirectional blood flow at high force (through synchronous contractions) in a closed vascular system is assured by the development of a conduction system and the appearance of valves in the vertebrate heart[1].

1. 2 Cardiac development in mammals

Cardiogenesis is an extremely sensitive developmental process. Any perturbation in the cells that participate in cardiac development results in embryonic/perinatal death or subtle cardiac anomalies that become evident with age. Congenital heart disease is the commonest human birth defect occuring in 1% of the population worldwide, whereas another 1% - 2% harbor mild cardiac developmental defects that deteriorate over decades[9].

The mammalian heart is a muscular pump that delivers blood (oxygen, nutrients) to all body cells through a closed vascular system. It consists of four specialized chambers, two atria and two ventricles, which have distinct functional roles. The left atrium collects the oxygenated blood from the lungs and sends it to the left ventricle, from where it is delivered to all body tissues through the aorta and the systemic circulation. On the other hand, the right atrium collects deoxygenated blood from all body cells and actively fills the right ventricle, from where it is sent to the lungs through the pulmonary artery. Unidirectional blood flow and separation between oxygenated and deoxygenated blood is ensured by the function of valves and the existence of ventricular and atrial septa. Moreover, the conduction system coordinates synchronous cardiac contractions by generating/conducting electrical signals in the myocardium. In addition, coronary vasculature plays a key role in cardiac function by supplying energy to all the cardiac cell populations (cardiomyocytes, smooth muscle cells, endothelial cells, fibroblasts)[10].

Recent fate-mapping studies in chick[11, 12] and mouse[13-16] embryos highlight two distinct mesodermal heart fields that contribute cells to the developing heart in a

temporally and spatially specific fashion, and were termed first and second heart fields. Interestingly, quail-chick graft experiments identified specific ectodermal cell populations at the dorsal neural tube that also contribute to portions of the heart and great vessels, referred to as cardiac neural crest (CNC) cells[17, 18].

First heart field

Mesoderm derives from the primitive streak during gastrulation and is the source of myocardial cells[19]. At embryonic day 6 (e6.5) of mouse development, cardiac progenitor cells are located at the anterior region of the primitive streak and start migrating to in an anterior-lateral fashion to regions under the headfolds[20]. At e7.5 these cells extend across the midline and form a crescent-shape epithelium, the cardiac crescent, where the first differentiated cardiomyocytes can be observed. It is believed that the first heart field (FHF) derives from the cardiac crescent, which later fuses at the midline in order to form the primitive heart tube at e8.0[21] (fig.1.2). At this stage, the primitive heart tube consists of an interior endocardial cell layer and an exterior myocardial cell layer that are separated by extracellular matrix allowing reciprocal signaling events. Next, the primitive heart tube undergoes rightward looping (e8.5) and simultaneous expansion of the myocardium which lead to formation of four recognizable chambers[22]. By e14.5 the cardiac chambers are well separated by septa, which ensure the separation of oxygenated and deoxygenated blood after birth. The left ventricle and parts of the atria are considered derivatives of the first heart field (FHF)[16, 21].

Second heart field

The notion that the primitive heart tube expands - exclusively - through myocardial cell proliferation *in situ* was recently challenged from studies in chick[11, 12] and mouse[13-16] embryos. These studies indicate that the heart tube derived from the first heart field (FHF) serves as a scaffold, where - later during cardiac development – cells from a second heart field (SHF) migrate and participate in chamber construction. During morphogenesis, the cardiac crescent (FHF) edges move to the midline and the SHF cells migrate and position themselves dorsal to the primitive heart tube in the pharyngeal mesoderm[14, 16]. SHF cells that lie dorsally to the heart tube contribute to right ventricular formation, whereas more anterior cells contribute to the outflow-tract myocardium and part of the atria[13] (fig.1.2). From the evolutionary point of view, the SHF appeared later than the FHF since the outflow tract with the right ventricular chamber are considered

later evolutionary advancements of the heart[13, 14, 23]. Notably, the migration and differentiation of the SHF derived cells are delayed if compared with the corresponding processes in the FHF derivatives[21].

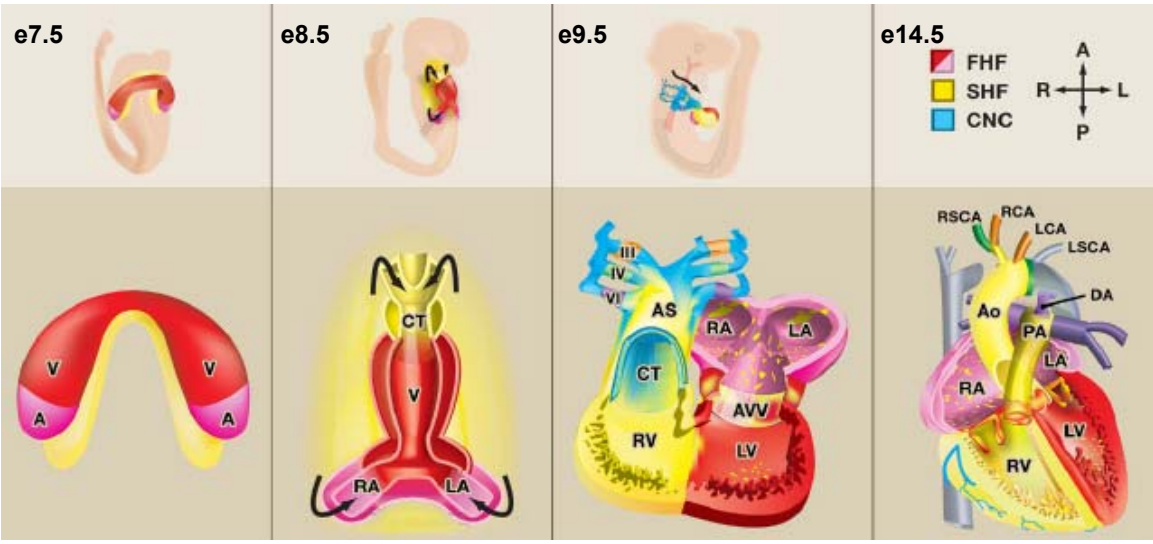

Figure 1.2 Mammalian Heart Development.
First panel: first heart field (FHF) cells form the cardiac crescent in the anterior region of the embryo, whereas the second heart field (SHF) cells are located medial and anterior to the FHF. ***Second panel:*** SHF cells are dorsal to the primitive heart tube and start to migrate into the anterior and posterior poles of the heart tube in order to build the right ventricle (RV), conotruncus (CT) and parts of the atria (A). ***Third panel*****:** Folowing rightward looping of the linear heart tube, cardiac nural crest (CNC) cells also migrate from the pharyngeal arches to the anterior pole of the heart and participate in outflow tract septation and aortic arch artery patterning (II, IV, VI). ***Fourth panel****:* Atrial and ventricular septation as well as formation of atrioventricular valves (AVV) results in the four-chambered heart. *Abbreviations: V, Ventricle; LV, left ventricle; LA, left atrium; RA, right atrium; AS, aortic ac; Ao, aorta; PA, pulmonary artery; RSCA, right subclavian artery; LSCA, left subclavian artery; RCA, right carotid artery; LCA, left carotid artery; DA, ductus arteriosus.* Arrows indicate direction of cell migration. *(Adapted from D. Srivastava, Cell, 2006)*

Cardiac neural crest

Powerful transplantation experiments in the chick embryo revealed a specific region of the dorsal neural tube that provided cells to regions of the heart and great vessels[17, 18]. These cells were named cardiac neural crest (CNC) cells and CNC-ablation experiments demonstrated a critical function in the septation of the outflow tract and the formation of the aortic arch arteries[24] (fig.1.2).

Remodeling after looping

After looping of the primitive heart tube, remarkable remodeling completes the cardiac developmental program. First, the transmural ventricular myocardium is

characterized by sponge-like structures, the trabeculae, which increase the surface area for oxygen uptake in the absence of coronary circulation at this stage[10]. Next, all the specialized components of the conduction system including sinuatrial (SA) and atrioventricular (AV) nodes are formed within myogenic tissue of the inflow tract (IFT) and proximal to atrioventricular canal (AVC), respectively[25]. Moreover, endocardial cushions are formed at the AVC and give rise to the formation of the tricuspid (right atrium - right ventricle) and mitral (left atrium - left ventricle) valves. Interestingly, endocardial cushions are also present in the outflow tract (OFT) and serve as a scaffold for the OFT septation and the development of the aortic and pulmonary valves[2]. Finally, the coronary circulation is formed through contributions of the epicardium and the cardiac neural crest (CNC)[24, 26].

Mutations affecting FHF, SHF and CNC contributions

Several evolutionary conserved molecules including ligands and transcription factors have been described to affect normal cardiac development when mutated in mice (table 1.1).

Heart and neural crest derivatives expressed transcript 1 (Hand1) mutants die from extra-embryonic defects and present left-ventricular hypoplasia, which reflects ***impaired FHF contribution*** to the cardiac development[27, 28]. Similarly, *NK2 transcription factor related, locus 5 (Nkx2.5)* mutant mice display single atrial and ventricular compartments accompanied with loss of ventricular tissue and absence of expression of the left-ventricular marker HAND1[29, 30]. Moreover, mice lacking the *T-box 5 (Tbx5)* gene show severe defects in the atria-inflow region of the heart and left-ventricular hypoplasia[31]. *Hand1* and *Tbx5* genes are also considered markers of the FHF because of their specific expression pattern at the cardiac crescent[22].

Insulin gene enhancer protein 1 (Isl1) is a LIM homeodomain transcription factor which serves as a marker of the ***SHF contribution*** to the developing heart since *Isl1*$^{-/-}$ mice show no outflow tract and loss of right-ventricular identity[13]. Moreover, *forkhead box H1 (Foxh1)* gene mutants demonstrate no right ventricle and abnormal outflow tract formation, which is reminiscent of impaired SHF contribution[32]. Similarly, *myocyte enhancer factor 2C (Mef2c)* mutants display a second heart field phenotype characterized by no right-ventricular formation and abnormal outflow tract[33]. In addition, *heart and neural crest derivatives expressed transcript 2 (Hand2)* and *T-box 20 (Tbx-20)*

enrich the battery of genes that can be considered markers of the second heart field since *Hand-2*[34, 35] and *Tbx-20*[36-38] mutants display hypoplastic right ventricle .

Fibroblast growth factor 8 (Fgf-8)[39, 40] and *T-box 1 (Tbx-1)* [41-44]mutants display similar phenotypes that possibly affect SHF and ***CNC contributions*** to the developing heart. These mutants die of cardiac failure due to malformations of the outflow tract. However, they also demonstrate a CNC phenotype because the aorta and the pulmonary trunk are also malformed. Similarly, mutants for Notch signaling components including *Jagged-1*[45, 46], *Notch-2*[47], and *Hey2*[48, 49] show defects in the outflow tract and tetralogy of Fallot (right ventricular hypertrophy, overriding aorta, ventricular septal defect and pulmonary stenosis), which indicate improper SHF and CNC contributions to the developing heart. From the latter examples, it becomes apparent that SHF phenotypes are usually associated with CNC phenotypes.

Gene	Crescent expression*	Second heart-field expression*	Cardiac tube expression*	Mutant phenotype in the cardiac tube
Nkx2-5	Yes	Yes	Yes	Single atrial and ventricular compartments; loss of ventricular tissue; no *Hand1* expression
Hand1	Yes	No	LV (high in outer curvature)	LV disrupted
Tbx5	Yes	No	LV, A, INF	Sinoatrial defects; hypoplastic LV
Fgf10	No	Yes	No	No early phenotype detected
Fgf8	No	Yes	No	OFT defects
Tbx1	Yes	Yes	No	OFT defects
Isl1	No	Yes	OFT, RV (LV), A, INF	Single atrial and ventricular compartments; *Hand1* and *Tbx5* expression, which indicates that LV identity is intact; no OFT; atria at the venous pole are abnormal
Foxh1	No	Yes	No	OFT reduced or absent; RV does not develop
Mef2c	(Yes?)	Yes	Yes	OFT reduced; RV does not develop (*Hand2* is downregulated); INF abnormalities
Hand2	Yes	Yes	RV	RV abnormalities
Hand1/Hand2	Yes	Yes	RV/LV	No ventricle; only atrial chamber forms
Tbx20	Yes	Yes	OFT, RV, LV	Chambers do not develop; no *Hand1* expression; hypoplastic RV; OFT disrupted

Table 1.1 Expression pattern and mutant phenotypes of genes involved in cardiac development.

* Only well-defined expression patterns are presented here. *Abbreviations: A, atria; Fgf8/10, fibroblast growth factor 8 and10; Foxh1, forkhead box H1; Hand1/2, heart and neural crest derivatives expressed transcript 1 and 2; INF, inflow region; Isl1, insulin gene enhancer protein, a LIM homeodomain transcription factor; LV, left ventricle; Mef2c, myocyte enhancer factor 2C; Nkx2.5, NK2 transcription factor related, locus 5; OFT, outflow tract; RV, right ventricle; Tbx1/5/20, T-box 1, 5, and 20. (Adapted from M. Buckingham et al. Nat Rev Genetics, 2005)*

1.3 Modes of cardiac growth

1.3.1 Hyperplasia

Pre-natal cardiac growth is mainly characterized by cardiomyocyte proliferation, where karyokinesis and cytokinesis are coupled processes, resulting in increases in mononucleated cardiac myocytes (hyperplasia)[50]. In mice, the first peak of cardiomyocyte proliferation (33%) is observed at mid-gestation (e12) and progressively decreases in late-gestation stages (2%), ceasing soon after birth. In the early post-natal period (day4-day6), a second peak of cardiomyocyte proliferation (10%) occurs; however, karyokinesis is not coupled with cytokinesis, resulting in binucleation of cardiomyocytes without an overall increase in cell number[51]. The mechanisms that regulate the uncoupling of nuclear division from cell division remain to be elucidated, as well as their functional significance.

Contrary to the long-standing dogma that cardiomyocytes are post-mitotic cells in post-natal life, various reports estimate 0.005% - 0.04% proliferation rate in the normal adult murine myocardium[52-54]. However, little is known regarding the molecular mechanisms that govern cardiomyocyte proliferation. Interestingly, cardiac-restricted overexpression of the cell-cycle regulator cyclin D1 in mice doubles the cardiomyocyte population at 2 weeks after birth[54]. Moreover, members of the Fibroblast Growth Factor (FGF) family, such as Fgf1 and Fgf2, can induce cell-cycle reentry and trigger cardiomyocyte proliferation in avians [55]. In addition, a recent report highlights the role of periostin as an extracellular molecule that induces proliferation of differentiated cardiomyocytes and promotes cardiac repair in a phosphatidylinositol-3-OH kinase (PI-3 kinase) dependent fashion[56]. However, it is becoming increasingly evident that further research is required to decipher the molecular mechanisms that control cardiomyocyte proliferation due to its therapeutic value in the context of cardiac regeneration.

1.3.2 Hypertrophy

In post-natal life, the predominant form of cardiac growth shifts from hyperplastic to hypertrophic, characterized by an increase in the size of cardiomyocytes, muscle mass and protein synthesis[57]. Cardiomyocytes are re-programmed to exit irreversibly the cell cycle and employ hypertrophic signals that complete the cardiac developmental program and eventually give rise to a functional adult heart. Hypertrophic cardiomyocyte growth is

initiated by multiple stimuli, including mitogens, canonical cardiac agonists, passive mechanical load or hemodynamic burden during postnatal cardiac development or in certain disease conditions[51, 58].

Depending on the stimuli, cardiac hypertrophy can be classified as physiological or pathological hypertrophy[57]. Chronic exercise or pregnancy can lead to **physiological hypertrophy** which is associated with proportional increases in cardiomyocyte length and width, no signs of interstitial fibrosis, and absence of cardiac dysfunction (fig.1.3, a,b). Moreover, physiological hypertrophy is characterized by proportional ventricular wall thickening and chamber volume enlargement, termed as eccentric hypertrophy[57]. On the other hand, stress signals including chronic hypertension, pressure overload and aortic valve disease can cause **pathological hypertrophy** in which the ventricular wall thickens and results in a net decrease in the ventricular chamber volume (concentric hypertrophy). The pathological cardiac hypertrophy is associated with increases in cardiomyocyte width since new contractile-protein units (sarcomeres) are assembled in parallel[57]. In addition, fibrosis and cardiac dysfunction can also accompany pathological hypertrophy. However, pathological hypertrophy or conditions such as myocardial infarction and certain cardiomyopathies can produce a phenotype of dilatory and eccentric cardiac growth, termed as **cardiac dilation** (fig.1.3, a,b). Cardiac dilation is characterized by increased myocyte length (sarcomere addition in series), extensive tissue fibrosis, myocyte death and advanced cardiac dysfunction[57, 59].

The molecular mechanisms that regulate the transition from normal to hypertrophic cardiac growth are poorly understood. Recent reports propose the re-employment of the GATA4[60], Mef2C[61, 62] and Nkx2.5[63, 64] transcription factors, crucial for differentiation and growth of the developing myocardium, in adult cardiac hypertrophy or its transition to dilation. According to this model, the aforementioned transcription factors mediate the reactivation of the “fetal gene program”, where re-expression of several genes -not normally expressed in the adult heart, but seen only in the embryonic heart- orchestrates hypertrophic cardiac remodeling. Common examples include increase in the expression levels of the embryonic genes *atrial natriuretic peptide (anp)* and *brain natriuretic peptide (bnp*), as well as the contractile genes *myosin heavy chain 7 (myh7) and skeletal α-actin (Acta-1)*[65].

Fetal gene program re-activation is essential for the dynamic cardiac adaptation to stress signals by regulating hypertrophic response. However, prolonged re-activation of the fetal gene program leads to maladaptive changes in cardiac function accompanied

by myocyte loss through apoptosis and by replacement fibrosis[66]. These landmark processes for the transition from cardiac hypertrophy to cardiac dilation/failure highlight the importance of survival pathways in this transition[67, 68]. In line with this notion, conditional inactivation of the survival pathway gp130 demonstrated rapid progression to cardiac dilation/failure due to myocyte apoptosis in a pressure-overload model[69], whereas several *in vitro* and *in vivo* approaches demonstrate cardiomyocyte-autonomous pro-apoptotic actions for the cytokine, tumor necrosis factor-α (TNFα)[70, 71].

Besides survival pathways, the progression from normal to failing heart involves severe changes in the expression of structural and calcium-regulatory proteins, which can reflect primary or secondary events[59, 72]. All these pathways are presented in detail in the **Background of Chapter 2.**

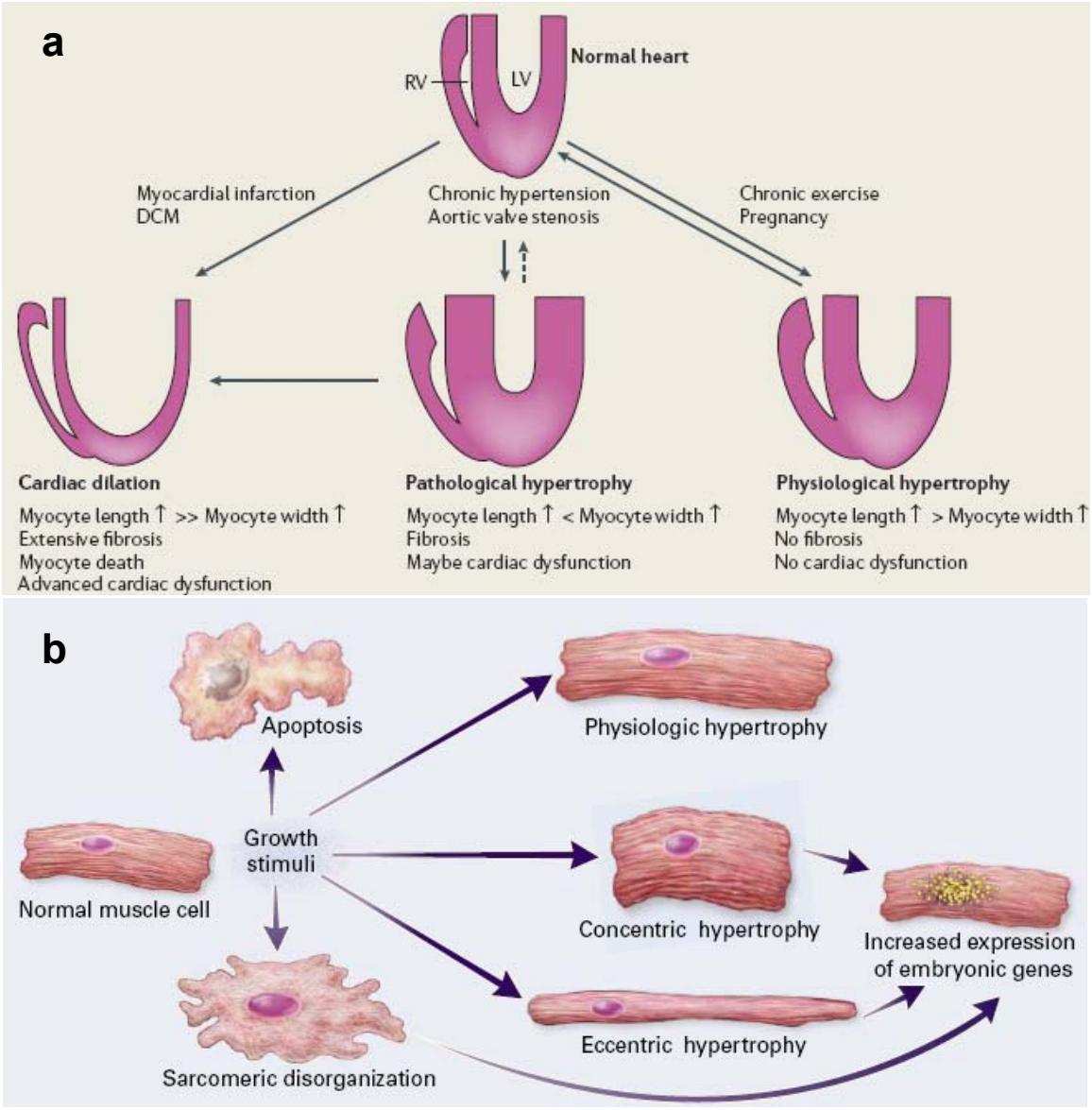

Figure 1.3 Cardiac hypertrophy and cardiomyocyte morphology changes. (a) Types of cardiac hypertrophy. Depending on the stimuli, the adult heart can acquire different types of hypertrophy (physiological, pathological and cardiac dilation). Detailed description of each condition is provided in the text. *(adapted from Heineke & Molkentin, 2006)*. **(b) Morphology of cardiomyocytes in hypertrophy and failure.** Various growth stimuli change the cardiomyocyte morphology and lead to distinct forms of hypertrophy. Sarcomeric disorganization, embryonic gene re-activation and apoptosis are typical of dilated cardiomyopathy (eccentric hypertrophy). *(adapted from Hunter & Chien, 1999)*.

1.4 Heart disease

Despite recent advances in therapy, heart disease remains the leading cause of mortality in the young and the old, accompanied with enormous social and economic impact for the Western populations[9, 73]. Cardiovascular research is continuously growing since population demographics clearly indicate a progressive future increase in the segment of the population at ages over than 65 years[74]. Depending on the time and the cause of its occurrence, heart disease can be classified as *congenital* or *acquired*.

Congenital heart disease refers to abnormalities in the heart's structure and function that arise before birth. It is the most frequent form of birth defects in humans, occurring in 1% of the population worldwide[9]. Congenital heart disease affects most parts of the heart and can be classified into three categories: *cyanotic heart disease, left-sided obstruction defects* and *septation defects* (fig.1.4). Infants with cyanotic heart disease appear blue as a result of the mixing of oxygenated and deoxygenated blood[75]. Cardiac defects that can lead to this condition include transposition of the great arteries (TGA), tetralogy of Fallot (TOF), tricuspid atresia, pulmonary atresia, Ebstein's anomaly of the tricuspid valve, double outlet right ventricle (DORV), persistent truncus arteriosus (PTA), and total anomalous pulmonary venous connection (fig. 1.4). The second main type of congenital heart disease includes left-sided obstruction defects, whose main cause can be hypoplastic left heart syndrome (HLHS), mitral stenosis, aortic stenosis, or interrupted aortic arch (IAA). Septation defects, the third main type of congenital heart disease, can affect septation of the ventricles (ventricular septal defects, VSDs), septation of the atria (atrial septal defects, ASDs), or formation of structures in the central part of the heart (atrioventricular septal defects, AVSDs). Two other congenital cardiac defects that do not fit into the three aforementioned categories include bicuspid aortic valve (BAV) and patent ductus arteriosus (PDA) (fig.1.4). The most common types of congenital heart disease include BAV and septation defects[75]. Mortality and morbidity rates are high and depend on the severity of the congenital heart disease.

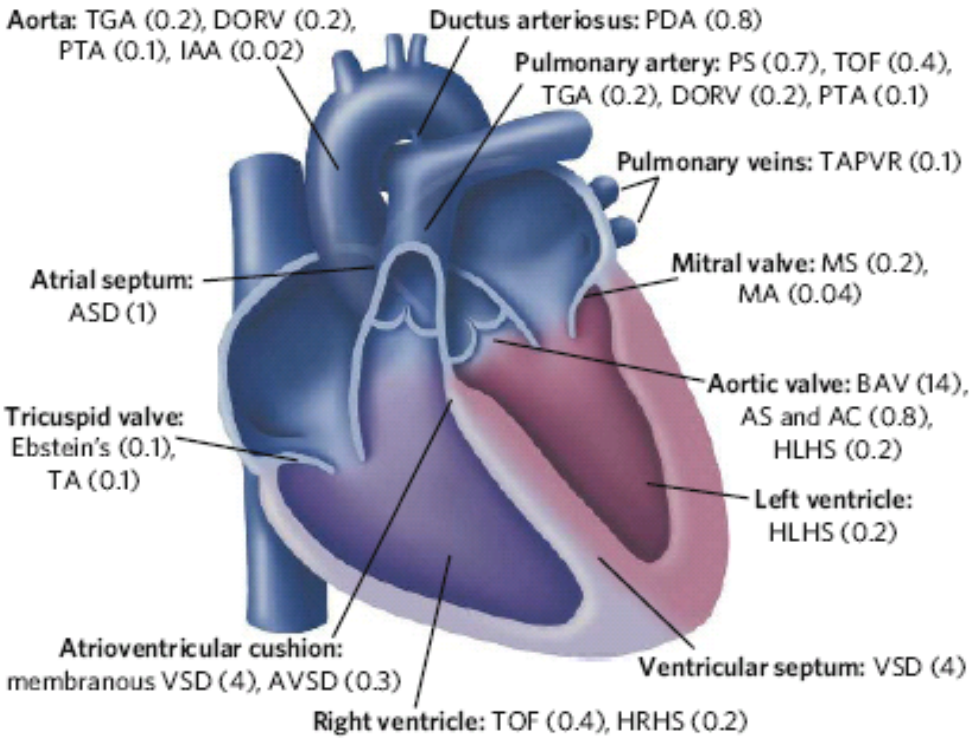

Figure 1.4. Congenital heart defects. Diagram of the adult heart demonstrating the cardiac structures affected by congenital defects, with the estimated incidence of each defect per 1,000 live births indicated in parentheses. AC, aortic coarctation; AS, aortic stenosis; ASD, atrial septal defect; AVSD, atrioventricular septal defect; BAV, bicuspid aortic valve; DORV, double outlet right ventricle; Ebstein's, Ebstein's anomaly of the tricuspid valve; HLHS, hypoplastic left heart syndrome; HRHS, hypoplastic right heart syndrome; IAA, interrupted aortic arch; MA, mitral atresia; MS, mitral stenosis; PDA, patent ductus arteriosus; PS, pulmonary artery stenosis; PTA, persistent truncus arteriosus; TA, tricuspid atresia; TAPVR, total anomalous pulmonary vein return; TGA, transposition of the great arteries; TOF, tetralogy of Fallot; VSD, ventricular septal defect. *(Adapted from Benoit Bruneau, Nature, 2008)*

Following birth, cardiomyocytes are re-programmed to exit irreversibly the cell cycle and employ hypertrophic signals post-natally. This characteristic cell cycle exit and switch to hypertrophic growth sets the ground for the ***acquired form of heart disease*** in later life, potentially leading to an epidemic of uncertain proportions[76]. For example, there are five million Americans currently diagnosed with acquired heart disease, which is characterized by a survival rate of approximately 50%[77]. Over the past 50 years, the incidence of the acquired heart disease has declined among women but not among men, whereas the survival rate after the onset of the disease has been improved in both sexes[73]. Acquired heart disease can lead to heart failure, a deficiency in the capability of the heart to adequately pump blood in response to systemic demands, which subsequently leads to premature fatigue, dyspnoea, and/or oedema. The clinical

syndrome of heart failure (HF) is the final pathway for myriad diseases that affect the heart and arise via interactions of environmental factors and genetic susceptibility. Common HF stimuli include longstanding hypertension, myocardial infarction, ischaemia associated with coronary artery disease, valve insufficiency/stenosis, myocarditis, subtle congenital defects, cardiomyopathy and cancer treatment-induced cardiotoxicity[78, 79]. Most of these stimuli initially induce a state of compensated/pathological hypertrophy in which cardiomyocytes grow in length and/or width in order to increase cardiac pump function and decrease ventricular wall tension. However, in the long term, individuals with compensated hypertrophy are predisposed to heart failure, arrhythmias and sudden death[80].

1.5 Strategies for cardiac repair

Warm-blooded animals lost their ability to effectively repair injured myocardium, whereas amphibians, fish, mollusks, and arthropods can replace lost cardiomyocytes through regeneration, suggesting that the ability for cardiac regeneration in mammals has been lost during evolution[1]. In contrast to skeletal muscle, the mammalian heart has limited restorative capacity following myocardial infarction or ischemia-reperfusion injury, rendering heart disease as the leading cause of mortality worldwide[58]. Until recently, the standard dogma in the cardiac field was that cardiomyocytes are terminally differentiated cells that have lost their capacity to divide[81]. Intriguingly, several groups have identified resident cardiac progenitor cells (CPCs) that may be activated in response to myocardial injury (such as an infarction) and facilitate tissue repair[58]. *Cell replacement*, *regulation of the cardiac cell cycle*, *identification of resident cardiac stem cells* and re-*employment of embryonic signaling* summarize the currently recognized strategies for cardiac repair.

Cell replacement

The principle of this approach is to implant additional myocytes to the injured myocardium. Studies with fetal cardiomyocytes proved the feasibility of this approach since these cells could survive in the myocardium after grafting and prevent left ventricular dysfunction after infarction[82]. Due to the limited clinical applications of this approach, following studies focused on the therapeutic potential of skeletal muscle and bone marrow derived stem cells (fig.1.5). Interestingly, skeletal myoblast transplantation improved cardiac function following infarction in mice[83]. However, further studies

demonstrated that skeletal myoblasts do not transdifferentiate into cardiomyocytes after cardiac grafting [84] and cases of arrhythmias have been reported in clinical trials with human skeletal myoblasts[85]. Interestingly, autologous hematopoietic stem cells do transdifferentiate into cardiomyocytes after direct injection into the ventricular wall and partially replace the necrotic myocardium after infarction[86, 87]. The therapeutic appeal of this approach is also limited since it requires removal of the spleen. Notably, mesenchymal stem cells from adult bone marrow contain high levels of telomerase activity and prevalent engraftment by these cells occurred after direct injection into the infracted myocardium in pigs[88, 89]. Finally, several reports propose endothelial progenitor cells derived from peripheral blood mononuclear cells as a source for adult cardiomyocytes[90, 91] (fig.1.5). Clinical trials on patients with myocardial infarction using bone marrow-derived cells or endothelial progenitor cells have been initiated with initial priority to safety rather than effectiveness[92, 93].

Regulation of the cardiac cell cycle

The principle of this approach is to delay terminal cardiomyocyte differentiation and promote cardiomyocyte cycling. Studies focusing on telomere length demonstrated enhanced cardiomyocyte proliferation and protection after infarction in transgenic mice where telomerase reverse transcriptase is expressed under the alpha-myosin heavy chain (αMyHC) gene promoter[94]. Conversely, mice lacking the telomerase RNA component (TERC) showed significant telomerase-shortening, ventricular thinning and apoptosis[95]. Moreover, a recent report demonstrates cell cycle reentry and new cardiomyocyte formation after infarction in mice with cardiac specific overexpression of the cell cycle regulator, cyclin A2[96]. Intriguingly, cardiomyocyte cell lines from ventricular myocardium have been recently created by expression of the SV40 large T antigen under the transcriptional control of an early cardiac-specific promoter from the *Nkx2.5* gene promoter[97].

Resident cardiac stem cells (CSCs)

Unlike skeletal muscle, cardiac muscle harbors a negligible resident progenitor cell population[1, 58]. However, recent studies have suggested the existence of “stem-like” cells in the adult myocardium that may be activated in response to injury. One possible CSC candidate is the side population (SP) of the heart, based on its ability to exclude the

Hoechst dye 33342 and demonstrates stem cell properties (fig.1.5)[98, 99]. Second, the hematopoietic stem cell marker c-kit appears to mark cardiac progenitor cells, which migrate into the injured myocardium, differentiate into cardiomyocytes and improve mechanical function following direct injection into the infarcted myocardium (fig.1.5)[100]. Moreover, telomerase activity appears to identify adult cardiac progenitor cells which express the stem cell antigen 1 (Sca-1)[101]. Sca-1+ cells are able to home the injured myocardium, fuse with endogenous myocytes and differentiate *in situ*.

Re-employment of embryonic signaling

It is becoming evident that genes involved in early cardiogenesis may be re-deployed in the adult stage to protect or regenerate the injured myocardium[21]. A landamark study by Bock-Marquette *et al.* demonstrates that recapitulation of embryonic thymosin-β4 signaling protects against myocardial infarction in mice[102]. Thymosin-β4 is abundantly expressed in the heart and regulates cell migration events during cardiogenesis, whereas it promotes survival and neo-angiogenesis in the adult ischemic myocardium[102]. In support of this notion, myocardial gene delivery of *sonic hedgehog (shh)* - regulator of the second heart field contribution to the developing heart – preserves cardiac function, inhibits fibrosis and promotes neo-angiogenesis after infarction[103]. Moreover, taking into consideration the recent identification of rare resident cardiac progenitor cells[104], it will be interesting to determine if these cells can differentiate to cardiomyocytes, endothelial cells, or conduction system cells following embryonic signaling recapitulation[21]. In line with this possibility, a recent report shows adult epicardial progenitor mobilization and neovascularization upon thymosin-β4 signaling activation[105]. Taken together, re-employment of embryonic signals during the acute ischemic period favors survival and neo-angiogenesis, while at the same time obviates the need for cell-based approaches.

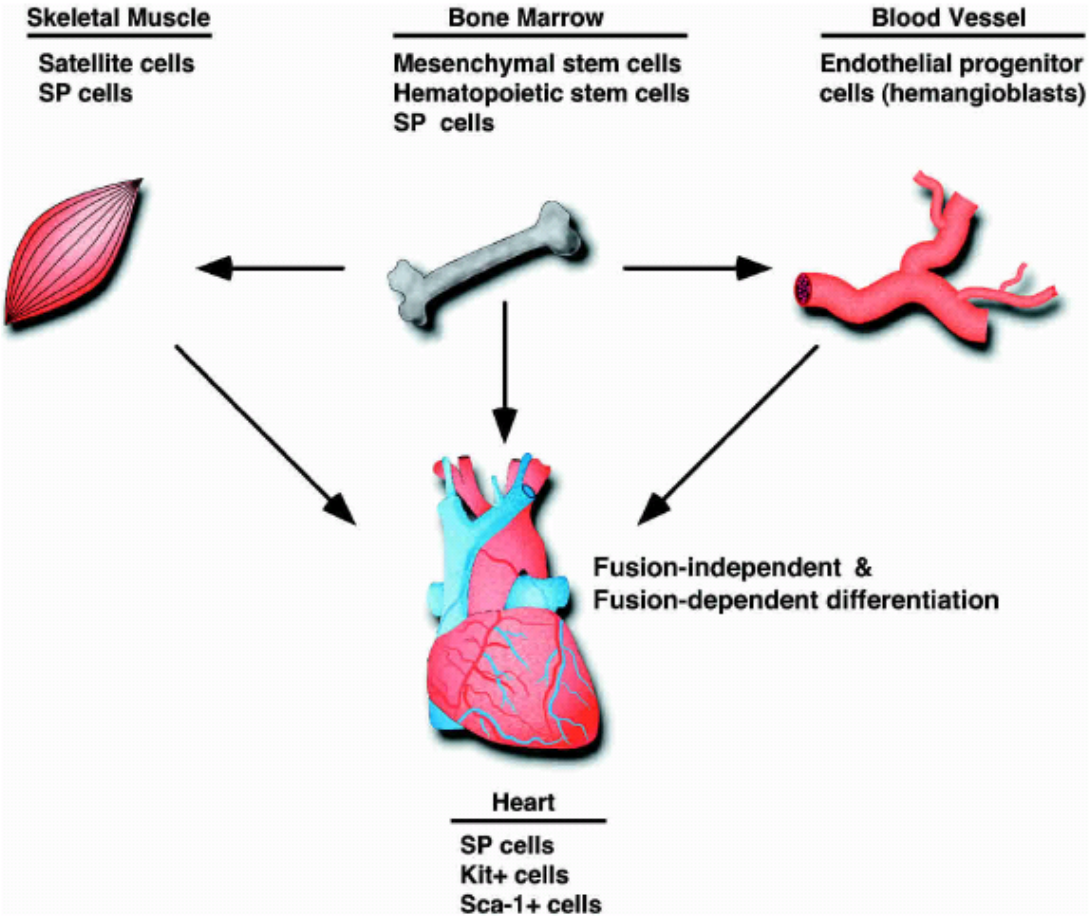

Figure 1.5 Stem cells from different tissues, including skeletal muscle, heart, bone marrow and blood vessels, could be of therapeutic value for the failing heart. See text for details. *Adapted from Olson & Schneider, G&D, 2003*

TRANSLATIONAL SCOPES OF THE THESIS

Scope 1

The paradigm of folic acid in the prevention of neural-tube defects provides hope for similar prevention of congenital heart disease[106]. Therefore, a precise understanding of the molecular mechanisms that govern cardiac development is imperative for deciphering the causes of congenital heart disease. The evolutionary conserved Notch signaling pathway has been linked to several forms of congenital heart disease, such as Alagille syndrome and aortic valve disease[107]. Intriguingly, the range of phenotypes observed in Notch mutant mouse models is much broader than those seen in patients with identified mutations in the Notch signaling pathway, suggesting that Notch pathway components are excellent candidate genes for involvement in a wide spectrum of congenital heart disease[107]. However, the cellular and molecular actions of Notch signaling remain largely obscure due to functional redundancy and early embryonic lethality that accompanies Notch pathway mouse mutants[107-109]. In the first chapter of the thesis, we investigate the role of Notch1 signaling specifically in cardiomyocytes -using Cre/loxP technology- in order to gain valuable insights regarding the involvement of Notch signaling pathway in the pathogenesis of congenital heart disease. In addition, based on the notion that recapitulation of embryonic signaling (essential for cardiogenesis) can promote cardiac repair, we examine the cardiac regenerative potential following Notch1 signaling re-activation.

Scope 2

Acquired heart disease comprises an epidemic more prevalent than all cancers combined[58]. Long-standing hypertension, myocardial infarction and cardiomyopathy are the most common causes of acquired heart disease that initially lead to compensated/pathological hypertrophy and progressively result in cardiac dilation and failure[57, 80]. Understanding the molecular mechanisms that govern the transition from normal to failing heart is highly desirable due to its enormous therapeutic value. It is becoming increasingly evident that survival pathways, such as gp130 and nuclear factor-κB (NF-κB) are implicated in this transition by regulating cardiomyocyte apoptosis[69-71, 110]. In the second chapter of the thesis, we evaluate the role of the canonical NF-κB pathway specifically in cardiomyocytes and its involvement in the transition to heart failure, following a conditional genetic approach.

CHAPTER 1

Notch-1 signaling activation in cardiac development and disease

1.1 BACKGROUND

1.1 Background

1.1.1 Cell Fate determination & Notch signaling

The formation of an organism relies on the generation of diverse cells types that provide the structural and functional units for tissue and organ formation. The gradual transition from one cell to a multicellular three dimensional organism is the result of coordinated gene transcription that directs the developmental fate of individual cells[111]. Adoption of different developmental cell fates creates a dynamic interplay of cell migration, growth, proliferation, differentiation and death[108]. Observations of the insect nervous system reveal two universal principles of cell fate determination: a) cells acquire their fate based on binary choices, and b) initially all cells in a given population can adopt a new fate, but only some maintain it stably, whereas others return to the initial (default) fate. The term *equivalence group* characterizes any cell population challenged with a binary choice and intrinsic or extrinsic events can influence gene expression of all the cells in an equivalence group[112]. However, only some cells will stably maintain the novel gene expression profile and attain a new cell fate by emitting inhibitory signals to their neighbor cells in order to return to their initial default state (fig.1.6, A). This developmental strategy is called lateral inhibition and has been acquired by organisms as a defense mechanism in order to maintain a reservoir of cells for each particular fate (in case anything goes wrong during the decision making process)[113].

Signaling through Notch receptors has been intimately associated with lateral inhibition and serves as a universal mechanism of cell fate determination in various cell types during development[111]. The gene encoding for Notch receptor was first discovered in *D. melanogaster* almost 90 years ago by Thomas Hunt Morgan and owes its name to the fact that partial loss of function of the gene (haploinsufficiency) results in notches at the wing margin (fig.1.6, C,D). *Notch*, which was cloned in the mid-1980's by the groups of Artavanis-Tsakonas and Young, encodes a receptor with a single transmembrane domain[114, 115]. Notch is an evolutionary conserved signaling pathway based on cell-to-cell interaction, and extensively studied in worms, flies and mammals[116]. It is nearly impossible to find a cell population which has not been exposed to Notch signals during development since Notch is implicated in cell fate determination events. Cells that adopt the new fate activate Notch receptors in surrounding cells in order to suppress them from acquiring the same fate [108] (fig.1.6, A). The involvement of Notch pathway in cell

fate determination becomes even broader with several studies demonstrating the requirement of Notch signals for induction of new cell fates after asymmetric cell division in boundary formation[108, 109] and vertebrate segmentation[117].

It is suggested that Notch signaling initially evolved for regulating segmentation or neural cell fate determination in common ancestors of the metazoan[118]. Later in the evolutionary axis, Notch signaling was co-opted for germ layer specification and gastrulation in *C.elegans*[119], zebrafish[120] and *Xenopus*[121]. However, the role of Notch in the evolution of mammals is distinctive in that it appears dispensable for early embryonic development[122-124].

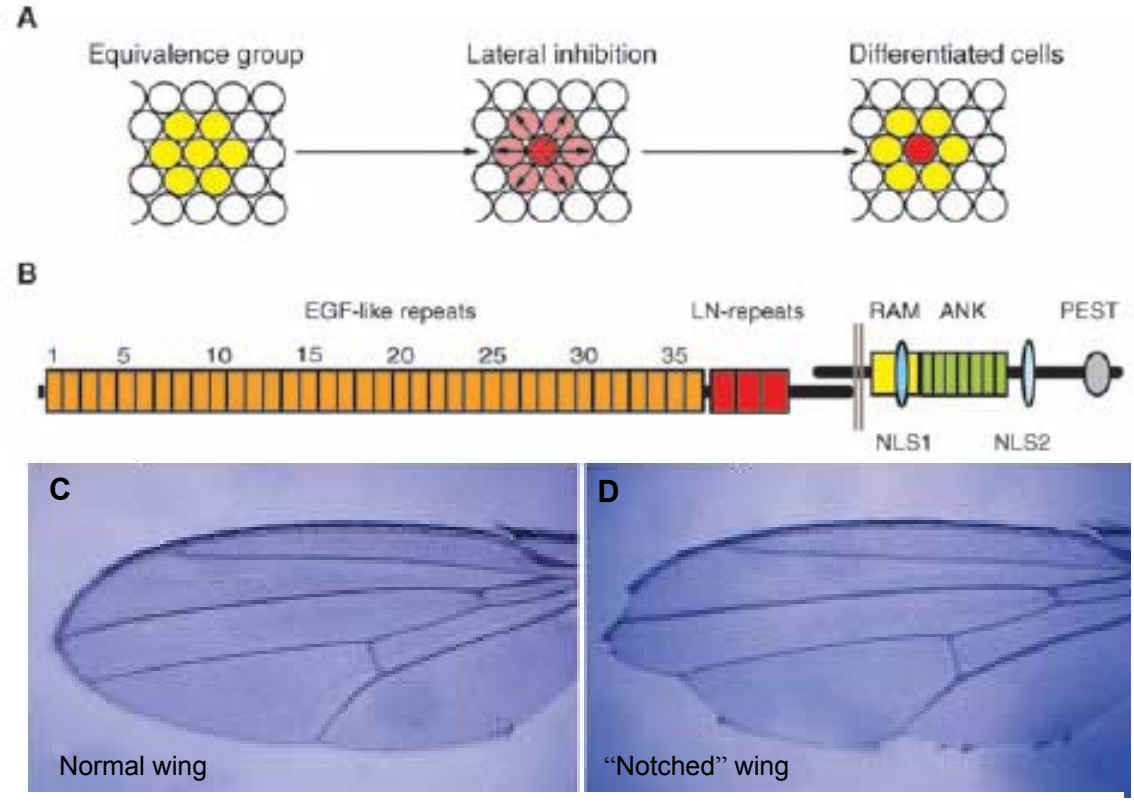

Figure 1.6 Lateral inhibition and structure of Notch receptor. A. All cells within an equivalence group express similar levels of Notch and Delta and are in a particular state (yellow cells). Stochastic (intrinsic or extrinsic) events induce a new state to some of these cells (light red) but the balance is shifted to one or some of these cells (dark red) which start producing increasing amount of Delta. Hence, Notch signaling is activated in the neighboring cells and that suppresses them from acquiring a new cell fate and return to the initial default state (yelow cells). **B**. Notch receptors are large single-pass (type I) transmembrane proteins with similar architecture. They are consisted of a long extracellular domain (NECD) and a smaller intracellular domain (NICD). The NECD is composed of up to 36 tandemly arranged epidermal growth factor (EGF)-like repeats followed by 3 similarly arranged calcium binding Lin12-Notch (LN) domains, which are a unique feature of the Notch receptor family. The NICD contains the recombination signal-binding protein for Jκ (RBP-Jκ) -associated molecule (RAM) region followed by 7 ankyrin repeats (ANK), 2 nuclear localization sequences (NLS), and a C-terminal Pro-Glu-Ser-Thr (PEST) degradation motif. **C.** Wing blade of a wild-type *Drosophila melanogaster*, and of a mutant with partial loss of the *Notch* gene **(D).** *A, B adapted by Ehebauer et al. Science, 2006. C, D adapted by Radtke & Raj, Nat Rev Cancer, 2003*

1.1.2 Notch signaling in mammals - core pathway

Below, the ubiquitous core components of Notch pathway are presented, although we should also take into consideration that tissue-specific Notch modifiers also exist, rendering Notch pathway a complex protein network rather than a linear signaling cascade.

Notch receptor family

The Notch receptor family in mammals consists of four members Notch1, 2, 3, and 4 of membrane-tethered transcription factors[116]. Notch receptors are large single-pass (type I) transmembrane proteins with similar architecture. They include a long extracellular domain (NECD) and a smaller intracellular domain (NICD). The NECD is composed of up to 36 tandemly arranged epidermal growth factor (EGF)-like repeats followed by 3 similarly arranged calcium binding Lin12-Notch (LN) domains, which are a unique feature of the Notch receptor family[114, 115]. The EGF-like repeats contain the receptor's ligand binding domain while the LN domains prevent ligand-independent signaling events[125, 126]. On the other hand, the NICD contains the recombination signal-binding protein for Jκ (RBP-Jκ) -associated molecule (RAM) region followed by 7 ankyrin repeats (ANK), 2 nuclear localization sequences (NLS), and a C-terminal Pro-Glu-Ser-Thr (PEST) degradation motif[127] (fig.1.6 B). Several lines of evidence demonstrate that the NICD relays signals from the cell-membrane to the nucleus[128, 129].

Delta/Serrate/Jagged family of Notch ligands

Notch ligands, such as Delta and Serrate proteins in *D. melanogaster* and the mammalian Jagged proteins are single-pass transmembrane proteins that share a very short intracellular domain[130]. The mammalian Notch ligand family consists of five members Delta-like 1/3/4, and Jagged1/2 proteins. Their extracellular domain contains several EGF-like motifs and an N-terminal DSL (Delta, Serrate, Lag2) domain (fig.1.7). Ubiquitination of Notch lignads by the E3 ubiquitin ligases Neuralized (Neur) and Mind bomb (Mib) is an essential step for ligand activation and internalization, which subsequently leads to Notch signaling activation[131-134]. Although little is known about ligand-to-receptor binding specificity, it has been suggested that certain EGF-like

repeats on the Notch receptor mediated the binding to Delta and Serrate ligands[125, 135, 136].

Unlike other signaling pathways which transmit signals from the cell membrane to the nucleus using protein cascades, upon ligand/receptor interaction the intracellular domain of Notch receptors is proteolytically cleaved by a multi-protein complex of proteases, referred to as **γ-secretase complex** (fig.1.7). Subsequently, the notch intracellular domain (NICD) is free for nuclear translocation and binds directly to downstream transcription factors of the C promoter binding factor/Suppressor of Hairless/Lag-1 (CSL) family. Upon NICD binding to the CSL family of transcription factors, transcriptional repressors are released from **Notch transcriptional machinery**, whereas transcriptional activators are recruited to regulate expression of **Notch target genes** (fig. 1.7).

γ-secretase complex

Although initially associated with Alzheimer's and problems in amyloid precursor protein (APP) processing[137, 138], genetic studies in C.elegans revealed the involvement of γ-secretase activity in Notch receptor processing[139, 140]. The γ-secretase complex owes its name to the enzyme that performs the proteolytic cut within an unusual site of the APP transmembrane domain. It is believed that the catalytic core of the γ-secretase complex is consisted of presenilin-1 and -2 in mammals (fig.1.7)[141, 142]. Presenilins are predominantly localized to the endoplasmic reticulum (ER) and Golgi compartments, as well as to the plasma membrane where they participate in receptor activation events[143, 144]. Although the proteolytic mechanism and the exact composition of γ-secretase complex remain poorly understood, nicastrin was recently identified as another component of the complex in flies and worms[145, 146]. Nicastrin is a type I membrane protein which associates with presenilins and is genetically required for Notch signaling activation[139, 147, 148]. More recently, studies in flies and worms identified two new components of the γ-secretase complex, the transmembrane Aph-1 and the small Pen-2 proteins[145, 149].

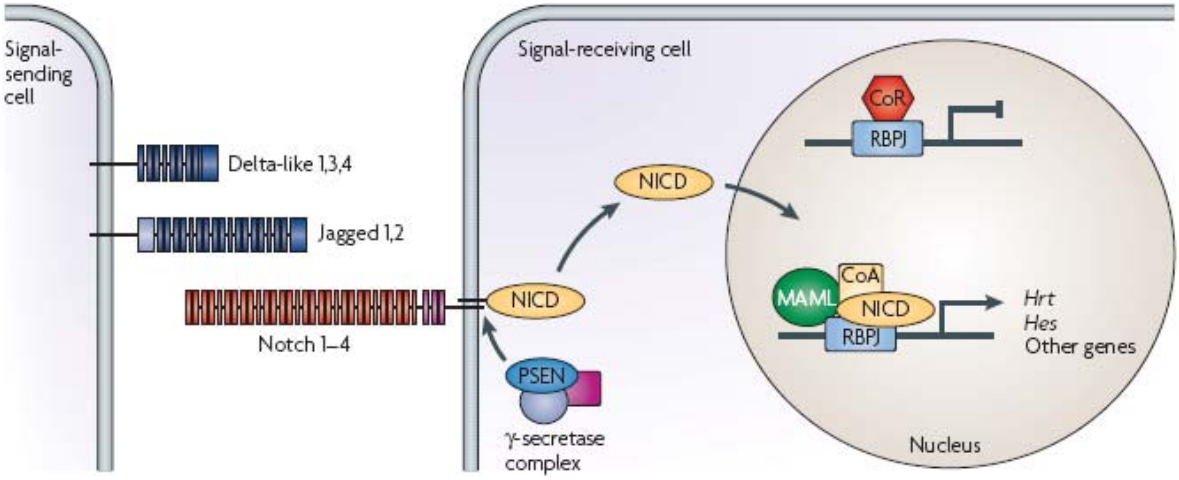

Figure 1.7. Notch signaling pathway in mammals
Four Notch receptors (Notch 1-4) and five ligands (Delta-like1, 3, 4, and Jagged 1,2) have been described in mammalian organisms. Notch signal transduction is achieved between neighboring cells since Notch receptors and ligands are single-pass membrane-tethered proteins. Upon ligand/receptor interaction, a multi-protein complex with γ-secretase proteolytic activity (presenilins -PSEN- are the catalytic components of the complex) cleaves the Notch receptor at the intramembrane S3 cleavage site and renders free the Notch intracellular domain (NICD). Once cleaved, the NICD translocates into the nucleus and forms a transcription-activating compex with recombination signal binding protein for immunoglobulin Jκ (RBP- Jκ). Conformational changes of the NICD-RBP- Jκ complex release transcriptional repressors (CoR) and recruit transcriptional activators (CoA) including Mastermilnd-like-1 (MAML-1) to the promoter of Notch target genes (see text for details). NICD nuclear translocation converts the transcriptional repressor RBP- Jκ to an activator. The most well-characterized Notch targets can be classified into two gene families, *Hes* and *Hey (Hrt),* with trancriptional repressor activity (see text for details). Seven *Hes (Hes1-7)* and three *Hey (Hey1, 2, L OR Hrt1, 2, 3) genes* have been described thus far, but many unidentified Notch target genes are likely to exist. *Adapted by High & Epstein, Nat Rev Genetics, 2007.*

Notch transcriptional machinery

The heart of Notch transcriptional machinery in mammals is a CSL family protein called recombination signal binding protein for immunoglobulin Jκ (RBP- Jκ) (fig.1.7). RBP- Jκ constitutively represses Notch target gene transcription by its direct binding to promoter sequences and recruiting of other transcriptional corepressors, such as SMRT (silencing mediator for retinoid and thyroid-hormone receptors)[150], CIR (CBF1 interacting corepressor)[151], SHARP (Class B Basic Helix Loop Helix Enhancer Of Split And Hairy Related)[152], and histone deacetylases (HDACs)[150]. However, upon NICD nuclear translocation, the aforementioned transcriptional repressors are displaced from RBP- Jκ and NICD binds directly to RBP- Jκ forming a transcription-activating complex[153-156]. Notably, the binding of NICD to RBP- Jκ causes conformational changes that lead to the

recruitment of the transcriptional coactivator Mastermind-1 in flies[157]. Mastermilnd-like-1 (MAML-1) gene has been also identified in mammals and plays a pivotal role in the activation of the NICD - RBP-Jκ complex by recruiting histone acetyltransferases (HATs)[157-160] (fig.1.7). Recent reports demonstrate that MAML couples transcriptional activation with Notch turnover since it promotes NICD phosphorylation and proteosome-dependent NICD degradation[161, 162]. It is also noteworthy that SKIP (skeletal muscle and kidney enriched inositol phosphatase) protein is also part of the transcription-activating complex although its function remains to be elucidated[162-164].

Notch target genes

The most well-characterized Notch targets can be classified into two gene families, *Hairy* and *Enhancer-of-split [E(spl)]* in *Drosophila* and their mammalian counterparts *Hes* and *Hey* gene families, respectively[165]. Seven *Hes (Hes1-7)*[166-169] and three *Hey (Hey1, 2, L)*[170-174] genes have been identified in the mouse genome. *Hes* and *Hey (Hrt)* gene families (fig.1.7) encode transcriptional basic helix-loop-helix regulators that act as repressors by binding to N (CACNAG) or E (CANNTG) box sequences of secondary Notch target gene promoters[173, 175, 176]. All members of the Hey gene family *(Hey1, 2, L or Hrt1, 2, 3)* are well conserved during evolution and can be induced by Notch[172, 175, 177]. In contrast to *Hey* genes, only *Hes1, Hes5* and *Hes7* can be induced by Notch[167, 178, 179], whereas Hes2, Hes3 and Hes6 appear to be Notch-independent[180, 181]. Moreover, several mammalian proteins, such as Helt, DEC1, and DEC2, display strong homology with Hairy and Enhancer-of-split [E(spl)] but evidence is missing regarding their possible Notch-dependent regulation[182].

Processing and trafficking regulate Notch receptor activity

Notch proteins are located at the plasma membrane in order to mediate ligand/receptor interactions and subsequent signal transduction to the nucleus[108]. However, a substantial amount of Notch is detected in the cytoplasm in compartments of the secretory pathway[109]. Notch is produced in the endoplasmic reticulum where it is fucosylated by the O-fucosyl transferase and later transported to the Golgi complex (fig.1.8)[183, 184]. Upon entering to the Golgi, the Notch single polypeptide is processed at S1 cleavage site by a Furin-like convertase but the two polypeptide fragments remain non-covalently associated through interactions between calcium (Ca^{2+}) and the LN Notch repeats[185]. Additionally, Notch can be glycosylated in the Golgi by the Fringe

glycosyl-transferase[186]. In vertebrates, this non-covalently associated glycosylated form is the commonest membrane-tethered form of the Notch receptor[186, 187]. The ligand binding promotes two additional proteolytic cleavages in the Notch receptor[109]. The ADAM-family of metalloproteases cleaves the receptor at the S2 extracellular cleavage site and leaves the rest of the receptor intact and membrane-tethered[163, 164, 178]. Subsequently – as discussed above – the γ-secretase complex mediates an intracellular proteolytic cleavage event at the S3 site of the receptor, generating the notch intracellular domain (NICD)[130]. However, in the absence of ligand/receptor interactions, Notch can be endocytosed from the cell membrane and either recycled or degraded[109]. Although the molecular mechanisms are not well understood, the Deltex ubiquitin ligase is associated with Notch recycling[188], whereas the Itch/NEDD4/Su(dx) ubiquitin ligase family targets Notch for degradation through the multi-vesicular body pathway (fig.1.8)[189].

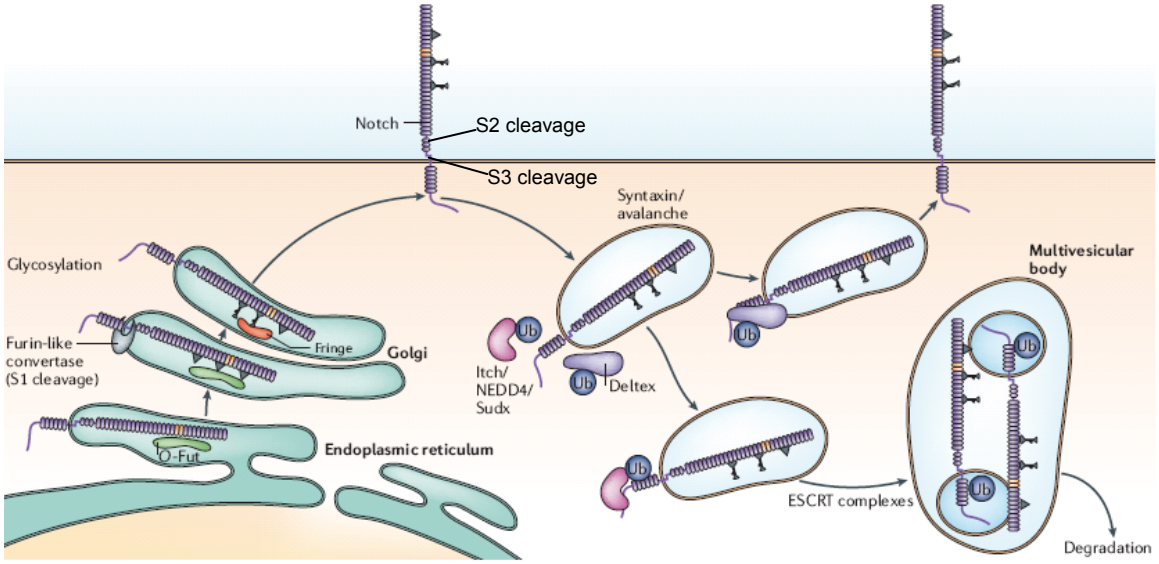

Figure 1.8 Processing and trafficking of Notch receptor. The Notch protein (purple) is produced in the endoplasmic reticulum and upon fucosylation by the O-fucosyl transferase (O-fut; green) it is transported to the Golgi complex. In the Golgi, Notch is processed by the Furin-like convertase (grey) at the S1 cleavage site and is further glycosylated by Fringe glycosyltransferase (red) before tranport to the plasma membrane. Once at the plasma membrane, Notch receptors can be activated by ligand binding, which induces further proteolytic events at S2 and S3 cleavage sites and subsequent Notch intracellular domain generation-NICD (see text for details). If ligand-mediated Notch receptor activation does not occur, Notch can be endocytosed and either recycled or degraded. Ubiquitin ligases, such as Deltex (purple), and other proteins (syntaxin) are possibly involved in Notch receptor recycling and transport to the plasma membrane. On the other hand, the family of Itch/NEDD4/Sudx ubiquitin ligases in association with ESCRT complexes mediates the Notch receptor degradation through the multivesicular-body pathway. *Adapted from S. Bray, Nat Rev Mol Cell Biol, 2006*

1.1.3 Notch signaling in the cardiovascular system

Expression pattern studies on several Notch pathway components in combination with the recent identification of numerous Notch mutations in several cardiovascular disorders in mice and humans highlight a pivotal role for Notch signaling in cardiovascular biology[107]. As described above, the cardiovascular system is the first organ system to be formed during embryogenesis undergoing simultaneous morphogenesis and differentiation events. During cardiac development, Notch signaling coordinates cardiomyocyte differentiation, valve development, and outflow tract remodeling[107]. The plethora of Notch-related events in heart development highlights the time- and cell type-dependent context of this signaling pathway[108].

1.1.3.1 Notch expression patterns

Notch signaling pathway components display dynamic expression patterns during cardiac development. Initially, Notch1, Notch4 and Delta-like 4 (Dll4) are expressed in the endocardium of the e8.0 murine heart[190-192]. At e12.5, Notch1 is also expressed at the outflow tract, the trabeculae, the epicardium and the aorta[193]. Although Notch2 expression has not been reported early (e8.0) in cardiac development following *in situ* hybridization approaches[194], Notch2 protein has been detected in the atrial and ventricular cardiomyocytes, the aorta, the coronary arteries and the pulmonary trunk at e13.5 and onwards by immunohistochemistry[47]. Similarly, Jagged1 protein is initially (e10.5) expressed in the atria and ventricles, and is also found later (e13.5) in the aorta, pulmonary trunk and coronary arteries[47, 195]. Although Notch3 is detected at the cardiac crescent during early cardiogenesis, its expression is only found in vascular smooth muscle cells of the heart at later developmental stages[190, 192]. Concerning Notch target genes, HRT1 (Hey1) has an endocardium-specific expression pattern at e8.5 in contrast to the myocardial ventricle specific HRT2 (Hey2) expression[191]. Remarkably, Hey2 maintains its ventricle specific expression pattern till adulthood, whereas Hey1 expression becomes atrium specific[196-199]. Moreover, HeyL expression pattern appears to coincide with Notch3 at the smooth muscle layer of the cardiac vessels[172, 182]. It is noteworthy that the dynamic *on-and-off* Notch expression in combination with different experimental approaches employed at narrow developmental windows confound

attempts for a *bona fide* classification of Notch expression patterns in the cardiovascular system.

1.1.3.2 Notch & cardiomyocyte differentiation

During early cardiogenesis, first heart field (FHF) derived cells differentiate into cardiomyocytes as the heart tube develops (fig.1.9)[22]. A growing body of *in vit*ro[200-202] and *vivo*[198, 203-206] studies propose Notch signaling as an inhibitor of early cardiomyocyte differentiation. For example, embryonic stem (ES) cells that lack Notch1 or RBP-Jκ show an increase in cardiomyogenesis following *in vitro* differentiation[200, 201]. On the contrary, forced Notch1 activation down-regulates cardiac differentiation marker expression in ES cells and indicates that Notch activation and cardiomyocyte differentiation are mutually exclusive events in early cardiogenesis[200, 202]. Moreover, *in vivo* gain-of-function approaches for Notch signaling demonstrate reduced number of differentiated cardiomyocytes during early cardiac development in *D. melanogaster*[204, 205] and *X.Laevis*[206]. In line with these findings, retroviral overexpression of constitutively active Notch intracellular domain (NICD) results in diminished expression of cardiomyocyte markers in the chick heart tube[203]. Similarly, overexpression of NICD1 in pre-cardiac mesoderm in mice leads to abnormal cardiac morphogenesis associated with abnormal cardiomyocyte maturation and sarcomeric structures[198].

Later in cardiogenesis, the myocardium differentiates into an outer compact zone and an inner trabeculated zone (fig.1.9 d) characterized by sheet-like outgrowths. Trabeculae formation is a result of signaling events between the primitive myocardium and the developing endocardium, which regulate cardiomyocyte proliferation and differentiation. Global *Notch1* and *RBP-Jκ* gene inactivation in mice results in defective trabeculation associated with decreased myocyte proliferation and trabecular marker expression[207]. Moreover, endothelial-specific inactivation of *Notch1* and *RBP-Jκ* phenocopies the *Notch1* and *RBP-Jκ* total knock-out defects and proves that endocardium-derived Notch signals control myocyte proliferation and differentiation[207]. Although these results do demonstrate an endocardial-specific requirement for Notch signaling in cardiomyocyte differentiation (ventricular maturation), the possibility that Notch functions in the developing or adult myocardium cannot be ruled out[107].

1.1.3.3 Notch & valve formation

Notch signaling is involved in boundary formation[108] (discussed in 1.1). During cardiogenesis, boundary formation between the primitive atrial and ventricular regions is required for the proper development of a four-chambered heart[107]. The boundary region in the developing heart is the atrioventricular (AV) canal (fig.1.9 b) and two recent in vivo studies suggest that the Notch target genes, *Hey1* and *Hey2*, control the boundary gene expression at the AV canal[208, 209]. Moreover, the AV canal and the outflow tract (OFT) are the cardiac regions where endocardial cushion formation takes place, a prerequisite for valve formation[21]. These cushions form the precursor structures of tricuspid and mitral valves at the AV canal and the precursors of aortic and pulmonary valves within the outflow tract (fig.1.9 c). Before cushion formation, the endocardium and the primitive myocardium are adjacent to each other and kept separated by extracellular matrix known as cardiac jelly[22]. At this stage, molecular cross-talk between endocardium and myocardium results in epithelial-to-mesenchymal transition (EMT)[210]. Endothelial cells from the endocardium migrate into the cardiac jelly and form cushions and, subsequently, valves[107, 210]. The first indication for the involvement of Notch signaling in EMT and valve formation comes from two *in vitro* studies where forced NICD overexpression in mammalian endothelial cells induces morphological changes that are consisten with EMT and upregulates the expression of mesenchymal markers[191, 211]. In addition, Notch1 and several Notch ligands are expressed in the endocardium at the time of cushion formation (discussed in 1.1.3.1). The requirement of Notch signaling for proper cushion/valve formation has been demonstrated in Notch-1 and RBP-Jκ mouse mutants where the endocardial cushions appear hypocellular and the endothelial cells fail to show morphological signs of EMT[191]. Moreover, the importance of Notch signaling in valve development was recently highlighted by the identification of human Notch1 mutations in hereditary forms of aortic valve disease (table 1.2), where Notch1 haploinsufficiency leads to structural valve abnormalities, such as bicuspid aortic valve[212, 213].

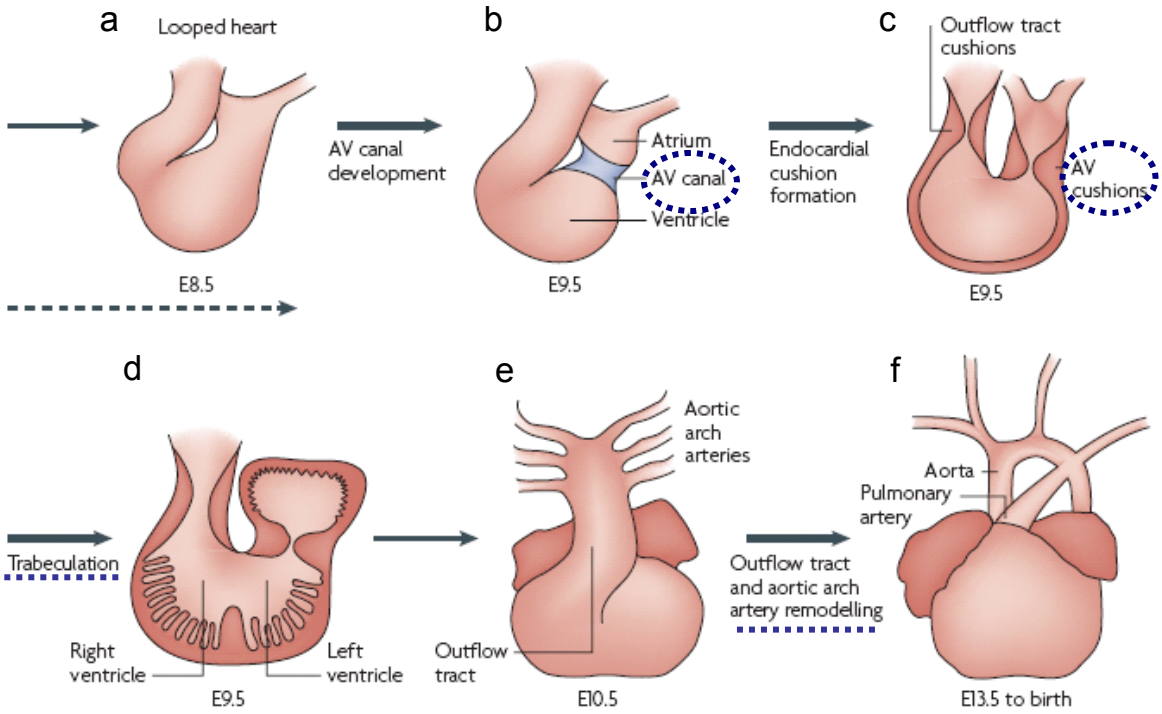

Figure 1.9 Notch signaling in cardiac development.
The stages of cardiac development from the looping of the primitive heart tube till outflow tract remodelling and formation of a four-chambered heart are depicted here (a-f) and have been discussed also in the 1.2 part of the introduction.
The involvement of Notch signaling in boundary formation at the atrio-ventricular (AV) canal region (b) and valve-cushion formation (c) has been discussed in 1.1.3.3 part of the introduction. Moreover, Notch is required for ventricular trabeculation (d) and outflow tract remodeling (f) and these processes have been also covered in 1.1.3.2 & 1.1.3.4 introductory parts, respectively. Blue dashed lines and circles highlight Notch involvement in the respective developmental processes. *Modified by High & Epstein, Nat Rev Genet, 2007.*

1.1.3.4 Notch & outflow tract remodeling

The cardiac outflow tract (OFT) is the arterial pole of the heart, where the right and left ventricles empty into the pulmonary artery and aorta, respectively (fig.1.9 e, f)[107]. OFT morphogenesis is a complex process that requires input from several cell types, including second heart field (SHF) precursors, cardiac neural crest and endothelial cells[22, 24]. The involvement of Notch signaling in OFT remodeling was first characterized in patients with Alagille syndrome, an autosomal dominant disorder that affects the heart, liver, kidneys, vertebrae and eyes[45]. Mutations in the genes encoding for Notch2[214] and Notch ligand Jagged 1[46] have been linked to Alagille syndrome (table 1.2), which is accompanied with OFT defects such as pulmonary artery stenosis and

Tatralogy of Fallot (right ventricular hypertrophy, overriding aorta, ventricular septal defect and pulmonary stenosis)[215, 216]. Similarly, combined haploinsufficiency of Jagged1 and Notch2 phenocopies Alagille syndrome in mice and strongly implicates this ligand-receptor pair in proper OFT development[47]. Moreover, *presenilin1* null mice further confirm the requirement of Notch signaling in OFT remodeling since these mice demonstrate ventricular septal defects, double-outlet right ventricle and pulmonary artery stenosis[217]. Recently, a landmark study associated Notch signaling events in cardiac neural crest (CNC) cells with OFT development using conditional mutagenesis[218]. Expression of a dominant negative form of the Notch transcriptional coactivator Mastermind-like1 (MAML1) under the control of a CNC-specific promoter in mice recapitulates many of the OFT defects observed in patients with Alagille syndrome and provides a model for CNC-autonomous Notch actions during OFT development[218].

Table 1.2. Human congenital cardiovascular disorders linked to Notch signaling pathway mutations. *Modified from High & Epstein, Nat Rev Genet, 2007.*

Gene name	Disease	Cardiovascular manifestations
JAG1	Alagille syndrome	Pulmonary artery stenosis, peripheral pulmonary artery stenosis, tetralogy of Fallot, ventricular septal defects, vascular anomalies
JAG1	Isolated congenital heart disease	Pulmonary artery stenosis, tetralogy of Fallot
NOTCH2	Alagille syndrome	Pulmonary artery stenosis, tetralogy of Fallot
NOTCH3	CADASIL	Cerebral arteriopathy resulting in stroke and dementia, granular deposits in vascular smooth muscle cells
NOTCH1	Aortic valve disease	Bicuspid aortic valve, aortic valve calcification
PSEN1, *PSEN2*	Dilated cardiomyopathy	Dilated cardiomyopathy, heart failure

CADASIL, cerebral autosomal dominant arteriopathy with subcortical infarcts and leukencephalopathy. *JAG*, jagged; *PSEN*, presenilin.

1.1.3.5 Notch signaling and vascular formation

During mammalian embryogenesis, development of the vascular system is one of the earliest events. *De novo* formation of the primitive blood vessel network occurs following differentiation of mesodermally-derived endothelial precursors (angioblasts) in a process termed vasculogenesis[175, 176]. This primary vascular network is then remodeled by the process of angiogenesis in order to generate both small and large vessels of the mature vascular system. Following vasculogenesis and angiogenesis, arteries and veins do not only differ in morphology and function but also in their gene expression profile[219]. Several Notch receptors and ligands, such as Dll4, have an artery-specific expression pattern, mainly in the endothelial cell layer, in zebrafish and

mouse[220-223]. Interestingly, Notch signaling mutations lead to loss of artery-specific markers whereas Notch ectopic activation results in repression of venous markers in zebrafish, establishing Notch as a key regulator of artery-vein identity[224]. Similarly, knock-down of *gridlock* gene in zebrafish (homologue to mammalian *Hey2*) suppresses the expression of arterial markers (such as ephrin-B2)[225]. In addition, several mouse mutants in Notch signaling (Notch1$^{-/-}$, Notch1$^{-/-}$/Noctch4$^{-/-}$, Mindbomb1$^{-/-}$, Delta-like4$^{-/-}$, RBP-Jκ$^{-/-}$, Hey1$^{-/-}$/Hey2$^{-/-}$) demonstrate defects in vascular remodeling and loss of arterial-marker expression[226-232].

In the adult, blood vessels acquire a quiescent state but retain considerable growth potential that can be activated by angiogenesis during wound healing or certain physiological processes[233]. Although angiogenesis is part of cancer pathogenesis and its blockage is highly desirable under these circumstances, controlled stimulation of angiogenesis might be beneficial in ischemic conditions[219]. The involvement of Notch signaling in postnatal arteriogenesis has been recently appreciated by functional studies focusing on the Notch ligand Dll-1[234, 235]. Dll-1 is mainly expressed in the arterial endothelium and its expression is strongly upregulated during ischemia-induced arteriogenesis[235]. Moreover, heterozygous *Dll-1*$^{+/-}$ mice, which survive till adulthood[236], fail to form collateral arteries and do not restore blood flow in a hindlimb ischemia model[235]. In addition, blood flow restoration in a hind limb ischemia model is also compromised in Notch1 heterozygous mice, demonstrating a critical role for Notch1 receptor in postnatal arteriogenesis[237].

The importance of Notch signaling in vascular development is underscored by the fact that Notch mutations are responsible for two congenital human conditions that affect the vasculature, the Alagille syndrome (discussed in 1.1.3.4) and cerebral autosomal dominant arteriopathy with subcortical infarcts and leukoencephalopathy (CADASIL). *Jagged1* and *Notch2* mutations have been identified in Alagile syndrome[46, 214], whereas *Notch3* mutations have been linked to CADASIL[238, 239] (table 1.2). CADASIL is a hereditary vascular degenerative disorder characterized by arteriopathy that affects mainly small arteries and leads to stroke and dementia[239]. Degeneration and loss of vascular smooth muscle cells (vSMC) is the main feature of CADASIL, which is attributed to impaired Notch3 function[240, 241]. In accordance with these observations, smooth muscle-specific overexpression of Notch3 containing a CADASIL mutation reproduces the disease symptoms, whereas Notch3$^{-/-}$ mice display dilated arteries

covered by a thin vSMC layer, suggesting a pivotal role for Notch3 receptor in vSMC differentiation and CADASIL pathogenesis[242, 243].

1.1.3.6 Notch target genes in cardiac development

The family of *Hey (Hey1, 2, 3)* basic helix-loop-helix transcriptional repressors has been well-documented as downstream target of Notch signaling *in vitro*[171, 173, 176]. Unlike *Hes* gene family[244, 245], *Hey* genes have been implicated in cardiovascular development[165]. All three members of this protein family show expression in the developing cardiovascular system, including the heart, endothelial cells and vascular smooth muscle[170, 172, 174, 246]. Hey2 knock-out mice have been generated by several research groups and demonstrate a wide range of cardiac defects accompanied with postnatal lethality[48, 49, 226, 227, 247-249]. These defects include ventricular enlargement and cardiomyopathy, atrial and ventricular septation defects, pulmonary artery stenosis, and atrio-ventricular valve dysfunction. Recently, conditional inactivation of *Hey2* gene specifically in cardiomyocytes recapitulated the cardiomyopathy observed in *Hey2* null mice and demonstrated a cardiomyocyte-autonomous requirement for Hey2[199]. In line with these findings, a cardiomyocyte-specific *Hey2* transgene is sufficient to rescue the cardiac defects in *Hey2* null mice. Interestingly, the wide spectrum of defects observed in *Hey2* mutants indicates that this gene is involved in multiple processes during cardiac development[107].

Whereas *Hey2* null mice display severe cardiac defects, *Hey1* and *Hey3* null mice are viable without presenting any cardiovascular abnormalities[196, 197, 226, 227, 250]. However, *Hey1/Hey2* double mutants display early embryonic lethality (e11.5) due to major vascular and cardiac defects, which is a more severe phenotype when compared to *Hey2* null mice and suggests possible functional redundancy between *Hey1* and *Hey2* during development[197, 250]. Moreover, the cardiac defects observed in *Hey1/Hey2* double mutants are reminiscent of the defects seen in *Notch1* and *RBP-Jκ* mutant embryos (abnormal cardiac looping, hypocellular endocardial cushions, and thin trabeculae layer)[197]. Interestingly, *Hey1/Hey3* double mutants have ventricular septation defects and atrio-ventricular valve dysplasia, indicating also possible redundancy for *Hey1* and *Hey3* during cardiac development[250]. The valve dysplasia and the hypocellular endocardial cushions observed in *Hey1/Hey2, Hey2* and *Hey1/Hey3* mutants are reminiscent of

impaired EMT and valve formation in *Notch1* and *RBP-Jκ* mutants, suggesting that *Hey* genes function downstream of Notch in this process[191].

Although little is known about the transcriptional regulation of *Hey* genes, it is not clear whether they act solely downstream of Notch *in vivo*[198, 208, 209]. Several groups have reported Notch-independent *Hey2* expression in the heart, while others propose signaling pathways, such as bone morphogenetic proteins (BMPs), as regulators of previously-thought Notch target gene transcription[251, 252]. Moreover, it seems unlikely that all Notch activity in the heart is only Hey-dependent[107]. In accordance with this notion, Ephrin B2 (EphB2) in the endocardium[207] and α-smooth muscle actin (α-SMA) in the vasculature[253] have been described as direct Notch targets. Notably, the battery of cardiac Notch target genes is likely to be enriched in the coming years since cross-talk between Notch and other signaling pathways (BMPs, Ras, and Wnt) essential for cardiac development exists[198, 254].

Table 1.3 Notch mutant mouse models. *Modified by High & Epstein, Nat Rev Genet, 2007.*

Mutation(s)	Stage of lethality	Cardiac phenotypes	Vascular phenotypes	Other significant phenotypes
NOTCH1$^{-/-}$	E9.5 to E10.5	Hypocellular endocardial cushions, impaired ventricular trabeculation	Yolk sac and embryonic vascular defects	Neural and somite defects
NOTCH2$^{-/-}$	E10.5 to E11.5	NR	NR	Widespread cell death
NOTCH2$^{del1/del1}$ (homozygous for a hypomorphic allele of *NOTCH2* with a deletion in the EGF repeat domain)	E11.5 to birth	Pericardial effusion, thinned myocardium	Haemorrhage, oedema	Kidney and eye defects
NOTCH3$^{-/-}$	Viable	NR	Defective maturation of arterial vascular smooth muscle cells	NR
NOTCH4$^{-/-}$	Viable	NR	NR	NR
NOTCH1$^{-/-}$, *NOTCH4*$^{-/-}$	E9.5	NR	Yolk sac, placental and embryonic vascular defects (more severe than *NOTCH1*$^{-/-}$)	Neural and somite defects
DLL1$^{-/-}$	<E12	NR	Haemorrhage	Neural and somite defects
DLL3$^{-/-}$	Postnatal	NR	NR	Somite and skeletal defects
DLL4$^{+/-}$	Variable (E9.5 to adulthood)	NR	Yolk sac and embryonic vascular defects, narrow aortae, AV malformations	NR
DLL4$^{-/-}$	E9.5	NR	Yolk sac and embryonic vascular defects, narrow aortae, AV malformations (more severe than *DLL4* heterozygotes)	NR
JAG1$^{-/-}$	E10.5	Pericardial oedema	Yolk sac vascular defects, abnormal head vessels, haemorrhage	NR
JAG1$^{+/-}$, *NOTCH2*$^{+/del1}$	Postnatal to adulthood	Pulmonary artery stenosis, ventricular septal defects, atrial septal defects	NR	Bile duct defects, jaundice, kidney defects, eye defects
JAG2$^{-/-}$	Perinatal	NR	NR	Limb, craniofacial and thymic defects
RBPJ$^{-/-}$	E9.5 to E10.5	Heart looping defect, hypocellular endocardial cushions, impaired ventricular trabeculation	Yolk sac vascular defects, narrow aortae, arterial–venous malformations	Neural and somite defects
PSEN1$^{-/-}$	Perinatal	Ventricular septal defects, double outlet right ventricle, pulmonary artery stenosis	NR	Neural and skeletal defects
PSEN1$^{-/-}$, *PSEN2*$^{-/-}$	E8.5 to E9.5	NR	Yolk sac vascular defects	Neural and somite defects
HRT1$^{-/-}$	Viable	NR	NR	NR
HRT2$^{-/-}$	Postnatal	Cardiomyopathy, ventricular septal defects, atrial septal defects, pulmonary artery stenosis, tetralogy of Fallot, tricuspid valve atresia, AV valve dysfunction	NR	NR
HRT1$^{-/-}$, *HRT2*$^{-/-}$	E11.5	Heart looping defects, impaired ventricular trabeculation, hypocellular endocardial cushions	Yolk sac, placental and embryonic vascular defects, haemorrhage	NR
HRT3$^{-/-}$	Viable	NR	NR	NR
HRT1$^{-/-}$, *HRT3*$^{-/-}$	Postnatal	Ventricular septal defects, AV valve defects	NR	NR

AV, atrioventricular; *DLL*, delta-like; EGF, epidermal growth factor; *HRT*, Hes-related transcription factor; *JAG*, jagged; NR, not reported; RBPJ, recombinat binding protein for immunoglobulin I-kappa region.

1.1.4 Notch signaling & tissue regeneration

Although there is little common agreement regarding cardiac progenitor cell markers[86, 87, 98, 255], identification of signaling pathways that govern the generation, maintenance, and differentiation of CPCs is highly desirable for its therapeutic value[21, 81, 107]. Notch signaling regulates multiple stem-cell populations, including hematopoietic, neural, skin, and intestinal stem cells[256]. In addition, Notch regulates the maintenance, activation and subsequent differentiation of the stem-cell-like population in skeletal muscle, referred to as satellite cells. Notably, Notch promotes skeletal muscle regeneration upon injury by maintaining the "stem-like" state and inhibiting skeletal muscle differentiation[257-259]. Interestingly, studies on several model organisms suggest that Notch signaling inhibits also cardiomyocyte differentiation (discussed in 1.1.3.2). Taking into account the parallels between skeletal and cardiac muscle development, it is intriguing to study the involvement of Notch signaling in myocardial injury.

Several studies across species associate Notch with tissue regeneration. Zebrafish is an organism with remarkable capacity of cardiac regeneration following injury[260]. When the apex of the zebrafish heart is amputated, cardiomyocytes re-enter the cell cycle and restore completely the loss of myocardial tissue[260]. It has been recently demonstrated that the ligand DeltaC and the receptor Notch1B are upregulated in the normal myocardium immediately following injury, suggesting that transient activation of Notch signaling pathway (although excluded from the regenerating region) precedes zebrafish heart regeneration[261]. In addition, *Xenopus* tail regeneration[262] and medaka fin regeneration[263] studies further demonstrate the requirement for Notch signaling in tissue regeneration.

It is also noteworthy that the cross-talk between Notch and the hypoxia pathway could provide valuable insights in the pathogenesis of cardiac ischemic disease[81]. The hypoxia pathway plays a key role in developmental organogenesis and tumor growth by inducing angiogenesis[264] and the hypoxia inducible factor 1α (HIF-1α) has been found up-regulated in patients with acute myocardial ischemia[265]. In addition, Notch signaling is activated in several models of *in vitro*[266] and *in vivo*[267, 268] hypoxia. Moreover, it has been demonstrated that hypoxia inhibits the differentiation of satelite cells and neural stem cells in a Notch-dependent fashion (stabilization of NICD by physical interaction with HIF-1α)[266]. Intriguingly, the beneficial outcome of Notch signaling activation in a model of cerebral ischemia has been recently demonstrated in mice[267], opening exciting avenues for the investigation of Notch signaling re-employment in cardiac ischemic disease.

1.2 RESULTS

Notch-1 signaling activation results in abnormal cardiac morphogenesis

1.2 RESULTS

1.2.1 Rationale

Recent studies establish Notch signaling as a fundamental pathway in cardiovascular development since *null* mice for Notch-1, Notch-2, Notch-4, Delta-like-1, Delta-like-4, Jagged-1 and Hey2 result in severe cardiac (myocardial hypoplasia, septation defects, and valve defects) and vascular defects leading to early embryonic lethality (table 1.3, INTRODUCTION). Cardiac and vascular formations are interlinked developmental processes that occur simultaneously during murine development and are completed after birth[22, 269]. As reviewed above, Notch-related proteins are expressed in both cardiac and vascular cell populations. To date, carious genetic approaches have increased our appreciation for the requirement of Notch signaling in cardiovascular development, however when Notch genes are globally mutated it is difficult to distinguish between primary and secondary events responsible for the resulting phenotypes. Thus, fundamental questions regarding molecular and cellular Notch actions remain to be answered.

Two recent reports [207, 218] highlight the involvement of Notch signaling in proper cardiac development since conditional inactivation of the Notch pathway in endothelial and cardiac neural crest cells results in ventricular maturation and outflow tract defects, respectively. However, forced activation of Notch-1 signaling at the entire cardiac lineage (myocardium, endocardium and endothelial cells) results in early embryonic lethality and provides limited evidence for the role of Notch-1 in cardiomyocytes[198]. In our approach, we bypassed embryonic lethality by genetically manipulating Notch-1 signaling specifically in cardiomyocytes. The *α-myosin heavy chain-Cre* (*α*-MyHC/Cre) transgenic mouse line, which drives Cre recombinase expression after embryonic day 8 (e8) and peaks after birth, was crossed with a conditional transgenic mouse line (CAG/CAT;NICD1) that upon Cre excision overexpresses the Notch-1 receptor intracellular domain (NICD1) in cardiomyocytes. Below, we present Notch-1 expression studies in the heart and a careful characterization of the αMyHC/Cre: CAG/CAT;NICD1 bisgenic mouse, hereafter referred to as NICD1:TG for simplicity.

1.2.2 Notch-1 is expressed in cardiomyocytes

Literature discrepancies regarding techniques and narrow developmental time windows chosen to study Notch expression in previous reports led us to carry out immunohistochemical analysis for Notch-1 receptor in the cardiac muscle (discussed also in 1.1.3.1 part of introduction, chapter 1). Expression of Notch-1 receptor (and not Notch-2) has been also reported at the endothelial cells (arrowheads, fig.1.10 d, f) of the vessels[175]. DAB staining revealed Notch-1 positive cells in the heart of mouse embryos at embryonic day 13.5 (fig.1.10 a-b) as well as in the adult ventricular (fig.1.10 d) and atrial (fig.1.10 e) myocardium. Staining for Notch-2 receptor (fig.1.10 f - g) was performed as a control since expression of this receptor in cardiomyocytes is well-documented[47].

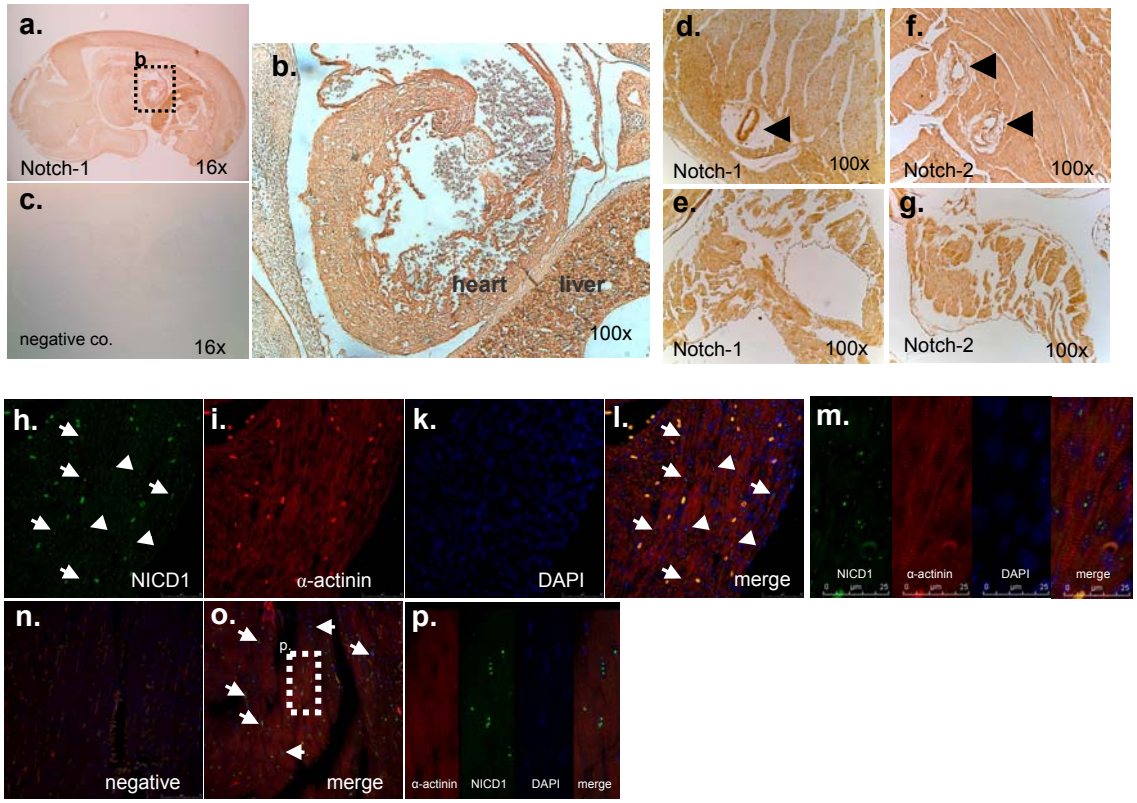

Figure 1.10 Expression pattern of Notch-1 and Notch-2 receptors in the heart. Immunohistochemistry (DAB staining) for Notch-1 (full molecule) reveals positive cells in the murine heart and liver at embryonic day 13.5 (e13.5) [**a;** 16x, **b**; 100x]. In the adult heart, Notch-1 positive cells are present in the endothelial cells of the vessels (arrowhead in **d**), the ventricular **(d)** and the atrial **(e)** cardiomyocytes. DAB staining demonstrates Notch-2 (full molecule) cardiomyocyte expression in the ventricles **(f)** and the atria **(g)** of the adult heart. Confocal double staining for the cleaved form of Notch-1 (NICD1) receptor **(h, l)** and the cardiomyocyte marker α-actinin **(i, l)** confirms the presence of NICD1 in the nuclei of neonatal **(h - m)** and adult **(o)** cardiomyocytes. DAPI was used for nuclear visualization **(k)** and high resolution images **(m, p)** images prove expression of NICD1 in neonatal **(m)** and adult **(p)** cardiomyocytes.

In order to prove that cardiomyocytes express Notch-1, we performed double staining for the cardiomyocyte marker α-actinin and the Notch-1 intracellular domain (NICD1). We demonstrate that NICD1 activity is found in the nuclei of neonatal (fig. 1.10,h-m) and adult cardiomyocytes (fig.1.10 o-p).

1.2.3 Genetic approach for cardiomyocyte-specific Notch1-mediated signaling activation

Having demonstrated that Notch-1 activity is present in neonatal (p1) cardiomyocytes, we took advantage of the Cre/loxP technology by crossing *α*-MyHC/Cre transgenic mice with CAG/CAT;NICD1 transgenic mice. As mentioned previously, the *α*-MyHC gene promoter is activated at embryonic day 8 (e8.5) and its activity peaks after birth (p1). The CAG/CAT;NICD1 transgenic mice carry the floxed chloramphenicol acetyl transferase (CAT) cassette and the Notch-1 intracellular domain (NICD1) under the control of the chicken β-actin gene promoter (CAG, ubiquitous promoter). Our genetic strategy allowed the cardiomyocyte-specific over-expression of Notch-1 intracellular domain (NICD1) in double transgenic mice (NICD1:TG) after Cre mediated excision of the CAT cassette (fig.1.11 a, b). To confirm that Cre recombinase activity was present at the time of birth (p1), we assessed the mRNA levels of *Notch-1* and several well-studied Notch target genes (*Hes-1, Hey-1, and Hey-2*) by quantitative TaqMan PCR (fig.1.11 c) Statistically significant differences for *Hes-1, Hey-1 and Hey-2* genes revealed that Notch-1 mediated signaling was activated in the neonatal (p1) heart of NICD1:TG mice. Moreover, the up-regulation of *Notch-1* gene expression was also confirmed by Western blot (fig.1.11 d)

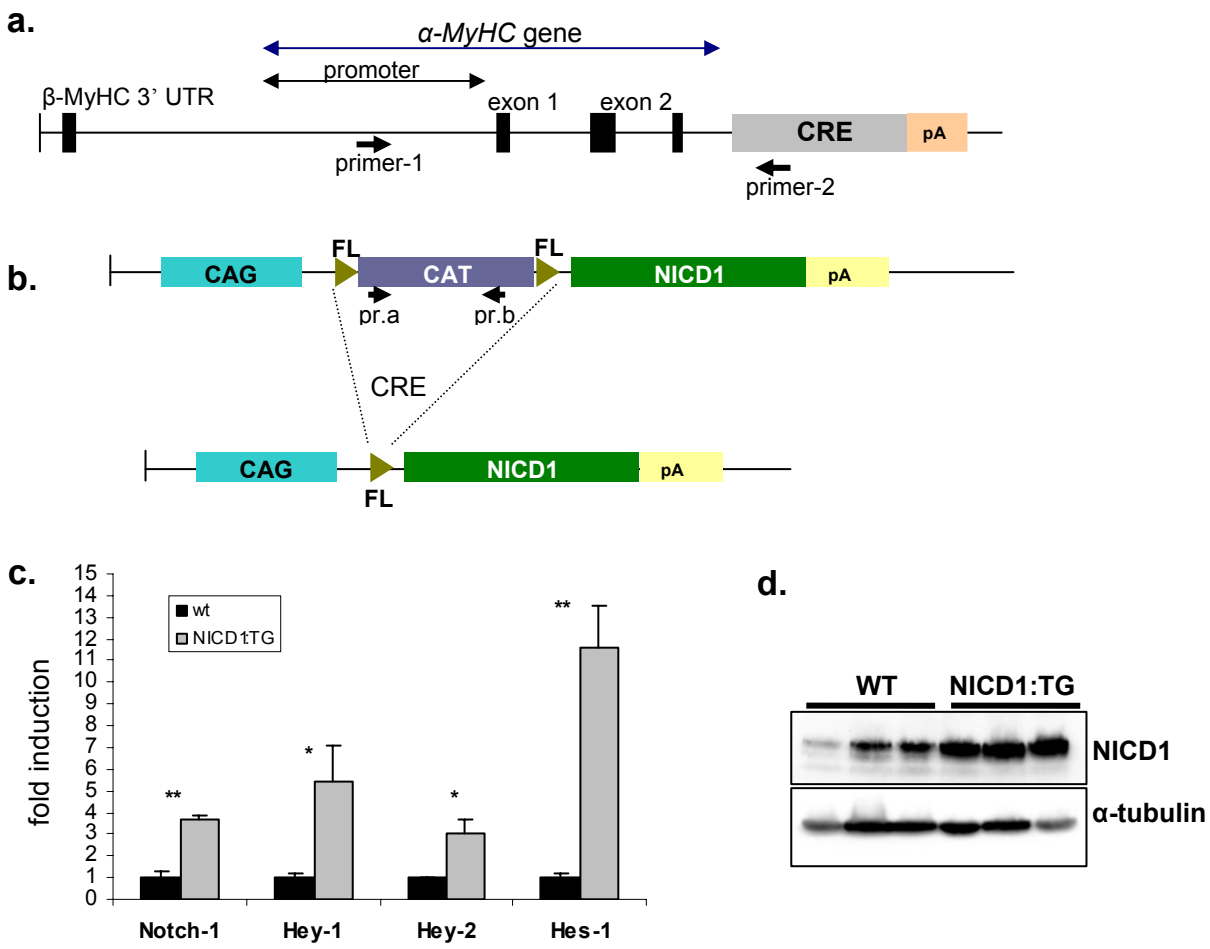

Figure 1.11 Genetic strategy for over-expression of Notch IntraCellular Domain-1 (NICD-1) in cardiomyocytes.

a). Construct structure of α-MyHC/Cre transgenic line; the regulatory region upstream of Cre recombinase consists of the 3'UTR of *β-Myosin heavy chain (β-MyHC) gene,* the entire promoter sequence and the first three exons of *α-myosin heavy chain (α-MyHC)* gene. Two primers (primer-1, primer-2) that bind to the α-MyHC gene promoter and the *Cre* recombinase gene, respectively, are used for genotyping the α-MyHC/Cre line and the expected PCR product is ~1kb. **b).** Construct structure of CAG/CAT-NICD1 transgenic line. The ubiquitous chicken β-actin gene (CAG) promoter has been placed upstream of the floxed (FL) chloramphenicol acetyl transferase (CAT) gene. The Notch IntraCellular Domain-1 (NICD-1) is located after the CAT gene and NICD-1 is over-expressed in the cardiomyocytes upon α-MyHC/Cre recombinase activation. The binding sites for primer a (pr.a) and primer-b (pr.b) -used for genotyping- are indicated. The Poly-A (pA) tail has been used in both transgenic constructs for enhancement of mRNA stability **c).** Quantitative TaqMan RT PCR reveals up-regulation of the mRNA levels of *Notch-1, Hairy enhancer of split-1 (Hes-1), Hes-related-1 (Hey-1) and Hes-related-2 (Hey-2)* genes in the neonatal (p1) heart of NICD1:TG mice. Taqman *glyceraldehyde 3-phosphate dehydrogenase (GAPDH)* probe was used for normalization. (t-test, * $p<0.05$, ** $p<0.01$, *** $p<0.001$). **d).** Notch-1 IntraCellular Domain (NICD1) is up-regulated in the neonatal (p1) heart of NICD1:TG mice at the protein level. Alpha-tubulin was used for normalization and samples were loaded in triplicates.

1.2. 4 NICD1:TG mice display perinatal lethality

NICD1:TG mice were born very close to mendelian ratio (20% instead of 25%, table 1.4) but die perinatally since only ~5% of them reached the weaning stage (table 1.5). Monitoring of the perinatal lethality demonstrated that the majority of the NICD1:TG mice (75%) died within the first 10 days of life while only 20% of them reached adulthood and eventually premature death at ~3 - 4 months of age (table 1.6).

Table 1.4 Statistics at birth					
F0	*age : P1*	αMyHC/CRE x CAG/CAT:Notch1			
F1	***total number of pups***	**αMyHC/CRE; (+/+)**	**(+/+): CAG/CAT;Notch1**	**(+/+); (+/+)**	**NICD1:TG**
	140	46	34	32	28
	%	32.86	24.29	22.86	20.00
	Mendelian %	25.00	25.00	25.00	25.00

Table 1.5 Statistics at the weaning stage					
F0	*age : weaning*	αMyHC/CRE x CAG/CAT:Notch1			
F1	***total number of mice***	**αMyHC/CRE; (+/+)**	**(+/+); CAG/CAT:Notch1**	**(+/+); (+/+)**	**NICD1:TG**
	117	40	39	32	6
	%	34.19	33.33	27.35	5.13
	Mendelian %	25.00	25.00	25.00	25.00

Table 1.6 Mortality rates over development				
total number of NICD1:TG mice	**p1 - p5**	**p6 - p10**	**p11- p20**	**p20….**
20	12	3	1	4
%	60.00	15.00	5.00	20.00

1.2. 5 Abnormal cardiac morphogenesis and impaired function in NICD1:TG mice

In order to decipher the cause of perinatal lethality (75% of NICD1:TG mice) or premature death at 3-4 months (20% of NICD1:TG mice), the cardiac morphology was examined at various developmental stages. At the whole mount level (fig.1.12 a), the NICD1:TG hearts appeared bigger when compared with WT littermates. A readily

enlarged right atrium (RA) was noticed at all developmental stages examined. In addition, trichrome staining on longitudinal sections revealed thick myocardial walls (fig.1.12 b), a finding suggestive of cardiomyocyte hyperplasia or hypertrophy. Heart to body weight measurements further confirmed the differences in heart size (fig.1.12 c,d), and cardiac function assessment by echocardiography at 1.5 months of age revealed significantly impaired fractional shortening in NICD1:TG hearts.

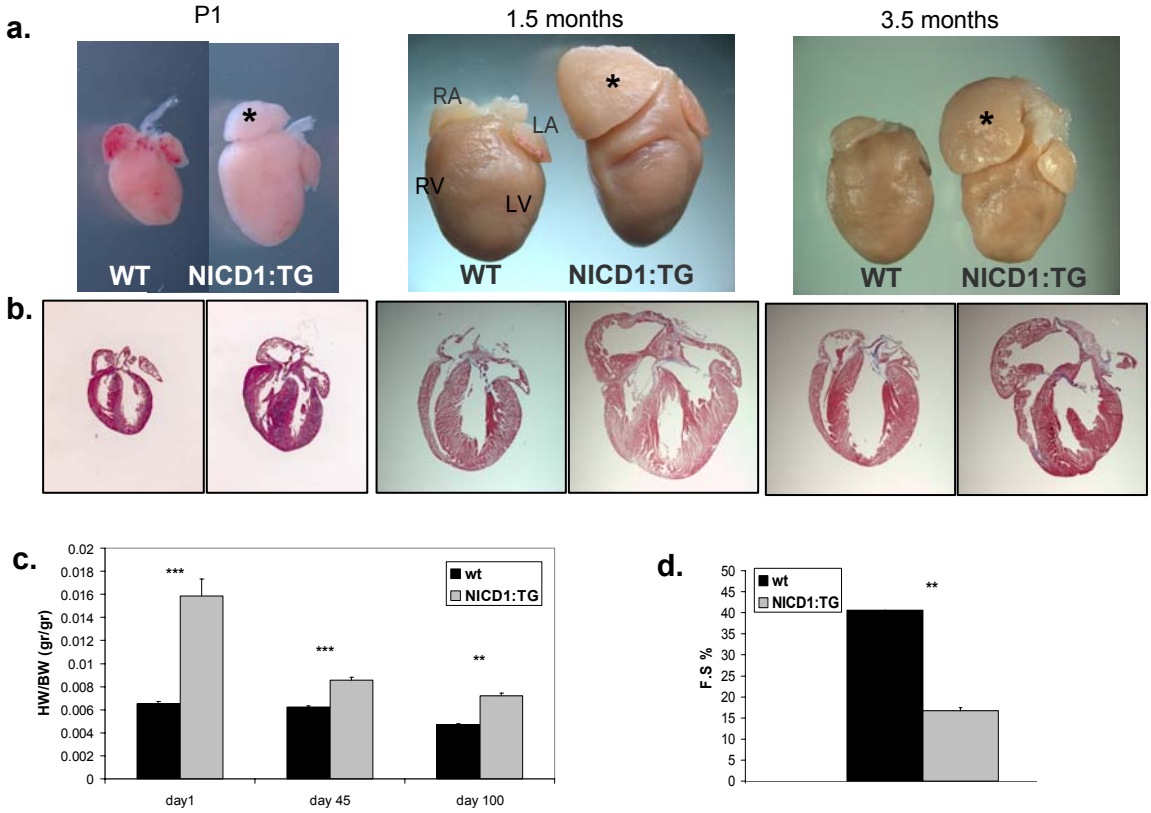

Figure 1.12 Impaired cardiac morphogenesis and function in NICD1:TG mice. Comparative whole mount analysis **(a)** as well as histological analysis (**b,** trichrome staining) on cardiac longitudinal sections reveals gross abnormalities in the heart of NICD1:TG animals over development (p1, 1.5months, 3.5months). At the whole mount level, the NICD1:TG hearts appear bigger in size with a readily enlarged right atrium (RA). At the histological level, the myocardium of the NICD1:TG animals is thicker when compared with WT littermates. Heart-to-body weight ratio over development **(c)** and assessment of the cardiac function by echocardiography (fractional shortening) at 1.5 months of age verify the establishment of a pathological cardiac phenotype. (t-test, * $p<0.05$, ** $p<0.01$, *** $p<0.001$).

Thorough examination of the neonatal hearts at the histological level revealed a variety of defects, explaining the perinatal lethality of the NICD1:TG mice. First, the myocardial walls were thicker and the septation between the right and the left ventricle

was incomplete (fig.1.13 a - b, e - f), a phenomenon known as ventricular septation defect (VSD)[21, 22]. Second, the tricuspid valve (between right atrium and right ventrile) appeared hyperplastic in the neonatal heart of NICD1:TG mice (arrows in fig.1.13 c, g). Finally, detailed analysis of serial sections showed that the atrial septation was also impaired in NICD1:TG hearts (fig.1.13 d, h), a condition known as atrial septation defect (ASD)[21, 22].

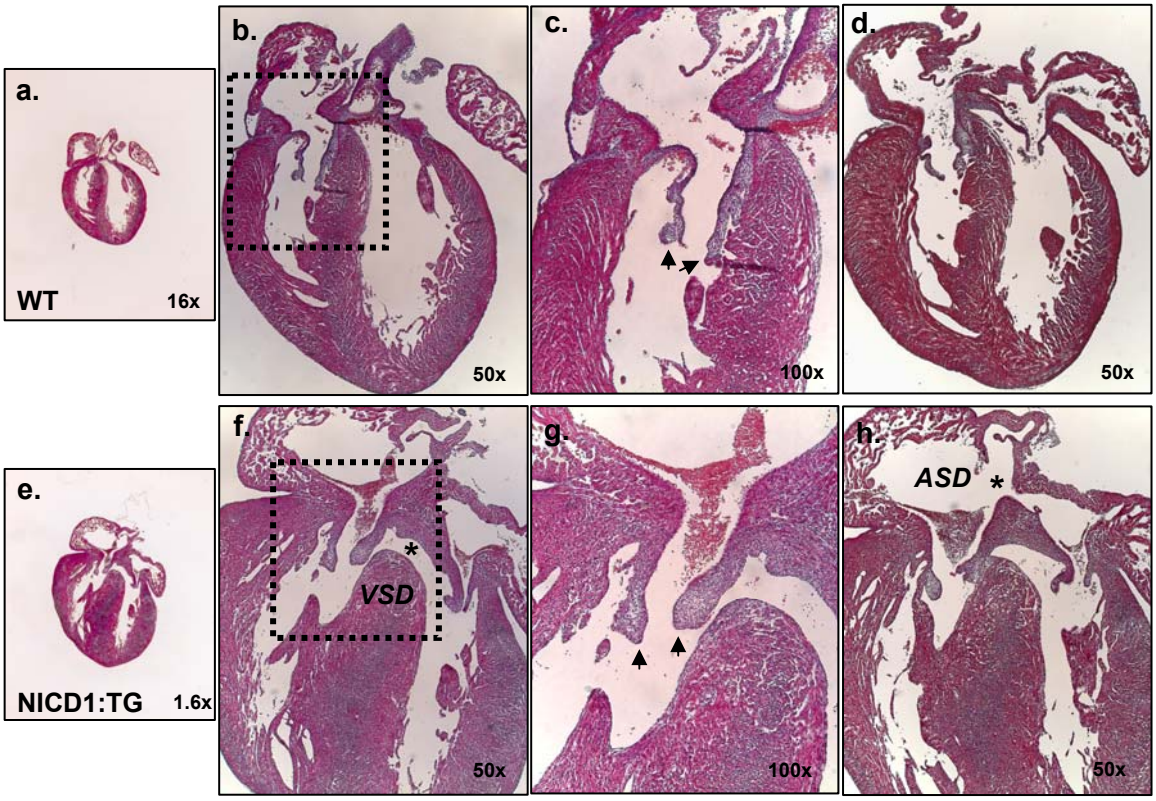

Figure 1.13 Septation defects and hyperplastic tricuspid valves in neonatal (p1) NICD1:TG hearts. a). The NICD1:TG hearts display Ventricular Septal Defect (VSD) [(**a, b ,e ,f**)] indicated by an asterisk (*). In addition, the tricuspid valve appears hyperplastic in NICD1:TG (**c, g**) indicated by arrows. Different planes (**d, h**) of the same WT (**a**) and NICD1:TG (**e**) hearts demonstrate also Atrial Septation Defect (ASD), which is also indicated by an asterisk (*).

The aforementioned findings provide evidence to explain the perinatal lethality that occured in the majority (75%) of the NICD1:TG mice, but it was still not clear why 25% of these mice survived until adulthood. Since combined ASD and VSD is inconsistent with life, histological analysis was performed on NICD1:TG hearts at postnatal day 10 (p10), 1.5 months and 3.5 months after birth. Although we were unable to detect VSD and

hyperplastic tricuspid valve at these stages, the NICD1:TG demonstrated consistently ASD at p10, 1.5months and 3.5month of age (fig.1.14). In conclusion, it appears that the ASD leads to premature death (3 - 4months of age) and impaired cardiac function in the 25% of the NICD1:TG that survive till adulthood.

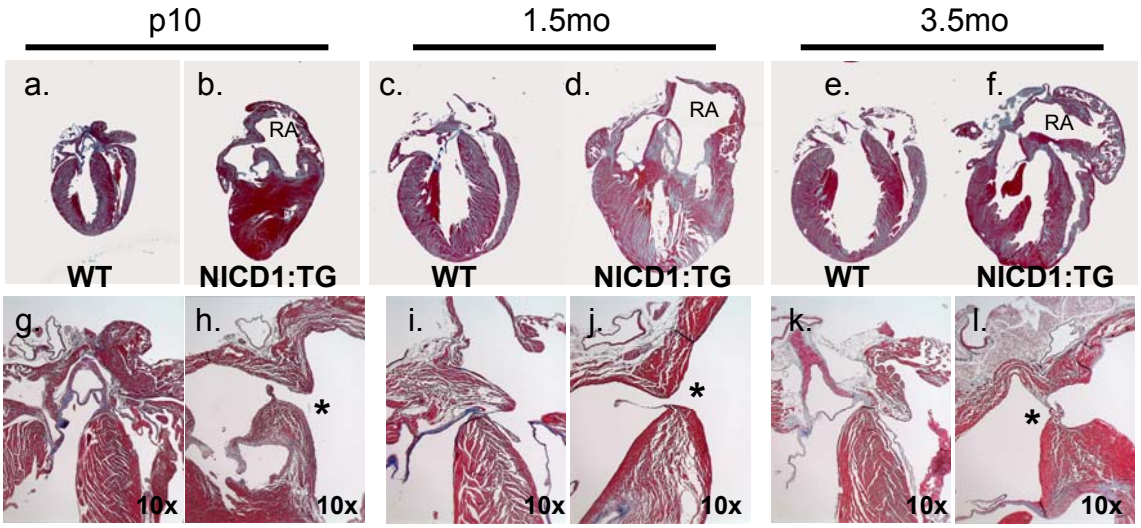

Figure 1.14 Atrial septation defect (ASD) is the cause of lethality in adult NICD1:TG mice. Trichrome staining demonstrates ASD and readily enlarged right atrium (RA) in NICD1:TG mice that escape perinatal lethality and reach adulthood **(a - f).** Higher magnification **(g - h**, 100x) images show the ASD (asterisk) in NICD1:TG hearts.

1.2. 6 Differentiation delay and enhanced cardiomyocyte proliferation in NICD1:TG hearts

Numerous studies have demonstrated that Notch signaling is involved in the fine balance between proliferation and differentiation in the neural and skeletal muscle system[257, 267, 270]. In addition, the ASD, VSD and valve defects observed in NICD1:TG hearts point in the direction of impaired cardiac differentiation. In order to test this possibility, we checked the expression levels of early cardiac genes such as *myosin heavy chain-6 (Myh6), myosin heavy chain-7 (Myh7), atrial natriuretic peptide (Anp), brain natriuretic peptide (Bnp), glucose transporter-1 (Glut-1), NK2 transcription factor related, locus 5 (Nkx2.5) and GATA binding protein 4 (GATA-4).* All these genes are normally highly expressed early during cardiac differentiation (e12.5 - e15.5) but *Anp, Bnp* and *Myh7* were futher up-regulated in the neonatal (p1) NICD1:TG hearts,

indicating differentiation delay in these hearts (fig.1.15). Moreover, the marker of energy regulation Glut-1 was up-regulated in NICD1:TG hearts, suggesting that these hearts are in energy demand.

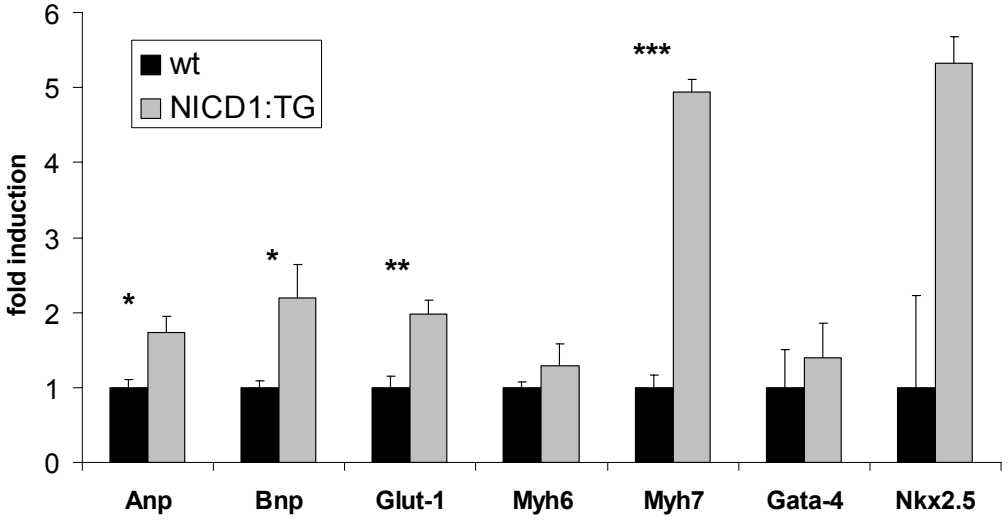

Figure 1.15 Differentiation delay in neonatal NICD1:TG hearts. Early cardiac gene expression was tested by Quantitative TaqMan RT-PCR. Probes for *myosin heavy chain-6 (Myh6), myosin heavy chain-7 (Myh7), atrial natriuretic peptide (Anp), brain natriuretic peptide (Bnp), glucose transporter-1 (Glut-1), NK2 transcription factor related, locus 5 (Nkx2.5) and GATA binding protein 4 (GATA-4)* genes were used. Taqman *glyceraldehyde 3-phosphate dehydrogenase (GAPDH)* probe was used for normalization. All these genes are normally highly expressed early during cardiac differentiation (e12.5-e15.5) but they are found significantly up-regulated in the neonatal (p1) NICD1:TG hearts, which indicates differentiation delay. (* $p<0.05$, ** $p<0.01$, *** $p<0.001$).

Since (a) differentiation and proliferation are usually mutually exclusive processes and (b) NICD1:TG hearts have thicker myocardial wall, we assessed the cardiomyocyte proliferation rate in these hearts. Double fluorescence staining was performed for the cardiomyocyte marker α-actinin (red) and the proliferation marker phospho-histone-3 (phospho-H3, green) on neonatal (p1) hearts. Since Notch signals are also required for left-right asymmetry[271, 272], we evaluated the cardiomyocyte proliferation rate separately at each region of the heart (left atrium, left ventricle, right atrium and right ventricle). After carefully controlled quantification of phospho-H3 positive cardiomyocytes, we conclude that there is a modest enhancement of proliferation in the left atrium and ventricle of the NICD1:TG hearts (fig.1.16,a-d), however the cardiomyocyte proliferation rate is comparatively higher in the right atrium and ventricle of the NICD1:TG hearts

(fig.1.16 e - h).Taken together, the enhanced proliferation rate at the right side of the heart and the up-regulation of the energy regulation marker Glut-1 suggest that enhanced cardiomyocyte proliferation is the cause of enlarged right atrium and thick myocardial wall in the neonatal (p1) NICD1:TG hearts.

Next page - Figure 1.16 Increased cardiomyocyte proliferation in neonatal (p1) NICD1:TG hearts. Double staining for the proliferation marker phospho-histone-3 (phospho-H3, green) and the cardiomyocyte marker α-actinin (red) demonstrates increased cardiomyocyte proliferation in neonatal (p1) NICD1:TG hearts **(a - h).** The differences reach statistical significance for the right side of the heart (**e - f**; right atrium and **g - h**; right ventricle). (t-test, *p<0.05, ** p<0.01, *** p<0.001).

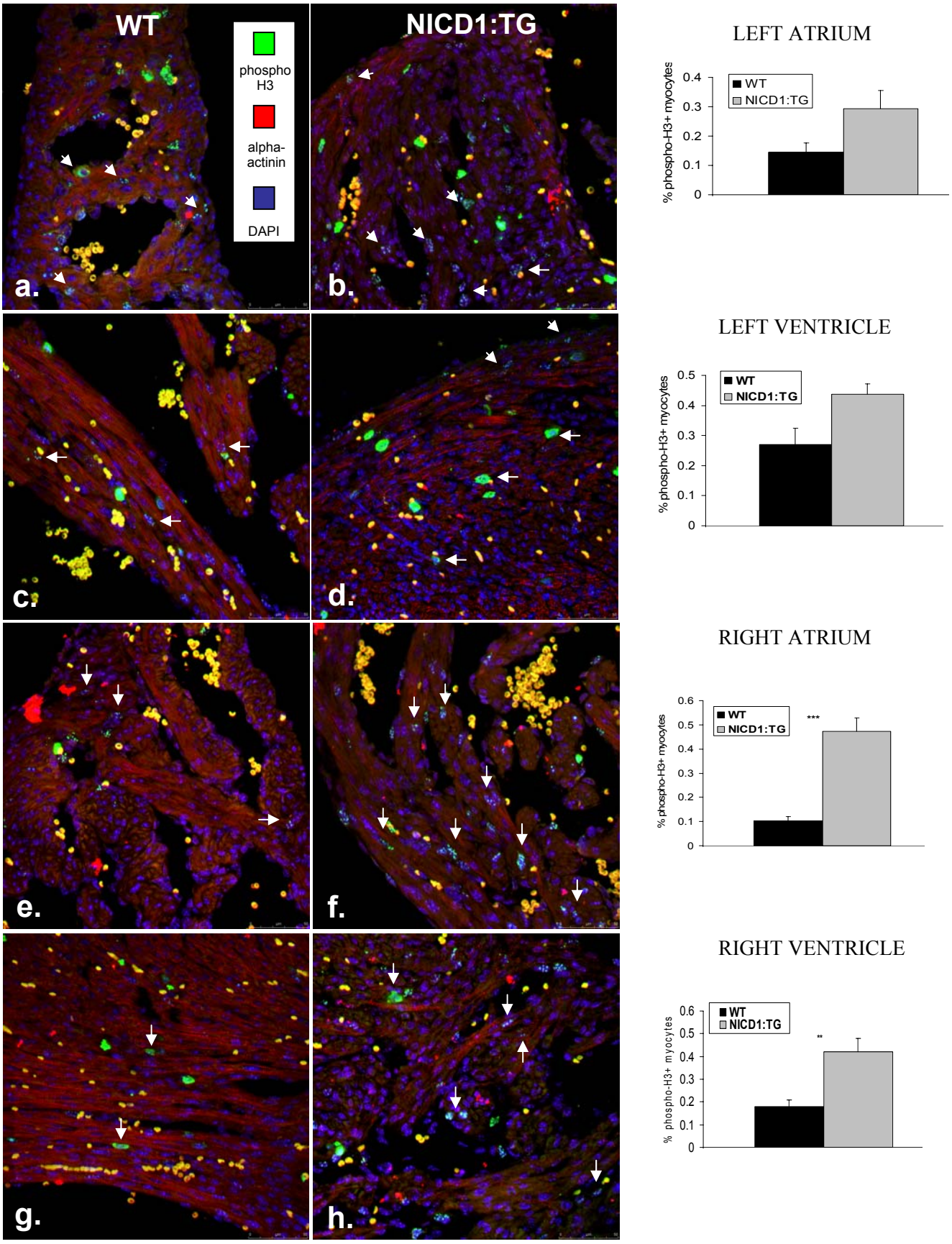
WT
NICD1:TG
phospho H3
alpha-actinin
DAPI
a.
b.
c.
d.
e.
f.
g.
h.
LEFT ATRIUM
% phospho-H3+ myocytes
WT
NICD1:TG
0.4
0.3
0.2
0.1
0
LEFT VENTRICLE
% phospho-H3+ myocytes
WT
NICD1:TG
0.5
0.4
0.3
0.2
0.1
0
RIGHT ATRIUM
% phospho-H3+ myocytes
WT
NICD1:TG
***
0.6
0.5
0.4
0.3
0.2
0.1
0
RIGHT VENTRICLE
% phospho-H3+ myocytes
WT
NICD1:TG
**
0.6
0.5
0.4
0.3
0.2
0.1
0

1.3 DISCUSSION

Notch-1 signaling activation results in abnormal cardiac morphogenesis

1.3.1 Discussion

Cardiogenesis is an extremely sensitive developmental process that requires myogenesis and morphogenesis to occur simultaneously with contractility[21, 198]. Poorly understood interactions among multiple mesodermally- and ectodermally-derived cell types, including cardiomyocytes, fibroblasts, endothelial, and smooth muscle cells, orchestrate the development of a four-chambered heart. Global inactivation in mice of several Notch pathway components, including Notch1[191, 231], Notch2[273], RBP-Jκ[191, 207, 230], PSEN1[217], HEY1[197, 226, 227, 250], HEY2[196, 197, 227], HEY3[182], demonstrates a wide range of cardiac defects, such as ASD, VSD, impaired ventricular trabeculation, and atrio-ventricular (AV) valve defects, implicating the Notch pathway as a central regulator of cardiogenesis, and suggesting that the precise outcome of Notch signaling employment is time- and cell type-dependent[108]. Although these studies have been informative, fundamental questions regarding molecular and cellular Notch actions in cardiac development and disease remain to be elucidated following conditional mutagenesis approaches.

Specifically, the role of Notch signaling in cardiomyocytes has been obscure, likely due to early embryonic lethality and functional redundancy issues reported in the aforementioned mouse mutants. In our approach, we bypass embryonic lethality and genetically manipulate Notch-1 signaling specifically in the cardiomyocyte compartment. Overexpression of Notch1 intracellular domain (NICD1) in cardiomyocytes results in perinatal lethality, impaired cardiac function and abnormal cardiac morphogenesis characterized by thick myocardial wall, enlargement of the right atrium, ASD, VSD, and hypercellular tricuspid valve. Although possible interactions between Notch1 and other signaling pathways cannot be excluded, the up-regulation of *Hey1, Hey2*, and *Hes1* in the heart of NICD1:TG animals underscores the Notch-dependent nature of the cardiac defects observed. Moreover, evidence for a Notch1 positive feedback mechanism in the heart already exists and could explain the wide range of cardiac defects seen in NICD1:TG mice[274].

Proper atrio-ventricular (AV) valve development requires the formation of endocardial cushions at the AV canal, where, in response to regionalized myocardial signals, a subset of endocardial cells undergo epithelial-to-mesenchymal-transition (EMT)[210]. Several Notch components, such as Notch 1, Delta-like 4 and Hey2, are expressed at the endocardium of the AV canal[191, 274]. Moreover, Notch1 and RBP-Jκ

total knock-out mice display early embryonic lethality (e9.5 - e10.5) and hypocellular endocardial cushions, highlighting the importance of Notch signaling in EMT and valve formation[191, 207, 231]. Importantly, valve development initiates at e9.0 and happens simultaneously with ventricular and atrial septation at e14.5 - e15.5[275, 276]. Consistent with this observation, several Notch mouse mutants, such as *Hey2*$^{-/-}$ [48, 49, 197, 247-249] *and Presenilin1*$^{-/-}$[217], demonstrate valve defects accompanied with VSD, suggesting the involvement of Notch signaling in these processes. Intriguingly, the NICD1:TG mice display a strikingly similar phenotype to *Hey2*$^{-/-}$ mice, where valve defects are observed only at the tricuspid valve accompanied by ASD and VSD, indicating that valve and septae formation are sensitive to critical dosages of Notch signaling, possibly through Hey2-mediated actions.

A growing body of evidence proposes Notch signaling as an inhibitor of early cardiomyocyte differentiation *in vit*ro [200-202] and *in vivo*[198, 203-206]. For example, *gain-of-function* approaches for Notch signaling demonstrate reduced number of differentiated cardiomyocytes or diminished expression of cardiac markers during early cardiac development in *D. melanogaster*[204, 205], *X.Laevis*[206], and chick[203], whereas *loss-of-function* experiments show the opposite effect. Similarly, overexpression of NICD1 in pre-cardiac mesoderm in mice leads to abnormal cardiac morphogenesis associated with abnormal cardiomyocyte maturation and sarcomeric structures[198]. In accordance with these findings, overexpression of NICD1 in the murine myocardium leads to differentiation delay since embryonic cardiac differentiation genes, such as Anp, Bnp, and Myh7, are significantly up-regulated in the NICD1:TG heart at the time of birth when compared to control hearts.

Apart from its role in differentiation, Notch signaling is also involved in proliferation events since it regulates stem cell maintenance/activation in the nervous[267, 277, 278] and skeletal muscle[257] systems, but it can also be oncogenic in epithelial cells[279-281] or T-cells[282, 283]. In accordance with these data, staining for phospho-histone-3 revealed increased levels of cardiomyocyte proliferation in NICD1:TG hearts, with differences that reached significance only at the right side of the heart (right ventricle and right atrium). Moreover, these findings could explain the abnormal size of the right atrium and the thick myocardial wall in NICD1:TG animals. Intriguingly, recent studies identify cardiac stem cells (CSCs) which regulate heterogeneous cardiomyocyte turnover; faster in the atria and slower in the ventricles[284]. In addition, the same study revealed that the Notch inhibitory protein, Numb, is expressed in atrial CSCs and possibly regulates asymmetric

cell division[284]. Although our study was not designed for identification of cardiac stem cells, we cannot exclude the possibility that the readily enlarged right atrium in NICD1:TG mice could be attributed to atrial CSC activation. Taken together, these data suggest that cardiomyocyte NICD1 overexpression favors proliferation at the expense of differentiation, since these processes are normally mutually exclusive.

Recent fate-mapping studies in chick[11, 12] and mouse[13-16] embryos highlight two distinct mesodermal heart fields that contribute cells to the developing heart in a temporally and spatially specific fashion. The first heart field (FHF) is established early in cardiogenesis and contributes cells to the left ventricle and parts of the atria[16, 21], whereas the second heart field (SHF) appears later and contributes to the formation of the right ventricle, two thirds of the atria and parts of the outflow tract[13, 14, 23]. Intriguingly, all the cardiac defects observed in NICD1:TG hearts, including enlarged right atrium, ventricular and atrial septation defects, hyperplastic tricuspid valve and increased proliferation in the right atrium and ventricle, indicate that SHF-derived structures are sensitive to Notch1 signaling. In line with this notion, a recent report demonstrates increased levels for NICD1 activity in the endocardium of the atria and the right ventricle during early (e13.5) cardiogenesis[274]. Moreover, cardiomyocyte-specific Hey2 inactivation results in right ventricular dilation and further indicates that the cardiac defects observed in NICD1:TG mice could be attributed to perturbations of Notch1-mediated Hey2 signaling[199]. However, *in situ* hybridization studies for SHF markers (Islet1, Mef2c, Hand2) in NICD1:TG hearts are required in order to elucidate the role of Notch1 in SHF contribution during cardiogenesis. In addition, examination of the Notch1 expression pattern in previously described SHF mutants (Isl1[13] or Fgf10[14] *null* mice) would provide complementary insights regarding the role of Notch1 in the SHF.

One could argue that spatial “preference” of the αMyHC-Cre line for the right side of the heart can lead to right-sided defects and reporter assays are underway to test this possibility. Moreover, the late contribution of the SHF to the right side of the developing heart combined with the minimal expression of the αMyHC promoter during early cardiogenesis (e8 and onwards, but peak at birth) raise the possibility that accumulation of Notch1 signals happens later during cardiogenesis and subsequently coincides only with processes that take place later in the developing heart, such as SHF contribution. However, the higher NICD1 endocardial activity at the right ventricle and atria[274] in combination with the right-sided defects observed in Hey2 mutant hearts[48, 199], rather

support the notion that SHF contribution is specifically sensitive to perturbation of Notch1 signailling in NICD1:TG hearts.

Cardiac function is severely impaired in NICD1:TG animals that reach adulthood. This defect could be explained by the ASD observed in NICD1:TG mice. Importantly, mice with global Hey2 inactivation also demonstrate ASD[48, 196, 197]. Moreover, two independent studies demonstrate that the chamber-specific expression pattern of Hey genes (Hey1 at the atria, Hey2 at the ventricles) are required for atrial and ventricular identity[199, 285]. Hence, Hey2 cardiomyocyte inactivation results in abnormal expression of atrial genes at the ventricles and severely impaired cardiac function. Although QRT-PCR analysis demonstrates Hey2 up-regulation in the heart of NICD1:TG animals, *in situ* hybridization studies are required in order to examine possible expression pattern alterations of *Hey1* and *Hey2* genes, that could lead to impaired cardiac function.

Our immunohistochemical approach allowed us to detect NICD1 activity in the nuclei of neonatal and adult cardiomyocytes, eliminating the possibility of ectopic NICD1 activation. Interestingly, previous reports suggest Notch1 as an endothelial and endocardial marker, but those studies were performed at earlier (e9 - e13) developmental stages[191, 198, 207, 274]. Taking into account the dynamic expression pattern of Notch genes, it is likely that Notch1 is expressed in several cell populations during cardiac development in an *on-and-off* fashion (discussed also in 1.3.3.1 part of introduction). Notably, Notch2 is consistently expressed in cardiomyocytes during development and in adult stages[47, 194]. Functional redundancy between NICD1 and NICD2 is supported by the normal phentype of mice carrying replacement of the NICD2 genetic region with NICD1[286]. Thus we cannot exclude the possibility that the cardiac defects observed in NICD1:TG mice could be attributed to perturbation of Notch2 downstream pathways as well.

The cardiac defects observed in our *gain-of-function* genetic approach, such as ASD and VSD, valve defects and impaired function, are reminiscent of defects seen in *loss-of-function* approaches for *Notch1*[191, 207, 231, 287], *Notch2* combined with *Jag1*[47], *Hey1* combined with *Hey3*[182], and *Hey2*[48, 248], allowing the speculation that Notch gene dosage is critical during the sensitive developmental process of cardiogenesis. Supporting this possibility, evidence from the recently emerging field of microRNA biology suggests that Notch signaling levels are regulated by microRNA1 and influence cardiac differentiation in *Drosophila*[288].

1.3.2 Future perspectives

Here, we explore the role of NICD1 activity in cardiomyocytes and report abnormal cardiac morphogenesis accompanied with impaired cardiac function in NICD1:TG animals. The observation of right-sided defects in the heart of NICD1:TG mice raises the exciting possibility that Notch1 signals influence the differentiation of SHF-derived cells. The involvement of Notch signaling in SHF contribution into the developing heart remains to be elucidated.

We plan to investigate the aforementioned possibility by crossing the *knock-in* Nkx2.5-CRE mice[289] with our inducible transgenic NICD1 mice[198]. The *Nkx2.5* gene promoter is cardiomyocyte-specific and active at e7.0 and onwards, temporally coinciding with FHF and SHF contributions to the developing heart tube[22, 289]. This cross will induce cardiomyocyte-specific NICD1 over-expression earlier compared to NICD1:TG mice, where *αMyHC* gene promoter drives minimal CRE recombinase expression at e8.5 and peaks at birth[290]. Moreover, this genetic approach could further confirm the right-sided defects observed in NICD1:TG, whereas *in situ* hybridization analysis for FHF (Hand1, Gata4) and SHF (Islet1, Mef2c, Hand2) markers could provide valuable information regarding the effects of NICD1 over-expression early during cardiogenesis. As a complementary *loss-of function* approach, we recently obtained a *knock-in* mouse line where the dominant negative form of the Notch transcriptional co-activator MAML1 (presented in the Introduction 1.1.3.2) has been introduced into the ROSA26 locus (provided by Jonathan Epstein, University of Pennsylvania, USA)[218, 291]. Crossing these mice with the aforementioned Nkx2.5-CRE mice will allow the cardiomyocyte specific Notch signaling inactivation and shed light into previously unanswered questions regarding the requirement of Notch signaling for cardiac development.

Another genetic approach to investigate the role of Notch signaling in the SHF includes the use of the SHF-specific Islet1-CRE mouse line[292, 293]. These animals could be crossed with the inducible NICD1 transgenic or dominant negative MAML1 mice, providing valuable genetic tools for SHF-specific Notch signaling activation or inhibition, respectively.

The examples given in this section provide only a few possible avenues for further investigation, but clearly show the significance of our study, which provides long-awaited insights regarding the role of Notch1 signaling specifically in cardiomyocytes.

1.3.3 Conclusions

Here, following a *gain-of-function* approach, we demonstrate that cardiomyocyte-specific NICD1 over-expression results in perinatal lethality and abnormal cardiac morphogenesis, favoring proliferation at the expense of differentiation. Besides, ASD and VSD, the NICD1:TG animals display right-sided cardiac defects, such as hyperplastic tricuspid valve and enlarged right atrium, setting the ground for future studies focusing on the role of Notch signaling in SHF contribution during cardiogenesis. In addition to the aforementioned cardiac defects, the NICD1:TG mice display impaired cardiac function and perinatal lethality and phenocopy the majority of abnormalities observed in *Hey2*$^{-/-}$ animals, indicating Hey2 as a possible downstream target of Notch1 signaling. Moreover, right ventricular hyperplasia, ASD and VSD have been reported in humans with Alagille syndrome and Jag1$^{+/-}$/Notch2$^{+/-}$ mice first highlighted the involvement of Notch signaling in this disorder by phenocoping the syndrome. Our findings provide evidence that Notch1 actions in cardiomyocytes could also explain the cardiac manifestations of Alagile syndrome and related forms of congenital heart disease.

1.4 RESULTS

Re-activation of Notch-1 signaling protects against myocardial infarction

1.4 RESULTS

1.4.1 Rationale

Current research focuses on the replenishment of injured myocardium using cell-based approaches or "re-employing" molecules that have a crucial role during cardiac development and morphogenesis[83, 102, 294-297]. The hypothesis that recapitulation of embryonic signaling such as *Thymosin β4, Sonic Hedgehog,* and *Notch* can promote tissue regeneration is increasingly supported by numerous studies in the nervous[267], skeletal[270] and cardiac muscle systems[102, 103]. Recently, it has been demonstrated that reactivation of Notch signals in mouse models of brain ischemia[267] and skeletal muscle injury[270] promotes regeneration by activation of resident stem cells. Moreover, the artery-specific expression pattern of various Notch receptors (Notch1,-3,-4) and ligands (Delta4, jagged1,-2) in mouse and zebrafish in combination with major vascular defects observed in Notch mutants[47, 222, 232, 298] establish Notch signaling as a critical player in vascular development and angiogenesis[299]. In addition, Notch appears to be activated in cases of *in vitro*[266] and *in vivo*[267, 268] hypoxia. Taking together, all these findings render Notch signaling an attractive target for therapeutics in case of heart ischemia.

Based on a recent study[270] where a single injection of a Notch-1 pseudoligand promoted skeletal muscle regeneration, we directly evaluated the cardiac regenerative potential of Notch-1 signaling activation. We employed a mouse model of myocardial ischemia (LAD operation) and evaluated Notch expression levels, cardiac performance and morphology as well as neoangiogenesis after Notch-1 signaling re-activation.

1.4. 2 Notch-1 is expressed in cardiomyocytes and endothelial cells of the adult heart

Initially, double staining for the *Notch-1 intracellular domain (NICD1)* and the vessel marker *smooth muscle α-actin* (*α-SMA*) was performed in order to identify the cell populations that express Notch-1 in the adult heart. As indicated by arrows, NICD1 activity is present at the nuclei of endothelial cells, which are located under the smooth muscle cell layer of the vessels in the adult heart (fig.1.17 a - d). Similarly, double staining for the *Notch-1 intracellular domain (NICD1)* and the cardiomyocyte marker *α-actinin* revealed NICD1 activity in the cardiomyocyte nuclei of the adult heart (fig.1.17 a, d, e - h), which is indicated by arrowheads. These findings were informative regarding

Notch1 expression in the adult heart since the dynamic Notch expression pattern has created literature discrepancies (see also 1.1.3.1 part of Background, Chapter 1).

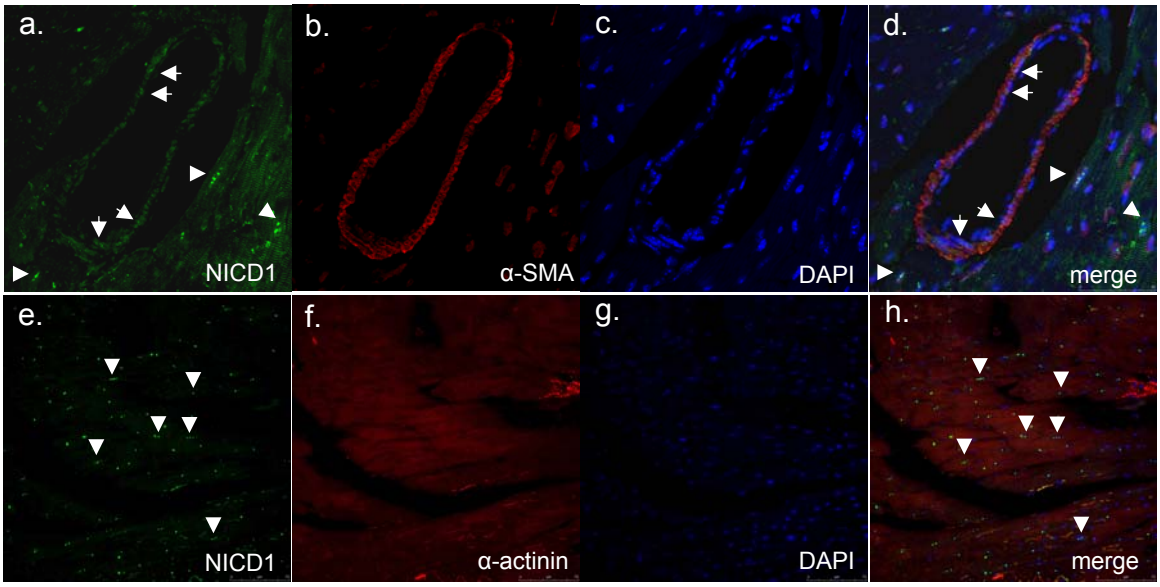

Figure 1.17 Notch-1 is expressed in endothelial cells and myocytes of the adult heart. Confocal microscopy for Notch-1 Intracellular Domain (NICD1) demonstrate NICD1 activity in the nuclei of endothelial cells (**a, d** - arrows) of vessels and cardiomyocytes (**a, d, e, h** - arrowheads) in the adult heart (**a, d**). Smooth muscle α-actin (**b**) was used for vessel visualization, α-actinin as a cardiomyocyte marker and DAPI for nuclear identification (**c, g**).

1.4. 3 Expression levels of several Notch pathway components are up-regulated after myocardial infarction

Several studies demonstrate changes in the Notch expression levels following hepatic[300, 301], arterial[302, 303] or skeletal muscle injuries[270]. TaqMan quantitative RT-PCR was employed in order to evaluate the expression levels of *Notch-2* and several well-documented Notch target genes [*Hairy enhancer of split-1 (Hes-1), Hes-related-1 (Hey-1) and Hes-related-2 (Hey-2)*] after the induction of myocardial ischemia (LAD operation). These analyses revealed that *Notch-2, Hes-1* and *Hey-2* transcripts were significantly up-regulated (when compared to sham) in a narrow time-window (8h-48h) after infarction (fig.1.18,a). Moreover, the Notch-2 protein levels were up-regulated 48hours to 4days after infarction, which is consistent with the earlier up-regulation of Notch-2 mRNA levels (fig.1.18,b). Furthermore, the protein levels of the Notch ligand *Jagged-1* and the cleaved form of Notch-1 receptor (NICD1) were up-regulated 48hours to 4days after myocardial infarction (fig.1.18 b). These findings on mRNA and protein

levels of several Notch pathway components do show activation of Notch signaling after myocardial infarction, but nevertheless they do not demonstrate which cell types are involved in this phenomenon.

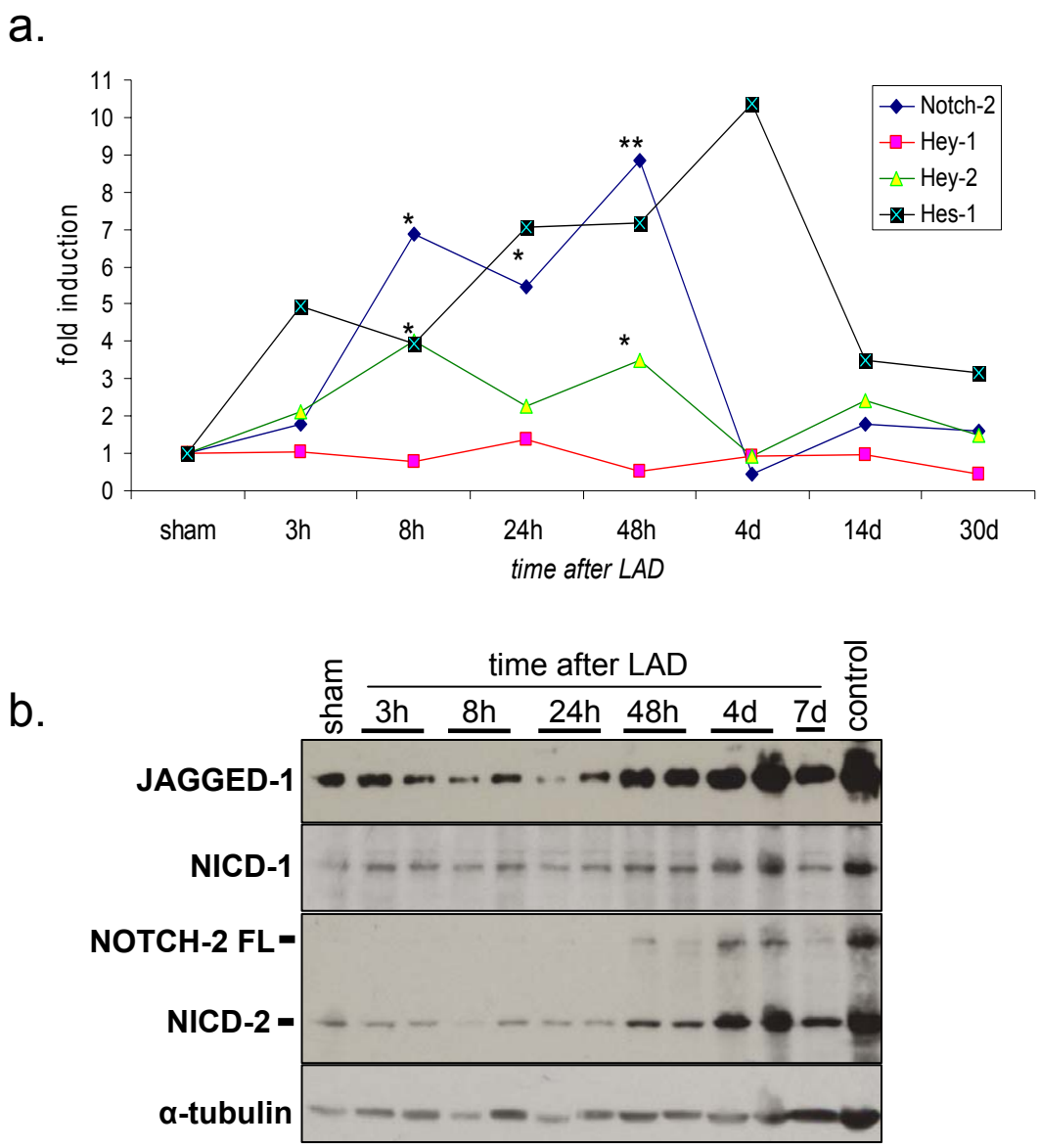

Figure 1.18 Notch pathway is activated after myocardial infarction. (**a**). Relative quantification of *Notch-2*, *Hairy enhancer of split-1 (Hes-1), Hes-related-1 (Hey-1) and Hes-related-2 (Hey-2)* transcripts reveals that *Notch-2, Hey-2* and *Hes-1* mRNA levels are up-regulated early (8h-48h) after myocardial infarction (LAD operation). TaqMan probes for the aforementioned genes were used and normalization was done with *glyceraldehyde 3-phosphate dehydrogenase (GAPDH).* (**b**). The protein levels of the Notch ligand *Jagged-1,* the cleaved form of Notch-1 receptor (NICD1) and the Notch-2 receptor [full molecule (FL) and cleaved form (NICD-2)] were up-regulated 2days-4days after myocardial infarction. The blots were normalized with an anti-α-tubulin antibody. SHAM indicates a non-infarcted heart.

1.4.4 Intramyocardial Notch-1 antibody (Notch1 ab) injection activates Notch signaling, improves survival and cardiac function

In order to evaluate the cardiac regenerative potential after Notch-1 signaling activation, myocardial infarction was caused to C57/Bl6 adult (2-3 month-old) mice. An antibody against the extra-cellular domain of Notch-1 receptor (pseudoligand) was injected at two sites (left and right) of the border zone five minutes after infarction. This test group was consisted of thirty mice (n=30) and will be referred as *Notch-1 ab* group. The same procedure was followed for the control group (n=30), which was injected with an isotype-matched hamster IgG1 antibody and will be referred as *IgG1* group. The antibody concentrations used were in accordance with the skeletal muscle study[270].

To confirm Notch-1 signaling activation, we checked the expression levels of well-studied Notch target genes such as *Hairy enhancer of split-1 (Hes-1), Hes-related-1 (Hey-1)* and *Hes-related-2 (Hey-2)* six hours after the Notch1 antibody injection. By separating the infarcted heart in ischemic and non-ischemic myocardium, we witnessed up-regulation of *Hes-1* and *Hey-1* mRNA levels only at the non-ischemic part of the myocardium in the Notch1 ab injected hearts (fig.1.19 a - c), suggesting that the local injection of the Notch1 antibody was sufficient to induce Notch signaling activation in the border zone of the infarcted heart.

Careful monitoring of the post-operational survival rate revealed improvement for the *Notch1 ab* group (47.06%) when compared with the *IgG1* group (38.24%) one month after the induction of myocardial ischemia (fig.1.19 d). Moreover, assessment of the cardiac function by echocardiography demonstrated improved fractional shortening for the *Notch1 ab* injected hearts at 2 weeks and 1 month after infarction (fig.1.19 e).

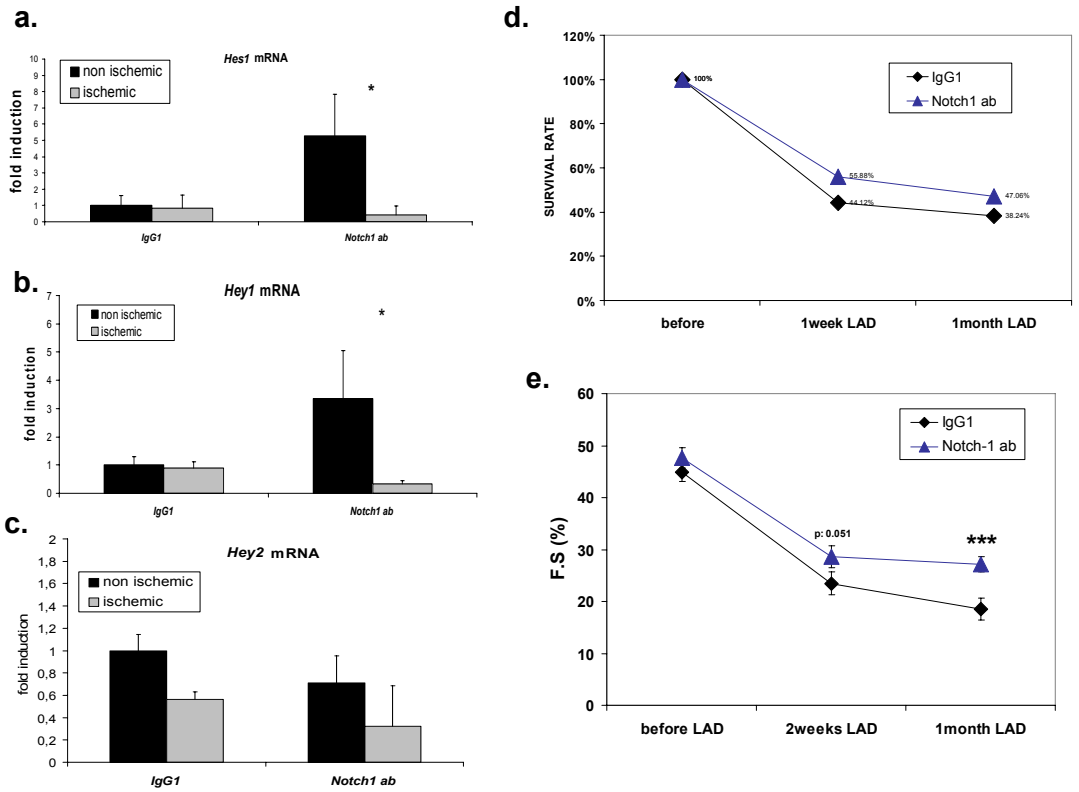

Figure 1.19 Activation of Notch signaling, improved survival and function after intramyocardial Notch-1 antibody (Notch1 ab) injection. Quantitative TaqMan RT PCR demonstrates up-regulation of *Hairy enhancer of split-1 (Hes-1)* and *Hes-related-1 (Hey-1)* but not *Hes-related-2 (Hey-2)* genes in the non ischemic myocardium 6 hours after Notch-1 ab injection in the infarcted heart. Taqman *glyceraldehyde 3-phosphate dehydrogenase (GAPDH)* probe was used for normalization (**a, b, c**). Monitoring of the post-operational survival rate reveals improvement for the Notch1 ab injected hearts (47.06%) when compared with the IgG1 injected hearts (38.24%) one month after LAD operation (**d**). Echocardiography shows improved fractional shortening for Notch1 ab injected hearts at 2 weeks and 1 month after infarction **(e).** (t-test, * p<0.05, ** p<0.01, *** p<0.001).

1.4.5 Early Notch-1 signaling activation protects against myocardial infarction

Detailed examination of the *Notch1 ab* and *IgG1* injected hearts showed absence of cardiac dilation and compromised fibrotic tissue deposition in the *Notch1 ab* injected hearts one month after infarction (fig.1.20 a - b). Furthermore, morphometry analysis revealed decreased left ventricular scar volume and increased muscle sustenance in the *Notch1 ab* injected hearts (fig.1.20 c - d). Next, we also checked well-documented markers of heart failure such as *myosin heavy chain-6 (Myh6), myosin heavy chain-7 (Myh7), glucose transporter-1 (Glut-1)* by TaqMan Quantitative RT-PCR (fig.1.20 e). *Myh6* and *Glut-1* mRNA levels were close to the sham operated heart levels, a finding

which further demonstrates protection against myocardial infarction in the *Notch1 ab* injected hearts. Taken together, these findings suggest that early Notch1 signaling activation protects against myocardial infarction by reducing fibrosis and heart failure marker expression.

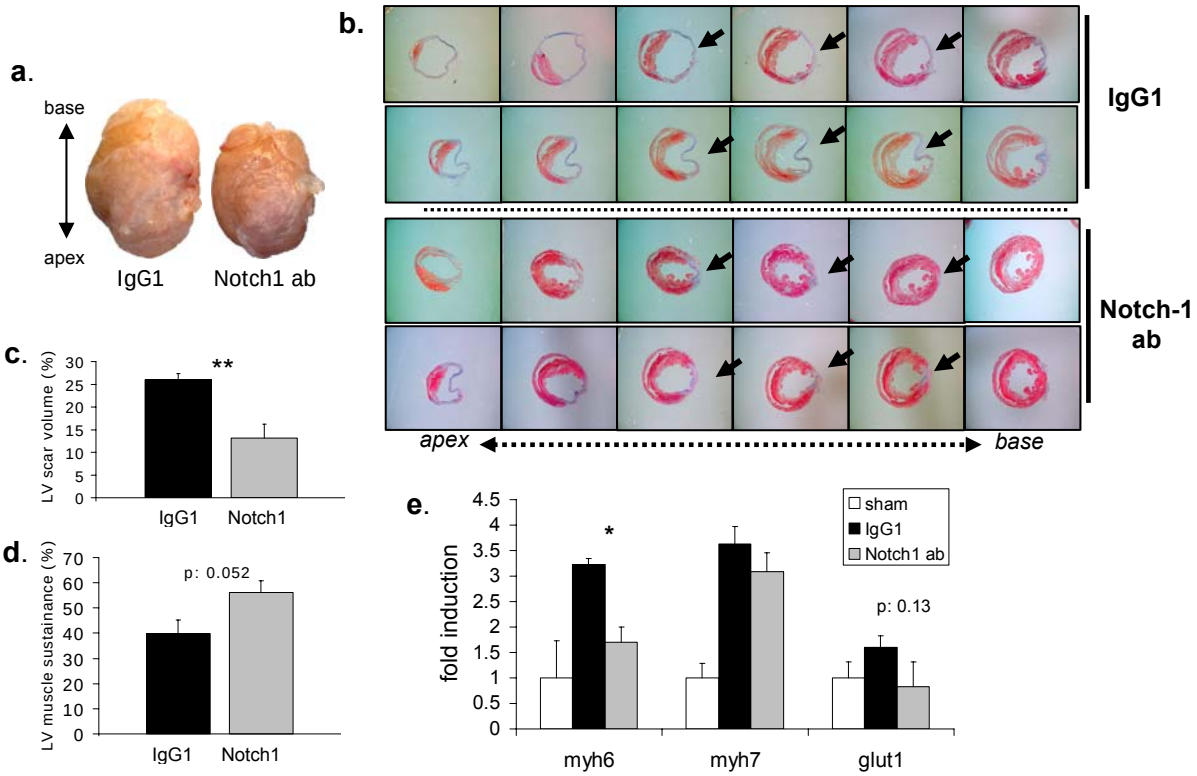

Figure 1.20 Early Notch-1 signaling activation protects against myocardial infarction. Whole mount comparison of IgG1 and Notch-1 antibody (Notch1 ab) injected hearts shows reduced scar formation in Notch1 ab injected hearts 30 days after infarction (**a**). Trichrome staining on serial cross-sections from apex to base of IgG1 and Notch1 ab injected hearts (samples in duplicates) demonstrates reduced scar tissue deposition (arrows) and no dilation in Notch1 ab injected hearts 30 days after infarction (**b**). Quantification measurements on left ventricular (LV) collagen tissue deposition (**c**) and LV muscle sustainance (**d**) reveals protection in Notch1 ab injected hearts 30 days after infarction. Quantitative TaqMan RT PCR for heart failure markers [*myosin heavy chain-6 (Myh6), myosin heavy chain-7 (Myh7), glucose transporter-1 (Glut-1)]* indicates moderate down-regulation of these markers in the heart of Notch1 ab injected animals 30 days aftre infarction. SHAM indicates a non-infarcted heart.

1.4. 6 Angiogenesis and/or proliferation; possible mechanisms for Notch-1 mediated cardiac repair

As mentioned in the Introduction, the role of Notch signaling in angiogenesis and proliferation is well documented. In order to test whether these processes are involved in Notch-1 mediated cardiac repair, DAB staining for the angiogenesis marker *smooth muscle α-actin* (*α-SMA*) and proliferation marker *(BrdU)* was performed. α-SMA staining revealed more vessels close to the infarcted (necrotic) myocardium in *Notch1 ab* injected hearts one month after infarction (fig.1.21 a, b). Importantly, numerous small-diameter vessels were noticed, which is suggestive of neoangiogenesis. In addition, staining for BrdU incorporation indicated a tendency towards enhanced proliferation in Notch1 ab injected hearts and quantification studies are underway (fig.1.21 d, e).

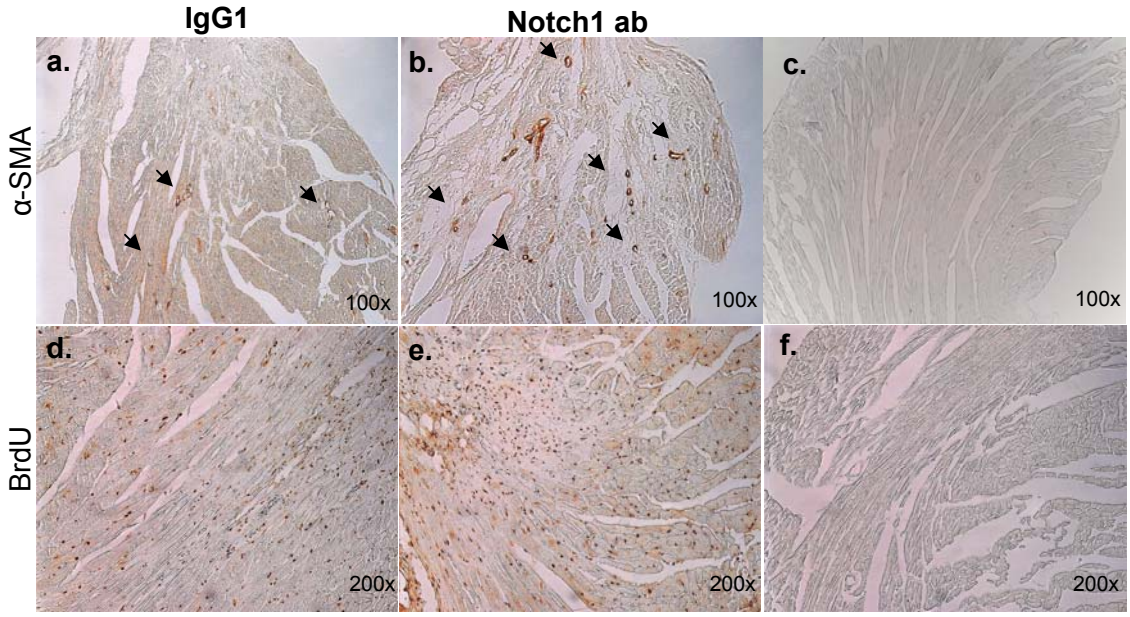

Figure 1.21 Improved angiogenesis and enhanced proliferation are possible mechanisms for Notch-1 mediated cardiac repair. Immunohistochemistry for smooth muscle α-actin reveals improved angiogenesis in Notch-1 antibody (Notch1 ab) injected hearts 30days after infarction (**a**, **b**). Staining for BrdU incorporation in the nuclei of proliferating cells indicates enhancement of proliferation after infarction in Notch1 ab injected hearts (**d, e**). Negative control images for smooth muscle α-actin and BrdU staining are presented in **c** and **f**, respectively.

1.5 DISCUSSION

Re-activation of Notch-1 signaling protects against myocardial infarction

1.5.1 Discussion

The involvement of Notch signaling in acquired cardiac conditions at the adult stage has been recently reported by the identification of human mutations in *Notch1*[212] and *Presenilin*[304] genes in aortic valve disease and dilated cardiomyopathy, respectively. However, the role of Notch signaling in myocardial infarction, the second most common cause of acquired heart disease, is largely unknown.

A growing body of literature provides hints at the involvement of Notch signaling in cardiac regeneration. First, activation of Notch signaling pathway precedes heart regeneration in zebrafish, a model organism with remarkable capacity to regenerate its heart following injury[260, 261]. Second, studies on *Xenopus* tail[262] and medaka fin regeneration[263] further demonstrate the requirement for Notch signaling in tissue regeneration. Third, Notch signaling regulates maintenance, activation and differentiation of multiple stem-cell populations, including hematopoietic, neural, skin, and skeletal muscle stem cells[256]. Specifically in skeletal muscle, Notch regulates the activation and subsequent differentiation of the resident stem cell-like population (satellite cells) and promotes skeletal muscle regeneration upon injury[257-259]. The parallels between skeletal and cardiac muscle development and the recent identification of resident cardiac progenitor cells (CPCs)[58, 255], prompted us to study the involvement of Notch signaling in myocardial injury. Finally, genes involved in cardiac development may be re-deployed in the adult stage to protect or regenerate the injured myocardium[21]. For example, *thymosin-β4*[102] and *sonic hedgehog*[103] genes are required for cardiogenesis and when re-employed during the acute ischemic period favor survival and neo-angiogenesis. In line with this notion, Notch signaling has an essential role in heart formation and angiogenesis[107], which further encourages investigation of Notch signaling re-employment in cardiac ischemia.

Here, based on a recent study[270] where a single injection of a Notch-1 pseudoligand (antibody against the extracellular domain of Notch-1 receptor) promotes skeletal muscle regeneration, we demonstrate that early activation of Notch-1 signaling improves functional outcome, minimizes fibrotic tissue deposition and promotes angiogenesis following myocardial infarction in mice. Our immunohistochemical analysis reveals Notch-1 intracellular domain (NICD1) activity in the endothelial cells of the cardiac vessels and cardiomyocytes during adulthood, suggesting that these cardiac cell populations are responding to Notch-1 antibody (ab) injection upon infarction. Moreover,

Notch-1 activation leads to upregulation of two well-documented Notch downstream targets, *Hey1* and *Hes1*, and not *Hey2*, indicating that the beneficial outcome of Notch-1 signaling re-employment after infarction is manifested possibly through *Hey1* and *Hes1* actions.

Importantly, our expression analysis of several Notch pathway components following myocardial infarction revealed features reminiscent of zebrafish heart regeneration[260, 261]. Following Notch-1 ab injection, we witness *Hey1* and *Hes1* mRNA up-regulation at the non-ischemic myocardium that surrounds the infarcted area. Similarly, *notch1b* and *deltaC* mRNA levels are increased in the normal myocardium that surrounds the injured area in the zebrafish heart[261], suggesting that the role of Notch extends beyond the regenerating cells themselves. Intriguingly, *notch1b* and *deltaC* mRNA levels are up-regulated during the first week of myocardial injury in zebrafish, which temporally coincides with the time window of Notch1, Notch2, Jagged1, Hes-1 and Hey-2 up-regulation following myocardial infarction in mice[261, 305], indicating that Notch signals are involved in early events after a myocardial injury.

Similarly to Notch-1-mediated skeletal muscle regeneration[270], early re-employment of Notch-1 signaling following myocardial ischemia results in curtailed cardiac dilatation, reduced fibrosis, increased muscle sustenance and improved cardiac function. Although Notch-1-mediated skeletal muscle regeneration is attributed to the activation of resident stem cells (satellite cells), discrepancies regarding potential cardiac stem cell (CSC) markers render difficult the investigation of possible CSC activation in Notch-1 ab injected hearts[255, 257].

The requirement of Notch signaling for embryonic angiogenesis has been highlighted in *Notch1*$^{-/-}$ and *Delta-like-1*$^{+/-}$ *Delta-like4*$^{+/-}$ mutant mice[230, 231, 235, 306]. Vascular endothelial growth factor (VEGF) is a central mediator of angiogenesis during development, ischemia and cancer, and lies upstream of Notch signaling[307-310]. Interestingly, little is known regarding the role of Notch signaling in postnatal angiogenesis in response to hypoxia in ischemic tissues. Under steady-state conditions, we report basal NICD1 activity in the endothelial cells of the cardiac vessels, which is consistent with previous studies demonstrating Notch-1 expression in the vascular endothelium[175, 176]. Accordingly, recent hind-limb ischemia studies report induction of endothelial *Notch1, Delta-like-1* and *Hes-1* expression upon injury[235, 237]. In line with this observation, we report up-regulation of *Notch1, Notch2, Jagged1, Hes-1* and *Hey-2* mRNA and protein levels following myocardial ischemia. However, the fact that we

examined RNA and protein samples from the entire infarcted heart, in combination with the observation of NICD1 activity in endothelial cells and cardiomyocytes, leave open the possibility that different cell populations could contribute to Notch signaling activation in models of skeletal muscle (hind limb) and cardiac muscle ischemia. Hence, we cannot exclude the possibility that the beneficial outcome of Notch-1 ab injection in the heart after infarction could be attributed to several cardiac cell populations, such as endothelial cells and cardiomyocytes.

We propose that Notch-1 ab injection promotes neovascularization in the infarcted heart and, subsequently, favors survival, decreases fibrosis, and improves cardiac function. This is supported by the finding that increased numbers of *smooth muscle alpha actin* (αSMA) positive vessels of small-diameter where observed at the border zone between infarcted and normal myocardium in Notch-1 ab injected hearts when compared with controls. In accordance with this observation, global or endothelial-specific *Notch1*$^{+/-}$ mice displayed impaired neovascularization in a model of hind-limb ischemia, suggesting that Notch1 signaling is required for endothelial cell proliferation, migration and survival[237]. In addition, smooth muscle alpha actin, which is an essential component of the vascular wall and is required for neovascularization, has been recently described as a direct Notch target gene in endothelial and smooth muscle cells[253]. The latter study raises the possibility that endothelial and smooth muscle cells are responsive to the Notch-1 ab injection after infarction. Moreover, the intriguing observation of NICD1 activity found also in the epicardial cells early after myocardial infarction (data not shown) is reminiscent of the thymosin-β4 inductive role in adult epicardial progenitor cell mobilization and neovascularization[105], and further illustrates a possible role for Notch-1 signaling in neoangiogenesis after infarction.

Interestingly, in our developmental approach (NICD1:TG mice) overexpression of NICD1 in cardiomyocytes results in increased proliferation and differentiation delay, consisted with the inhibitory role of Notch in cardiac differentiation across species[198, 203-206]. Following this rationale, BrdU staining one month after infarction reveals a tendency towards increased proliferation in Notch-1 ab injected hearts when compared with controls. However, additional studies using proliferation (phospho-histone 3, Ki67) and cardiomyocyte (α-actinin) or endothelial (Flk-1) markers are required in order to unravel the specific molecular mechanism triggered upon Notch-1 ab injection. Moreover, taking into account the NICD1 activity observed in adult cardiomyocytes in combination with the

well-documented role of Notch signaling in cell survival[108, 254, 266, 311], evaluation of cardiomyocyte apoptosis would further elucidate the molecular mechanism of Notch-1 mediated cardiac protection.

.

1.5.2 Future perspectives

Our current approach reveals alterations in the expression levels of several Notch pathway components following myocardial infarction in mice. In accordance with the notion that embryonic signaling re-employment could promote tissue regeneration, we show that re-activation of Notch1 signaling protects against myocardial infarction. Due to the specificity of the Notch1 antibody (pseudoligand) used for intramyocardial injection, our study highlights the potential therapeutic value of Notch signaling manipulation following myocardial infarction.

To further support the clinical implications of our study, future research assessing the cardiac regenerative potential upon re-activation of Notch1 signaling at later time points following myocardial infarction would provide valuable insights.

However, little is known regarding the Notch1-mediated molecular mechanism that leads to protection against myocardial infarction. Hind-limb ischemia studies[237, 253] show that Notch1 signaling is required for endothelial cell proliferation and survival, further confirming our observations that neovascularization could provide the mechanistic explanation for protection against myocardial infarction after Notch1 antibody injection. Nevertheless, the possibility that Notch1 orchestrates cardiomyocyte proliferation or survival cannot be ruled out. Conditional manipulation of Notch1 signaling in the cardiomyocyte compartment in a temporally-controlled manner would increase our understanding regarding the Notch1-mediated mechanism following myocardial infarction. Hence, we have crossed our inducible NICD1 transgenic animals with a cardiomyocyte-specific temporally-controlled CRE mouse line (αMyHC-mER-CRE-mER)[312], which will allow NICD1 over-expression immediately after myocardial infarction (following tamoxifen-mediated CRE recombinase activation). As a complementary approach, we plan to inhibit Notch signaling specifically in cardiomyocytes by crossing the αMyHC-mER-CRE-mER animals with the dominant negative MAML1 mice[218, 291] and assess cardiomyocyte proliferation and survival following myocardial infarction.

1.5.3 Conclusions

Here, we investigate the role of Notch signaling in acquired heart disease following myocardial infarction in mice. We witness early changes in the expression levels of several Notch pathway components after infarction, which are reminiscent of skeletal muscle ischemia responses and zebrafish heart regeneration. Taking advantage of a previous well-designed report in skeletal muscle regeneration, we examine the cardiac regenerative potential upon re-activation of Notch-1 signaling following myocardial infarction. Similar to *thymosin-β4*[102] and *sonic hedgehog*[103] signaling re-employment during the acute ischemic period, forced activation of Notch-1 signaling immediately after myocardial infarction favors cardiac protection, likely through neovascularization, decreases fibrosis and dilatation, and improves function. Comparison of our developmental approach (NICD1:TG mice) with the study of Notch-1 signaling in the adult infarcted myocardium demonstrates that the outcome of Notch signaling activation is always context-, cell type-, and time-dependent, and further supports the notion that embryonic signaling re-employment could prove beneficial for tissue regeneration[21].

1.6 MATERIALS & METHODS

Chapter 1

Notch-1 signaling activation in cardiac development and disease

1.6 Materials & methods

1.6.1 Animals

1.6.1.1 Genotyping

Transgenic mice expressing Cre recombinase under the control of the *alpha-Myosin Heavy Chain (a-MyHC)* gene promoter[290] were crossed with *CAG/CAT;NICD1* transgenic mice[198] in order to generate transgenic animals that overexpress the intarcellular domain of Notch-1 receptor only in cardiomyocytes. Genotyping was performed by PCR using genomic DNA from tail biopsies and the PCR products were analyzed by electrophoresis on 2% agarose gels; primer sequences (table 1.7) and PCR programs (table 1.8) are provided below.

Table 1.7 Primer sequences for genotyping of *αMyHC/CRE* & CAG/CAT;NICD1 mice

transgene	PCR primers (5'- 3')
αMyHC/CRE	ATG ACA GAC AGA TCC CTC CTA TCT CC (sense) CTC ATC ACT CGT TGC ATC ATC GAC (anti-sense)
CAG/CAT;NICD1	CAG TCA GTT GCT CAA TGT ACC (sense) ACT GGT GAA ACT CAC CCA (anti-sense)

Table 1.8 PCR programs for genotyping of *αMyHC/CRE* & CAG/CAT;NICD1 mice

PCR program for *αMyHC/CRE* mice		PCR program for *CAG/CAT;NICD1* mice	
30 cycles	94°C for 1min 59°C for 1min 72°C for 45sec 72°c for 10min	35 cycles	94°C for 30sec 60°C for 30sec 72°C for 1min 72°c for 10min

1.6.1.2 Husbandry

Animals were housed in a clean, temperature controlled (22^{o}C) mouse facility on a 12-hour light/dark cycle, and standard diet was provided. Mice were weaned at post-natal day 21 (p21) and housed in same-sex groups of 3-5 per cage with pellet food and water *ab libidum*. All mouse procedures were approved by European Molecular Biology Laboratory Monterotondo Ethical Committee (Monterotondo, Italy) and were in accordance with national and European regulations. Male mice were used in all experiments.

1.6.1.3 Induction of myocardial ischemia (LAD operation)

Male C57BL6 10-12 week old mice (HARLAN) were anesthetized with isoflurane during the operation. The animals were orally incubated using a Harvard Apparatus ventilator. A small thoracoctomy was performed to expose the heart and after pericardial opening the left anterior descending (LAD) artery was ligated using 8-0 ETHILON nylon suture (ETHICON) through a dissecting microscope. After the closure of the thorax and skin using 6-0 ETHILON nylon suture (ETHICON), the animals were allowed to recover in a clean temperature controlled (22^{o}C) mouse facility and sacrificed at the indicated time points.

1.6.1.4 *In vivo* Notch-1 activation

Five minutes after myocardial ischemia induction, 10μl of a 1:4 dilution of the Notch-1 pseudoligand (Chemicon International, MAB5414) were injected in two sites (left and right) at the border zone of the ischemic myocardium. Isotype-matched hamster IgG (AbCam, ab18426) was used at the corresponding concentration for the control group of animals.

1.6.1.5 Echocardiography Analysis

Animals were anesthetized with 2% isoflurane and left hemithorax was shaved. The mice were placed on a temperature-controlled pad and heart rate was continuously monitored (400-550bpm). Ultrasound transmission gel (Parker Laboratories Inc.) was used and the heart was imaged in the parasternal short-axis view. Two-dimensional B-mode images were obtained at the papilary muscle level using the Vevo 770 Ultrasound system (VisualSonics) and fractional shortening was calculated using the using the Vevo 770 V2.2.3 software (VisualSonics).

1.6.2 Histology

1.6.2.1 Cardiac morphology & morphometric analysis

Hearts were excised at the indicated developmental stages and fixed over-night at 4% paraformaldehyde. Following progressive tissue dehydration with ethanol and xylene, the heart samples were embedded in paraffin. Eight micrometer (μm) thick cross-sections were subjected to trichrome staining (Sigma-Aldrich) for nuclei, cytoplasm and collagen visualization. Images were collected using a Leica DMR microscope and a Leica DC 500 camera (Leica Microsystems). Morphometric analysis for collagen tissue deposition was performed with MetaMorph software (version 6.2r5; Universal Imaging Corporation).

1.6.2.2 Immunohistochemistry

1.6.2.2.1 Immunofluorescence

Animals were sacrificed at the indicated time points after myocardial ischemia and the heart was excised and then fixed over-night in 4% paraformaldehyde. Following standard dehydration procedures, the heart tissue was embedded in paraffin. Eight μm thick cross-sections were produced and deparaffinized in xylene. After immersion in ethanol solutions with different concentrations (100%, 95%, 85%, 70%, 50%), antigen unmasking was performed submerging the slides in R-buffer BG (PickCell Laboratories) in a pressure-cooker apparatus. Next incubated with blocking solution (10% goat serum, 0.2% fish skin gelatin and 0.01% Tween 20). Antibodies against cleaved Notch-1 (1:100, Abcam), smooth muscle α-actin (1:200, Sigma), α-actinin (1:200, Sigma) and phospho-histone-3 (1:50, Cell Signaling) were diluted in 0.2% fish skin gelatin/0.01% Tween 20 in PBS and the slides were incubated over-night at 4^{o}C in a humidified chamber. After washing in PBS, the sections were incubated with the appropriate Cy-2, Cy-3 secondary antibodies (1:500, Jackson ImmunoResearch) for 1.5hours in the dark at room temperature. The nuclei were counterstained with DAPI and the slides were analyzed using the Leica TCS SP5 spectral confocal and multiphoton microscope system and the LAS AF software (Leica, Microsystems).

1.6.2.2.2 DAB staining

Slides were deparaffinized in xylene and rehydrated in serial ethanol concentrations. Antigen unmasking was performed in citrate buffer (10mM sodium citrate, pH 9.0 for membrane/cytoplasmic proteins or pH 6.0 for nuclear proteins) for

30min at 80°C. Quenching of endogenous peroxidase activity took place in 0.5% H_2O_2/ dH_2O for 10min and then the slides were blocked with 5% normal goat serum (DAKO) for 1h at room temperature (RT). Incubation with primary antibodies (Notch-1; 1:200/Santa Cruz, Notch-2; 1:200/Santa Cruz, smooth muscle α-actin; 1:200/Sigma) was done over-night (O/N) at 4°C. After washing in PBS, the slides were incubated with the appropriate secondary antibody (peroxidase conjugated) for 60min at RT. The slides were again washed in PBS and the DAB chromogenic reaction (Vector Laboratories) was employed in order to visualize the staining (brown color). Then, slides were dehydrated through serial ethanol concentrations and xylene and mounted permanently.

1.6.2.2.3 BrdU staining

0.1% BrdU (Sigma) was administered *ad libitum* in the drinking water for the first 2 weeks after the induction of myocardial infarction. A two-week wash-out period (normal drinking water) followed and the mice were sacrificed. Hearts were perfused and embedded in paraffin. Eight micrometer (μm) thick sections were produced and deparaffinized in xylene. Next, the slides underwent rehydration by submersion in ethanol serial solutions with different concentrations (100%, 95%, 80%, 70%, 50%) and endogenous peroxidase activity was quenched with 0.3% H_2O_2/methanol for 30min at RT. Antigen retrieval was done using citrate buffer (10mM, pH 6.0) in a microwave. Then, the slides were allowed to cool down for 30min and later incubated with the primary antibody (mouse IgG) against BrdU in the nuclease solution (RPN20EZ, Amersham Biosciences) for 1hour in a humidified chamber at 37°C. After three washes in PBS, the secondary incubation with an anti-mouse IgG horseradish peroxidase conjugated (Jackson ImmunoResearch) was performed for 2hours at RT and signals were detected with the DAB chromogenic reaction (Vector Laboratories). Dedydration in ethanol series took place and the slides were mounted permanently. Images were collected using a Leica DMR microscope and a Leica DC 500 camera (Leica Microsystems).

1.6.3 Molecular Biology

1.6.3.1 Western blot analysis

Whole protein extracts were obtained after homogenization (douncing) of the heart tissue in protein extraction buffer (20mM Tris-HCl pH 8.0, 100mM NaCl, 5mM EGTA, 2mM EDTA, 0.5% Triton-X, 100mM PMSF in ETOH, 200mM sodium orthovanadate, 1

μgr/ml aprotin) and subsequent centrifugation at maximum speed (14.000rpm) at 4°C. The supernatant was recovered and protein determination was done using Brandford method (Biorad). Forty μgr of protein lysates were separated in 10% SDS polyacrylamide mini-gel (Biorad system) and transferred onto a hybond ECL nitrocellulose membrane (Amersham). Filters were blocked with 5% milk, blotted with specific antibodies o/n at 4°C, washed with 3 times for 30min with washing buffer (TBS and 0,1% Tween-20) and blotted with specific secondary antibodies (horseradish peroxidase-conjugated, 1:5000, Amersham) with 5% milk for 1h at RT. The filter was incubated for 1 min using ECL kit (Amersham) before exposure. The following primary antibodies were used: anti-Notch-1 (1:500, Sigma), anti-Notch-2 (1:500, Hybridoma Bank, University of Iowa) and anti-jagged-1 (1:500, Santa Cruz). Anti-α-tubulin (1:2000, SIGMA) was used for normalization.

1.6.3.2 Quantitative Real Time PCR

Total RNA was isolated from hearts using TRIzol (Invitrogen). RNA was treated with DNaseI enzyme (Promega) for 1h at 37°C and then cleaned by column purification (Qiagen). The RNA concentration was determined with a spectrophotometer. After RNA quality verification, 1-2μg were used to prepare cDNA (Ready-To-Go, T-Primed First-Strand Kit, Amersham Bioscience). Inventoried TaqMan FAM probes (Applied Biosystems) were used for the relative quantification of the mRNA levels of *Notch-1, Notch-2, Notch-3, Notch-4, Jagged-1, hairy enhancer of split-1(Hes-1), hes-related-1(Hey-1), Hes-related-2 (Hey-2), myosin heavy chain-6 (Myh6), myosin heavy chain-7 (Myh7), atrial natriuretic peptide (Anp), brain natriuretic peptide (Bnp), glucose transporter-1 (Glut-1), actin-alpha–1 skeletal muscle (Acta-1), GATA binding protein 4 (Gata-4),* and *NK2 transcription factor related, locus 5 (Nkx2.5)* genes. Taqman VIC *Glyceraldehyde 3-phosphate dehydrogenase (GAPDH)* probes were used for normalization (table 1.9).

Table 1.9 Genes & TaqMan assays used	
gene	*assay part number*
Anp	Mm01255747_g1
Bnp	Mm00435304_g1
Myh6	Mm00440354_m1
Myh7	Mm00600555_m1
Glut1	Mm00441473_m1
Acta1	Mm00808218_g1
Nkx2.5	Mm00657783_m1
Gata-4	Mm00484689_m1
Notch1	Mm00435245_m1
Notch2	Mm00803077_m1
Hey1	Mm00468865_m1
Hey2	Mm00469280_m1
Hes1	Mm01342805_m1
Gapdh	4352339E

1.6.4 Statistics

Statistical analysis was performed using the student's *t* test (tail 2, type 2). Values were expressed as mean ± SEM and differences with p value < 0.05 were considered significant (* $p < 0.05$, ** $p < 0.01$, *** $p < 0.001$).

CHAPTER 2

Cardiac-restricted *Nemo* gene inactivation leads to dilated cardiomyopathy

2.1 BACKGROUND

2.1 Background

2.1.1 Dilated cardiomyopathies - Introduction

Dilated cardiomyopathy (DCM) is the most common form of heart disease (60% of all cardiomyopathies) characterized by ventricular dilation, impaired systolic function and distortion of the mitral valve apparatus, leading to mitral regurgitation[313, 314]. DCM is one of the major causes of sudden cardiac death and can manifest at any age, though predominantly after middle age. Patients with DCM either demonstrate severe heart failure or are symptomless. The incidence of DCM has been estimated to 5 - 8 in 100,000 per year in the United States and Europe[315, 316].

2.1.2 Common genetic mutations in dilated cardiomyopathy (DCM)

It is estimated that 70% of all DCM are acquired due to sporadic mutations, whereas 30% of DCMs are considered to be inherited[317]. DCM form a heterogeneous group of disorders with different patterns of inheritance, including autosomal dominant (~60%), autosomal recessive (~16%), X-linked (~10%) and mitochondrial transmission (8%)[318]. Besides genetic mutations, biomechanical stress resulting from myocardial ischaemia, hypertension and other forms of myocardial injury can also cause progression to DCM[72]. Recent advancements in mouse genetics and publicly available databases of gene sequence variants associated with disease conditions have advanced our understanding regarding the genetic basis for the development of DCM. The progression from normal state to DCM involves severe changes in gene expression of structural, calcium-regulator, and survival proteins which can reflect the primary cause of dilation or a secondary effect[59, 72]. Hence, genes that transcribe for *cytoskeletal*, *calcium-handling* or *apoptosis/survival* related proteins have been identified as genetic modifiers of dilated cardiomyopathy.

2.1.2.1 Cytoskeletal mutations in dilated cardiomyopathy

(i) Dystrophin. The dystrophin gene (X-linked) is the largest human gene, spanning more than 3Mb, with 79 exons and 7 different promoters[319]. Dystrophin links the sarcomere to the extracellular space and plays a key role in force transmission and intracellular organization (fig.2.1). Mutations in the dystrophin gene contribute mainly to

syndromes affecting the skeletal muscle such as Duchene and Becker muscular dystrophies[319, 320]. Mutations on the 5' end of the gene change the ratio between cardiac and skeletal muscle dystrophin isoforms and lead to DCM development with no skeletal muscle defects[321-323]. This disease is often present in young males and termed X-linked dilated cardiomyopathy (XLDC)[324-326].

(ii) *δ-sarcoglycan.* Mutations in the *δ-sarcoglycan* gene cause limb girdle muscle dystrophy (LGMD), which is sometimes associated with dilated cardiomyopathy[327, 328].

(iii) *Cadiac muscle LIM protein (CLP).* CLP is a key component of the cardiomyocyte stretch-sensor machinery and interacts with α-actinin and telothin (fig.2.1)[329] . Human and mouse mutations in the CLP gene cause changes in the secondary structure of the protein, defects in the cardiomyocyte stretch-sensor machinery and dilated cardiomyopathy[330, 331].

(iv) *α-actinin*. The α-actinin protein is localized as a homodimer at the Z-disc and facilitates to anchor actin filaments. Rare mutations linked to the development of DCM have been identified in the α-actinin gene[330].

(v) *Lamin A/C*. Lamins (A, B, and C) are located at the inner layer of the nuclear envelope and connect it with the nuclear matrix and chromatins (fig.2.1). Human and animal studies demonstrate that the absence of lamin A/C gene leads to dilated cardiomyopathy and highlight that mutations throughout the entire cytoskeletal network could lead to chamber dilation[332, 333].

It is noteworthy that mutations affecting proteins in the sarcomere (contractile machinery of the heart muscle) lead to familial hypertrophic cardiomyopathy, which is not accompanied by chamber dilation. Mutations in *cardiac actin*[334], *β-myosin heavy chain*[335], *desmin*[336], *titin*[337] and other sarcomeric genes affect force transmission and heart muscle contractility resulting in hypertrophic cardiomyopathy. It is believed that unknown genetic modifiers can promote the transition from hypertrophic to dilated cardiomyopathy[338].

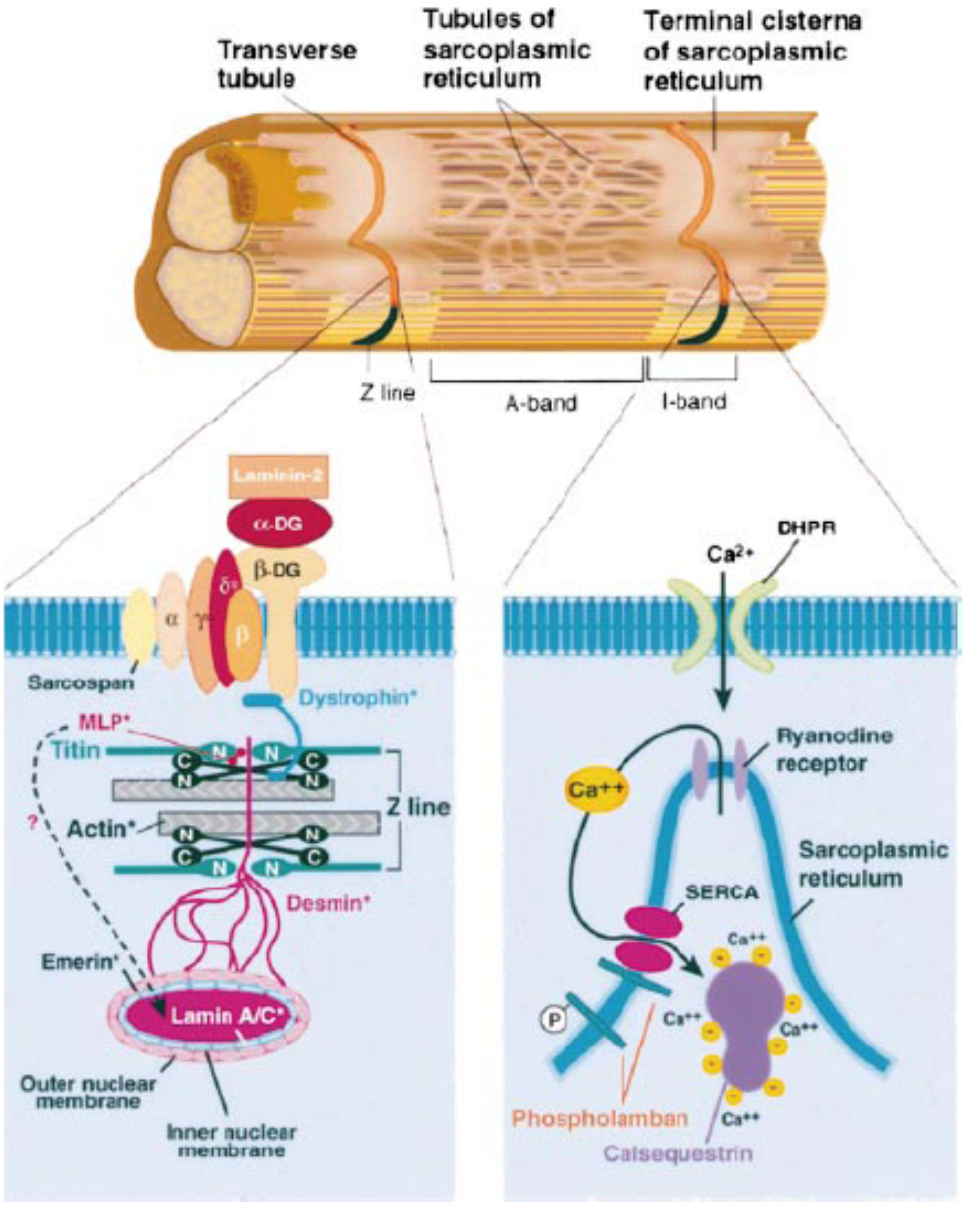

Figure 2.1 Cytoskeletal protein network and calcium-cycling in cardiomyocytes. The upper panel represents two myofibrils and associated sarcoplasmic reticulum within a cardiomyocyte in three-dimensional fashion. The bottom left panel illustrates the cytoskeletal protein network that connects the extracellular matrix (laminin-2) and the nucleus (lamin A/C) via the dystrophin-glycoprotein complex. Asterisks indicate mutations that cause dilated cardiomyopathy. The bottom right panel shows the calcium cycling mechanism in the sarcoplasmic reticulum of cardiomyocytes. Details about the proteins involved are provided in the text *(adapted from Chien, 1999)*

2.1.2.2 Impaired calcium-handling in dilated cardiomyopathy

The primary functional defect in end-stage heart failure and dilated cardiomyopathy is profound loss of cardiac contractility. Although the distinction between primary and secondary events is difficult, mutations in calcium regulatory genes highlight the fundamental role of calcium currents in cardiac muscle contraction.

(i) *sarcoplasmic reticulum calcium ATPase-2 (SERCA-2).* During systole, calcium enters into the cardiomyocytes through the dihydropyridine receptor (DHPR) and sequesters in the sarcoplasmic reticulum via the SERCA-2 action, leading to cardiac relaxation (fig.2.1). Moreover, SERCA-2 activity is negatively regulated by phospholamdan, an endogenous muscle-specific inhibitor[339]. Intriguingly, mice lacking phospholamban display an augmentation in cardiac contractility and relaxation, whereas transgenic mice carrying a point mutation (Arg9Cys) recapitulate the DCM phenotype.

(ii) β-adrenergic receptor pathway. β-adrenergic receptors are G-coupled receptors activated by catecholamines. In cardiac muscle, activation of b-adrenergic receptors leads to an increase in heart rate, energy consumption and vasodilation. *β-adrenergic* pathways regulate phospholamban activity by phosphorylation and lead to increases in SERCA 2 ATPase activity in the sarcoplasmic reticulum. Several mutations in β-adrenergic pathway components have demonstrated increased ventricular contractile function in mice[340-342]

2.1.2.3 Survival pathways in dilated cardiomyopathy

Cardiomyocyte cell death promotes the transition from pathological hypertrophy to cardiac dilation. Critical signaling pathways that tune the fine balance between hypertrophy and apoptosis are presented below.

(i) Gp130 cytokine receptor pathway

Cytokines play critical roles in mammalian physiology and their increased expression levels in the circulation or at the myocardium have been associated with heart failure[343]. The interleukin-6 (IL-6) family of cytokines consists of IL-6, leukemia inhibitory factor (LIF), ciliary neurotrophic factor (CNTF) and IL-11 receptor α. Gp130 has been identified as a co-receptor of the IL-6 family of cytokines and complete deficiency of gp130 in mice results in embryonic lethality and hypoplastic ventricular myocardium[110]. In addition, conditional inactivation of gp130 demonstrated normal

cardiac function under baseline conditions but rapid progression to dilated cardiomyopathy and myocyte apoptosis in a pressure-overload model[69].

(ii) *Ga_q pathway.* The α subunit of the heterotrimeric quinine nucleotide-binding proteins (G proteins) of the Gq family (Ga_q) is a widely expressed regulator of growth and death downstream of G-protein-coupled receptors (GPCRs). Studies in neonatal cardiomyocytes demonstrated a direct link between initiation of apoptosis and constitutively active Ga_q[344]. Moreover, overexpression studies in mice associated increased Ga_q activity with marked chamber dilation accompanied by excessive cell death[345, 346].

(iii) *TNFα/NFκB pathway.* A growing body of evidence suggests that cytokines, such as tumor necrosis factor α (TNFα) and cardiotrophin-1 (CT-1), are expressed in the cardiomyocytes upon ischemic or hypertrophic stress, as well as in infiltrating macrophages and leucocytes[347, 348]. TNFα is a soluble, widely expressed cytokine involved in inflammatory/antiviral responses, cell death and proliferation. *In vitro* and *in vivo* approaches demonstrate cardiomyocyte-autonomous actions for TNFα which are required for pro-apoptotic pathway activation and progression to dilated cardiomyopathy[70, 71]. Another arm of TNFα signaling activates the canonical Nuclear Factor- κB (NF-κB) pathway, and more detailed information regarding the involvement of NFκB in pathological hypertrophy is provided below.

2.1.3 NF-κB signaling pathway

2.1.3.1 Introduction

Nuclear Factor- κB (NF-κB) was first identified in the lab of the Nobel Prize laureate David Baltimore in 1986. Although initially described in B cells of the immune system, a growing body of literature suggests that NF-κB is a pleiotropic and almost ubiquitously expressed transcription factor[349]. Twenty years following the discovery of NF-κB signaling, much of our understanding derives from studies in the immune system. However, *in vitro* and *in vivo* findings extend the actions of NF-κB beyond innate and adaptive immunity to influence gene expression events with a pivotal role in cell survival, differentiation and proliferation[350, 351]. The diversity of the NF-κB biological roles is reflected in recent reports where dysregulation of the pathway is described to be associated with a broad spectrum of human and mouse pathologies [350, 352-356].

2.1.3.2 NF-κB pathway components

The NF-κB signaling pathway demonstrates several levels of regulation and a series of positive and negative feedback mechanisms. In brief, a plethora of endogenous (cytokines) or exogenous (viruses, bacteria) stimuli can activate NF-κB signaling through binding to several membrane receptors (presented below). Signal transduction via receptor proximal adaptor molecules leads to the activation of the Inhibitor of κB Kinase (IKK) complex, a central component in the NF-κB pathway. Upon IKK activation, the Inhibitor of κB (IκB) is phosphorylated and degraded through the proteosomal pathway. As a result, the NF-κB dimers translocate to the nucleus, bind to their DNA binding sites and regulate expression of genes involved in apoptosis, survival, proliferation and immune responses. A simplified attempt to describe the key NF-κB signaling components is presented below.

(i) NF-κB/Rel family proteins.

The NF-κB family of transcription factors consists of five members, p50, p52, p65 (RelA), RelB and c-Rel, which all share a Rel homology domain (RHD) critical for homo- or heterodimerization and DNA binding[357]. NF-κB transcription factors act in a dimeric fashion by binding to consensus κB sites (5' GGGRNWYYCC 3', N-any base; R-purine; W- adenine or thymine; and Y-pyrimidine) within promoters or enhancers of NF-κB targets[358] and regulate transcription through recruitment of coactivators or corepressors. Moreover, structural studies reveal that p65, RelB and c-Rel contain a C-terminal transcription activation domain (TAD) necessary for positive regulation of NF-κB target gene transcription (fig.2.2). On the other hand, the NF-κB proteins p50 and p52 are generated by proteolytic cleavage of precursor p105 and p100 proteins, respectively. It is believed that p50 or p52 homodimers, which lack TAD, repress target gene transcription until displaced by transcriptionally competent NF-κB dimers. The main activated form of NF-κB is a heterodimer of the p65 subunit with p50 or p52 subunit[359].

(ii) IκB family proteins.

In unstimulated cells, the NF-κB dimers are kept inactive in the cytoplasm through association with Inhibitor of κB (IκB) proteins. The IκB proteins are characterized by ankyrin repeat domains which mediate protein-protein interactions[360]. The IκB family consists of three typical IκB proteins, IκBα, IκBβ,and IκBε and the precursor p100 and

p105 proteins (fig.2.2). IκBα is the most extensively studied member of the family, masking the nuclear localization signal (NLS) of p65 protein and preventing the nuclear translocation of NF-κB p50/p65 dimers. Moreover, a nuclear–export signal (NES) unique to IκBα protein regulates the shuttling of NF-κB dimers out of the nucleus. Interestingly, three atypical, inducibly expressed IκB proteins have been recently identified, IκBγ, IκBζ and bcl-3. In contrast to the inhibitory function of the other IκBs, bcl-3 has been shown to interact with p50 or p52 homodimers and induce transcription of NF-κB target genes[361].

(iii) IKK complex.

The IκB kinase (IKK) complex is a converging point for NF-κB signal responsiveness. It consists of two catalytic subunits, IKK1/IKKα or IKK2/IKKβ, and a regulatory subunit, IKKγ/NEMO (NF-κB essential modulator). All IKKs contain a leucine zipper (LZ) and a helix-loop-helix (HLH) domain that are involved in protein-protein interactions but a kinase activity domain is exclusive to IKK1 and IKK2 (fig.2.2). Upon ligand/receptor induced activation, the IKK complex is activated and subsequently phosphorylates the IκB proteins (IκBα, IκBβ, and IκBε) which become targets for ubiquitination and proteosomal degradation. Hence, the translocation of NF-κB dimers to the nucleus is achieved. The molecular mechanisms regarding IKK activation are poorly understood but can be summarized in two senarios. One possibility is that upon receptor activation, an upstream kinase becomes activated and phosphorylates the IKK complex. Alternatively, upon receptor activation, a scaffold protein could recruit the IKK complex at the receptor's vicinity and induce IKK conformational changes and autophosphorylation[351].

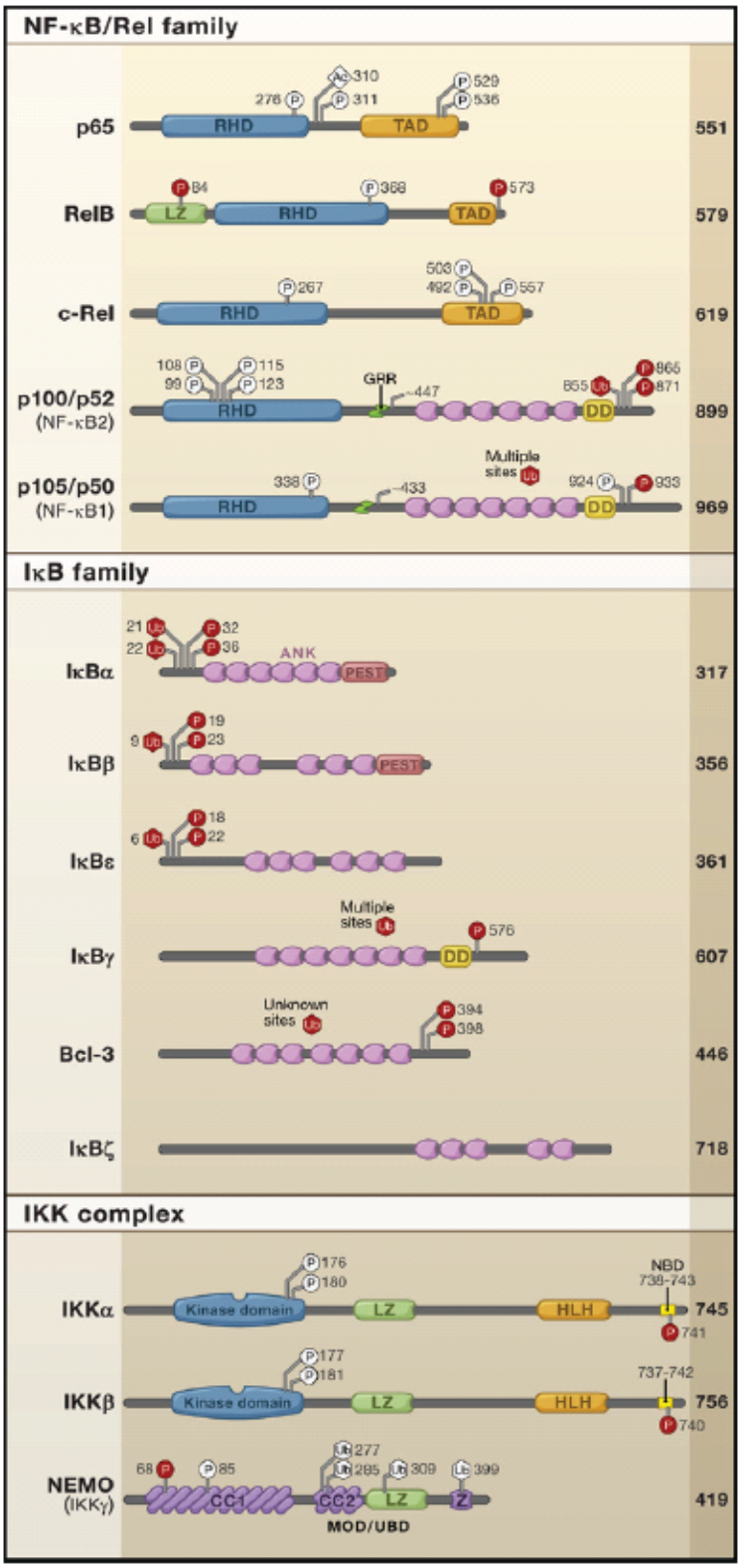

Figure 2.2 The NF-κB, IκB, a nd IKK protein families. All the members of NF-κB, IκB, and IKK protein families are presented. The number of amino acids of each human protein is given at the right highlighted column. The structure of each protein is discussed in the text. Post-translational modifications - that regulate IKK activation and NF-κB transcriptional activity - such as acetylation, phosphorylation and ubiquitination are indicated with Ac, P, and Ub, respectively. Moreover, inhibitory events of ubiquitination and phosphorylation on p100, p105 and IκB proteins that lead to proteosomal degradation are highlighted with red Ub and P, respectively. RHD, Rel homology domain; TAD, transactivation domain; LZ, leucine zipper domain; GRR, glycine-rich region; HLH, helix-loop-helix domain; Z, zing finger domain; CC1/2, coiled-coil domains; NBD, NEMO binding domain; MOD/UBD, minimal oligomerization domain/ubiquitin binding domain; and DD, death domain. *(adapted from Hayden & Ghosh, 2008)*

IKK1/IKKα & IKK2/IKKβ. IKK1 and IKK2 dimerize using the LZ domain and they both bind to NEMO through their C-terminal hexa-peptide NEMO-binding domain (NBD) (fig.2.2). In vitro findings reveal that NF-κB signal transduction is completely blocked in the absence of IKK1 and IKK2 proteins[362]. Competition assays reveal higher NEMO-binding affinity for IKK2 respective to IKK1 and genetic analysis of several IKK1 and IKK2 mutants demonstrates their distinct *in vivo* roles[363]. The IKK2 subunit is an essential component of the so-called canonical NF-κB pathway, where NF-κB-related receptors are activated and signal via the IKK1/IKK2/NEMO complex allow the p50/p65 nuclear translocation. In support of this notion, IKK2-mutant mice display similar phenotype with p65 knock-out mice characterized by embryonic lethality due to massive liver apoptosis[364]. Importantly, the IKK2 mutant phenotype can be rescued if *Ikk2*$^{-/-}$mice are crossed with mice lacking the *tumor necrosis factor receptor -1 (Tnfr1*$^{-/-}$*)* mutant mice, which indicates that TNFR1 is a key receptor in the canonical NF-κB pathway[364].

Alternatively, IKK1 is a crucial signaling component of the so-called alternative NF-κB pathway as it is suggested by several lines of evidence. First, *Ikk1*$^{-/-}$ mice display different phenotype from the *Ikk2*$^{-/-}$ mice characterized by perinatal lethality, defects in keratinocyte differentiation, and impaired transcription of certain NF-κB target genes[365, 366] . Second, the alternative NF-κB pathway is characterized by processing of the p100 precursor to p52, an event solely dependent to the activation of IKK1 by the NF-κB-inducing kinase (NIK)[367] . Next, *Ikk1*$^{-/-}$ and *Nik*$^{-/-}$ mice display similar phenotypes while IKK2 and NEMO actions are dispensable for the alternative NF-κB pathway[368, 369]. Finally, IKK2-dependent NF-κB signaling is required for activation of innate immunity whereas IKK1-dependent signals are important for regulation of adaptive immunity and lymphoid organogenesis[370].

IKKγ/NEMO. NF-κB essential modulator (NEMO) was initially described as a component of the IKK complex by genetic complementation experiments in a cell line non-responsive to NF-κB stimuli[371, 372]. Although structural data for NEMO is missing, structure prediction algorithms suggest that NEMO is a helical protein containing large coiled-coil domains (CC), a leucine-zipper (LZ), and a zinc-finger (ZF) domain, all important for protein-protein interactions (fig.2.2). The precise role of NEMO in the IKK complex is still obscure. Biochemical analysis reveals that the IKK complex has a high molecular weight that cannot be justified by the presence of IKK1, IKK2 and NEMO alone. In accordance with these observations, it has been proposed that the IKK

complex contains two IKK1/IKK2 dimers and the NEMO oligomer within this complex forms a tetramer[373]. Most probably, NEMO serves as a scaffold that brings together IKK1 and IKK2 and promotes their trans-autophosphorylation. Alternatively, it has been proposed that NEMO brings the IKK complex at the vicinity of other proteins, most likely kinases, which phosphorylate and subsequently activate the IKK subunits[374].

Although NEMO is not required for the activation of the IKK1-dependent NF-κB alternative pathway, *in vivo* findings suggest that NEMO is required for activation of the IKK2-dependent classical NF-κB pathway and the IKK complex formation[369]. Mice lacking *Nemo* die embryonically due to massive liver apoptosis and *Nemo*-deficient cells exhibit no response to known NF-κB stimuli[375]. *Nemo* gene is located on the X chromosome and mutations of the *Nemo* gene are associated with two human conditions – anhidrotic ectodermal dysplasia with immunodeficiency and incontinentia pigmenti[376, 377]. Interestingly, NEMO-mutant heterozygous female mice phenocopy the symptoms of the human condition incontinentia pigmenti characterized by keratinocyte hyperproliferation and increased apoptosis[378, 379]. Recently, an additional role for NEMO has been described where DNA double-strand breaks induce NEMO sumoylation, subsequent ubiquitination, nuclear shuttling and regulation of NF-κB target gene transcription[380].

(iv) Converging signals to IKK complex.

A remarkable variety of stimulus/receptor interactions leads to activation of receptor-proximal adaptor molecules that converge and transduce signals to the IKK complex. The main pathways that lead to NF-κB activation are presented below (fig.2.3).

Toll-like receptor mediated NF-κB activation. Several pathogens such as lipopolysacharide (LPS), peptidylglycans, lipoproteins, bacterial or viral nucleic acids can be recognized by specific-pattern recognition receptors (PRR) that have evolved in order to initiate immunological responses. The most known family of PRRs is the Toll-like receptor family which counts ten members (TLR1-10) in mammals (fig.2.3). Upon activation by various bacterial wall components (LPS, zymosan, lipoprotein, peptidoglycan), TLRs mediate the activation of intracellular signaling pathways that result in NF-κB activation[381]. Biochemical and genetic evidence demonstrates that LPS stimulation activates several adaptor proteins (MYD88, IRAK) downstream of TLR4 and

causes the formation of a trimeric TAB1/TAB2/TAK1 complex that eventually relays signals to IKK complex[359, 382]. *(abbreviations in fig. 2.3)*

Cytokine-mediated NF-κB activation. Cytokines such as tumor necrosis factor (TNF) and interleukine-1 (IL-1) represent a very common group of NF-κB stimuli. TNF is mainly produced by macrophages and monocytes and binds to the TNF receptor family proteins (fig 2.3). Two receptors, TNF-R1 and TNF-R2 comprise the TNF-R family and display a wide range of expression but lack enzymatic activity. TNFR family members can activate either the canonical or the non-canonical NF-κB pathway. Upon TNF stimulation, adaptor proteins like TRADD and TRAF are being recruited to the receptor and lead to IKK complex activation via receptor interacting proteins (RIP) and MEKK3[383, 384]. In addition, it has been shown that RIPs can bind to NEMO and mediate the interaction between IKK complex and upstream signaling cassettes[385, 386]. As far as it concerns IL-1 mediated NF-κB activation, a similar to TNF mechanism of action takes place since the intracellular domain of the IL-1 receptor (IL-1R) and TNF-receptor (TNF-R) share remarkable homology[387] *(abbreviations in fig. 2.3)* .

T-cell receptor-mediated NF-κB activation. Upon antigen presentation to the peripheral T-cells, the T-cell receptor (TCR) requires co-stimulation by CD28 in order to induce signaling cascades that activate NF-κB pathway (fig.2.3). Protein kinase Cθ (PKCθ) is the adaptor molecule required for the activation of the membrane-associated kinase complex of MAGUK/MALT1/BCL-10 and subsequent activation of the IKK complex[388-390]. Consistent with this senario, PKCθ$^{-/-}$ T cells fail to activate NF-κB signaling and display impaired IL-2 production[391]. It is also noteworthy that antigen presentation to the B cell receptor induces NF-κB activity following similar signaling cassettes[392] *(abbreviations in fig. 2.3)* .

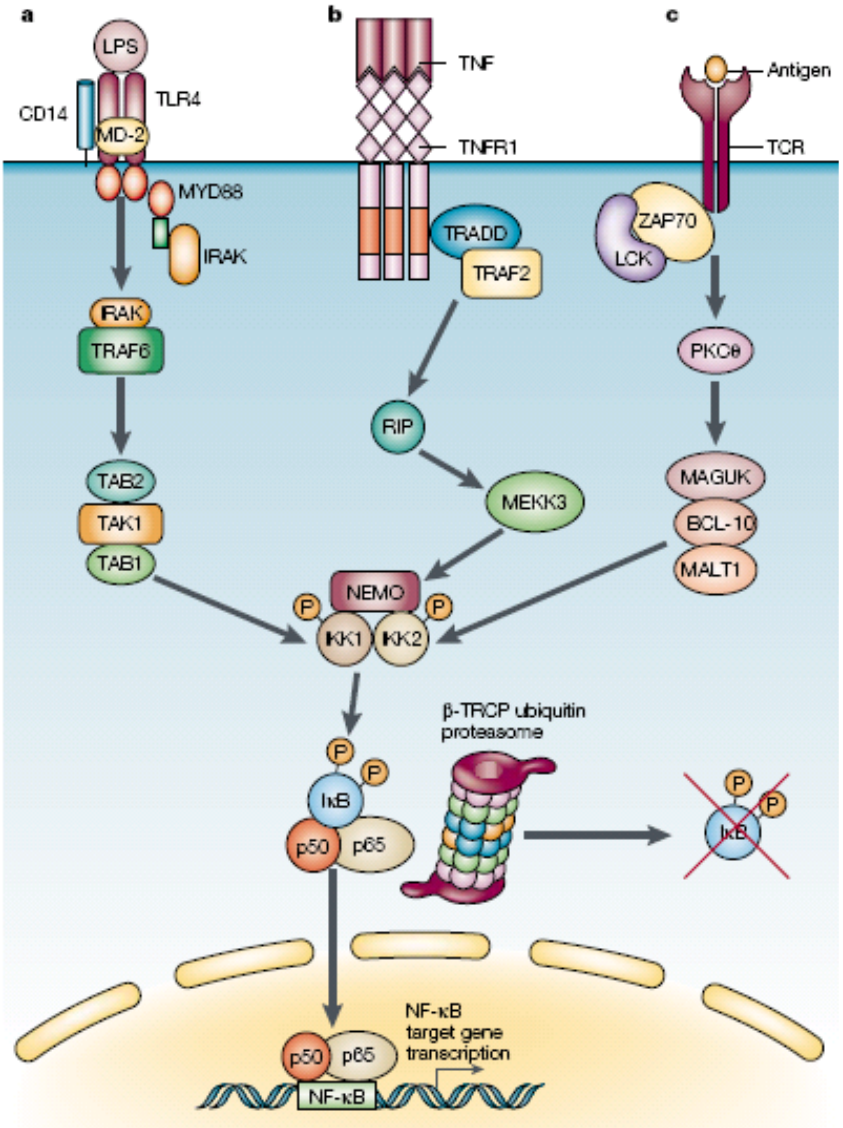

Figure 2.3 Main NF-κB signaling pathways. Toll-like receptor (TLR)-, tumor necrosis factor receptor (TNFR)-, and T-cell receptor (TCR)-mediated signaling summarizes the main inductive signals for NF-κB transcriptional activity. The IKK complex (IKK1, IKK2, and NEMO) is a converging point downstream these receptors and allows the nuclear translocation of NF-κB dimers (p50/p65) upon phosphorylation of the inhibitor of κB (IκB) proteins. **a.** LPS stimulation of the Toll-like receptor 4 (TLR-4)-CD14-MD-2 transmembrane complex induces intracellular signaling events through the recruitment of MYD88 (myeloid differentiation primary response gene 88) and IRAK (interleukin-1-receptor-associated kinase). Activation of IRAK induces the phosphorylation of TNF-receptor-associated factor 6 (TRAF6), which through the TAB1/TAK1/TAB2 complex relays signals to the IKK complex. **b.** TNF signals induce TNF receptor 1 (TNFR1) trimerization and recruitment of the adaptor proteins TRADD and TRAF2. Next, the signal is transduced to the MAP/ERK kinase 3 (MEKK3) through the receptor interacting protein (RIP), which subsequently leads to IKK complex activation. **c.** Following antigen presentation to the T-cell receptor (TCR) adaptor proteins (LCK, ZAP70) are recruited to the intracellular domain of the receptor and activate the protein kinase Cθ (PKCθ). Although the mechanism for the PKCθ-mediated IKK complex activation is poorly understood, the trimolecular complex MAGUK/BCL-10/MALT1 is likely to be the intermediate link. (membrane-associated guanylate kinase homologue, MAGUK; mucosal-associated lymphoid tissue protein 1, MALT1; extracellular signal-regulated kinase, ERK; mitogen activated protein, MAP; TAK1-binding protein, TAB1; transforming-growth-factor β-activated kinase 1, TAK1; TNF receptor associated via death domain protein, TRADD; leukocyte-specific tyrosine kinase, LCK; ζ-chain-associated protein kinase 70 kDa, ZAP70) *(adapted from Li & Verma, 2002).*

2.1.3.3 NF-κB target genes

NF-κB dimers bind to the promoter sequences of a plethora of genes and regulate their transcription. Although the spectrum of NF-κB target genes is continuously growing, the majority of them encode inflammatory proteins. Chemokines such as macrophage inflammatory protein 1α (MIP-1α), monocyte chemoattractant protein 1 (MCP-1) and interleukin-8 (IL-8) and cytokines such as IL-1β, IL-4, IL-5, IL-6 and tumor necrosis factor α (TNFα) are well-described NF-κB targets. In addition, enzymes (cyclooxygenase-2, cox-2; inducible nitric oxide synthase, iNOS) and adhesion molecules (vascular cell adhesion molecule 1, VCAM-1; intracellular cell adhesion molecule 1, ICAM-1) important for the resolution of inflammatory responses are regulated by NF-κB. It is also noteworthy that several NF-κB targets such as TNFα and IL-1β can also activate the NF-κB pathway through a positive feedback loop mechanism upon their binding to corresponding receptors (TNF receptors, TNFRs and interleukin receptors, ILRs)[351] .

2.1.4 NF-κB signaling in cardiac development

The role of NF-κB signaling in cardiac development is poorly understood possibly due to embryonic lethality and functional redundancy observed in NF-κB mutant mice[364, 393-395]. Despite the numerous approaches for global targeting of several NF-κB pathway components, only two reports suggest the challenging scenario of NF-κB signals being required for proper cardiac formation. First, mice deficient for Fas-associated death domain (FADD) protein display early embryonic lethality (e11.5), thin myocardial wall and impaired trabeculae formation[396]. FADD is an adaptor protein downstream the TNF receptor family that mediates signal transduction to the caspase cascade or the canonical NF-κB pathway. Second, mouse mutants for *NF-κB interacting protein 1 (Nkip1)* show abnormal skin and cardiac development[397]. Signs of inflammatory lesions are present in the right ventricular wall at birth and dilated cardiomyopathy is established rapidly in the *Nkip1* mutants as a result of excessive inflammation in the myocardial wall. Although these findings suggest possible involvement of the NF-κB signaling in cardiac development, conditional inactivation of several NF-κB pathway components is necessary to provide further insight into the role of NF-κB in cardiac development.

2.1.5 NF-κB signaling in cardiac hypertrophy

Studies on humans or animals with heart failure reveal up-regulated systemic or cardiac cytokine levels and highlight the involvement of NF-κB signaling in the pathology of myocardial infarction and cardiac hypertrophy[398-401]. Despite the early embryonic lethality observed in mice lacking crucial NF-κB pathway components[364, 393, 402] and possible functional redundancy issues, the potential importance of NF-κB signals in cardiac hypertrophy is indicated by several lines of evidence[394, 395, 403].

It has been recently demonstrated that NF-κB pathway is activated in primary neonatal cardiomyocytes or in adult cardiomyocytes that undergo hypertrophic growth[399, 400]. These reports raise the possibility that NF-κB activity may be required for cardiac hypertrophy in the adult heart. Consistent with this hypothesis, mice with targeted disruption of the p50 subunit ($p50^{-/-}$) display attenuated hypertrophy, improved survival and cardiac function in experimental models of induced-pathological hypertrophy[404, 405]. In support of these findings, transgenic mice that express an NF-κB "super-suppressor" (mutated IκBα) in cardiomyocytes display also attenuated hypertrophy in the same model of induced cardiac hypertrophy and provide the first indication of a cardiomyocyte-autonomous NF-κB requirement in the development of cardiac hypertrophy[406].

Recent advances in mouse genetics demonstrate a cardiomyocyte-autonomous pro-apoptotic role for the tumor necrosis factor α (TNFα) in the transition from pathological hypertrophy to dilated cardiomyopathy[70, 71, 407]. Transgenic mice that overexpress TNFα in cardiomyocyte-restricted fashion develop pathological hypertrophy associated with myocyte apoptosis and transition to dilated cardiomyopathy[408, 409]. The proposed model for TNFα-induced cardiomyocyte apoptosis involves binding to TNF receptor 1 (TNFR) and subsequent activation of the caspase cascade[408, 410].

The other arm of TNF signaling involves NF-κB pathway activation and subsequent regulation of matrix metalloproteinase expression. Matrix metalloproteinases (MMPs) and their inhibitors (tissue inhibitors of matrix metalloproteinases, TIMPs) are key mediators of myocardial remodeling after an insult. Interestingly, MMP promoters contain NF-κB binding sites and TNFα stimulation of adult rat cardiac fibroblasts leads to increased MMP activity[411]. Increased levels of MMPs have been described in myocardial samples from patients with heart failure and mice lacking TIMP1 develop dilated cardiomyopathy[412-414]. Further evidence for the notion that NF-κB pathway regulates MMP activity is provided by a clinical study where increased TNF receptor activity was associated with increased MMP activity in patients with heart failure[405, 415].

In addition to its role in apoptosis, NF-κB pathway regulates the transcription of anti-apoptotic genes, such as inhibitor of apoptosis (IAP) and Bcl-2 family members[416]. The anti-apoptotic effects of NF-κB in the heart have been appreciated in several reports where NF-κB inhibition led to increased myocyte apoptosis and deterioration of cardiac function after infarction[417-419]. Interestingly, it has been demonstrated that the anti-apoptotic protein A20 can inhibit NF-κB signaling and hypertrophic response in primary cardiomyocytes[420]. Moreover, cardiac-restricted over-expression of the anti-apoptotic gene *bcl-2* partially rescues the TNFα-induced cardiomyopathy in mice[408].

Additional lines of evidence also indicate the involvement of NF-κB signaling in pathological hypertrophy; a) the interleukin-6 (IL-6) family of cytokines mediates hypertrophy in primary cardiomyocytes[421], b) Toll-like receptor-4 (TLR4) is activated in human cardiomyopathy samples [422] and is required for cardiac hypertrophy in mice[423], and c) the NF-κB target gene iNOS (Inducible Nitric Oxide Synthase (iNOS) and the cytokine IL-1β gene are abundantly expressed in patients with dilated cardiomyopathy[424, 425].

In summary, the role of NF-κB in cardiac pathophysiology has yet to be demonstrated since null mice for several NF-κB elements demonstrate either fetal lethality or functional redundancy[394, 426 393, 395, 402, 427]. Recent studies using pharmacological NF-κB inhibitors or null mice for NF-κB elements demonstrated confusing results concerning the role of NF-κB pathway in ischemia-induced heart failure possibly due to lack of specificity or functional redundancy issues, respectively[428, 429]. Furthermore, it has been shown that NF-κB activation is required for the development of cardiomyocyte hypertrophy *in vitro*[400] and *in vivo*[399, 404, 406]. However, the precise role of NF-κB in physiological and pathological cardiac conditions is highly debatable due to the fact that NF-κB activation has diverse effects on different cell types and/or different stages of cardiovascular disorders.

2.2 RESULTS

2.2 Results

2.2.1 Rationale

To overcome the aforementioned limitations in the field, I sought to study the role of NF-κB pathway in heart development and disease by targeting the NEMO (NF-κB essential modulator) subunit specifically in cardiomyocytes. Due to the early embryonic lethality of *null Nemo* mice, the specific role of *Nemo* gene in the myocardium remains to be elucidated[378]. Generation of loxP-flanked alleles of the *Nemo* gene allows the generation of cardiac-specific *Nemo* knockout ($Nemo^{hko}$) mice by crossing mice carrying the floxed *Nemo* alleles to driver strains expressing Cre recombinase under the control of α-Myosin Heavy Chain (α-MyHC) gene promoter. The following sections describe the details of this approach to achieve cardiomyocyte specific inhibition of the NF-κB pathway, and the resulting effects on cardiac function.

2.2.2 Conditional inactivation of the *Nemo* gene in the myocardium

Transgenic mice expressing CRE recombinase under the control of α-MyHC gene promoter[290] (fig.2.4 a) were crossed with *Nemo* floxed mice ($Nemo^{fl/fl}$)[378] in order to allow conditional inactivation of the *Nemo* gene in cardiomyocytes. *Nemo* floxed ($Nemo^{fl/fl}$) mice have been previously generated by placing the second exon of the gene between two loxP sites[378]. Cre recombinase-mediated excision of the second exon results in a frameshift followed by a premature stop codon (fig.2.4 b).

The regulatory region upstream of Cre recombinase consists of the 3'UTR of *β-Myosin heavy chain (β-MyHC) gene,* the entire promoter sequence and the first three exons of *α-myosin heavy chain (α-MyHC)* gene. Cre reporter assays demonstrated gene excision in atrial and ventricular cardiomyocytes, beginning of Cre expression at embryonic day 8 (e8) and peak of Cre recombinase activity after birth. It has to be also reported that the *α-MyHC* gene promoter is also active in the pulmonary vessels (pulmonary myocardium)[290].

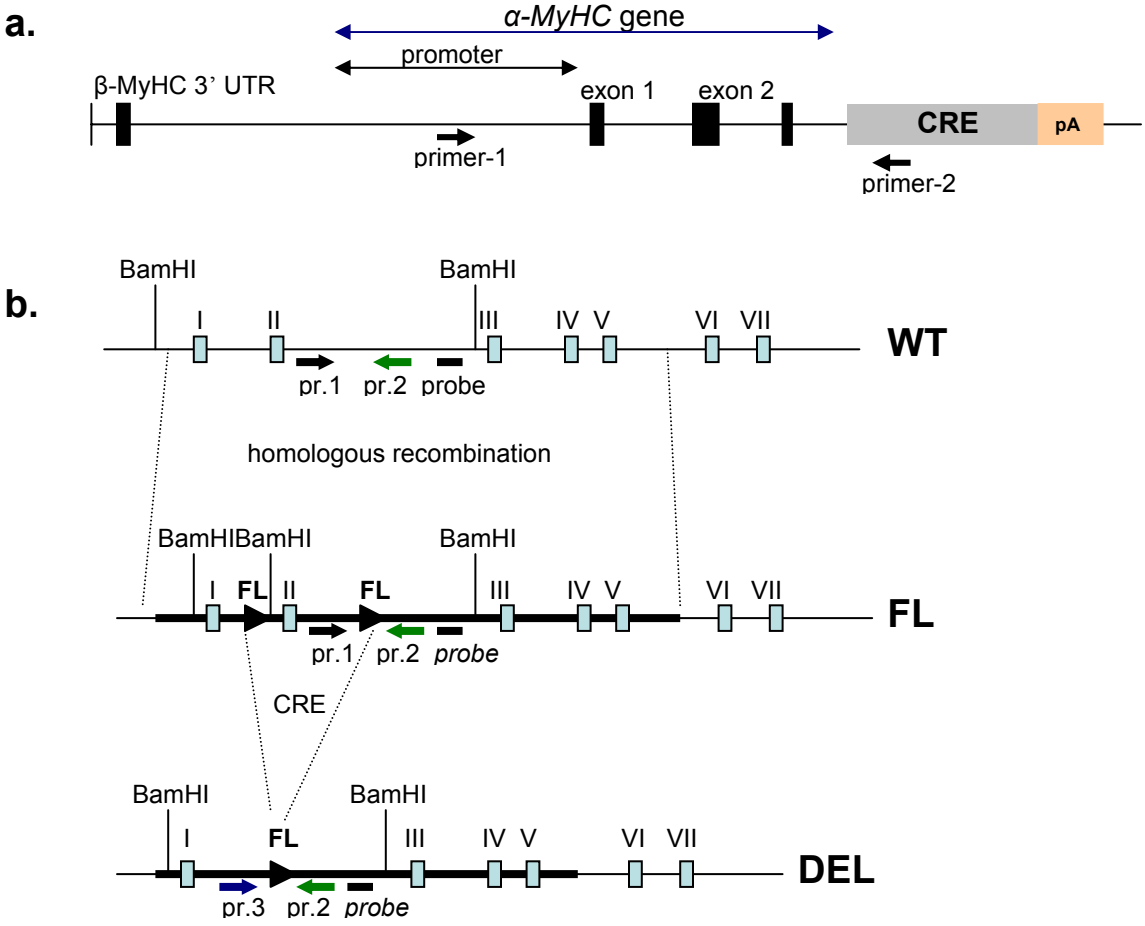

Figure 2.4 Genetic strategy for *Nemo* gene inactivation in cardiomyocytes
a). Construct structure of α-MyHC/Cre line; the regulatory region upstream of Cre recombinase is consisted of the 3'UTR of *β-Myosin heavy chain (β-MyHC) gene,* the entire promoter sequence and the first three exons of *α-myosin heavy chain (α-MyHC)* gene. Two primers (primer-1, primer-2) that bind to the α-MyHC gene promoter and the *Cre* recombinase gene, respectively, are used for genotyping the α-MyHC/Cre line and the expected PCR product is ~ 0.5kb. The poly-A (pA) tail has been used for enhancement of mRNA stability.
b). Targeting the second exon of the *Nemo* gene. The first seven exons of the *Nemo* gene are depicted and following homologous recombination loxP sites have been introduced upstream and downstream of the second exon. The three arrows (black, blue, green) indicate the genomic location of the three primers used to genotype the offsprings of the α-MyHC/Cre; Nemofl/fl. The PCR product sizes for the WT, floxed (FL) and deleted (DEL) alleles are ~200bp, 450bp and 600bp respectively. The genomic location of the probe used for Southern blotting as well as the BamHI restriction sites are given and the expected sizes of the BamHI fragments are 6.8Kb for WT, 3.2Kb for floxed (FL) and 1.2Kb for the deleted (DEL) allele respectively the BamHI fragments are 6.8Kb for WT, 3.2Kb for floxed (FL) and 1.2Kb for the deleted (DEL) allele respectively.

2.2.3 Characterization of *Nemo^{hko}* mice

The *Nemo^{hko}* animals are viable and fertile suggesting that *Nemo* is not required for proper cardiac formation and development. In order to prove that our genetic strategy was effective, PCR and Southern blot were performed on genomic DNA from various mouse tissues (brain, lung, heart, skeletal muscle, kidney, spleen and liver) which verified the *Nemo* gene ablation at the DNA level (fig.2.5 a, b). Notably, a faint PCR product corresponding to the Nemo deleted (DEL) band is also observed in the lungs of the *Nemo^{hko}* mice which is consisted with the minimal *α-MyHC* gene promoter activity in the pulmonary myocardium[290]. Next, we checked NEMO protein levels and Western blot analysis confirmed the significant reduction of NEMO protein only in the heart (and not in other tissues) of *Nemo^{hko}* mice (fig.2.5c, d), while the expression levels of the catalytic IKK subunits (IKK1 & IKK2) were unchanged. Finally, we performed electrophoretic mobility shift assay (EMSA) in order to check the transcriptional activity of NF-κB dimers, which are downstream of NEMO (fig.2.5 d). Under steady-state conditions, NF-κB activity is negligible and in order to stimulate the system we injected *Nemo^{hko}* mice intra-peritoneally with lipopolyscharite (LPS), a well-documented NF-κB stimulus[351]. NF-κB binding activity to the target sites was decreased 15min and 45min after LPS stimulation in *Nemo^{hko}* animals. Moreover, Western blot for the inhibitor of NF-κB alpha (IκBα) further confirmed the down-regulation of NF-κB activity since the IκBα levels were higher in the *Nemo^{hko}* hearts 15min and 45 min after LPS injection (fig.2.5 d). It is likely that the observed moderate decrease in NF-κB activity in the heart of *Nemo^{hko}* mice 15min and 45min after LPS stimulation is due to the fact that other cardiac cell populations (smooth muscle cells, endothelial cells, fibroblasts) contribute to this phenomenon.

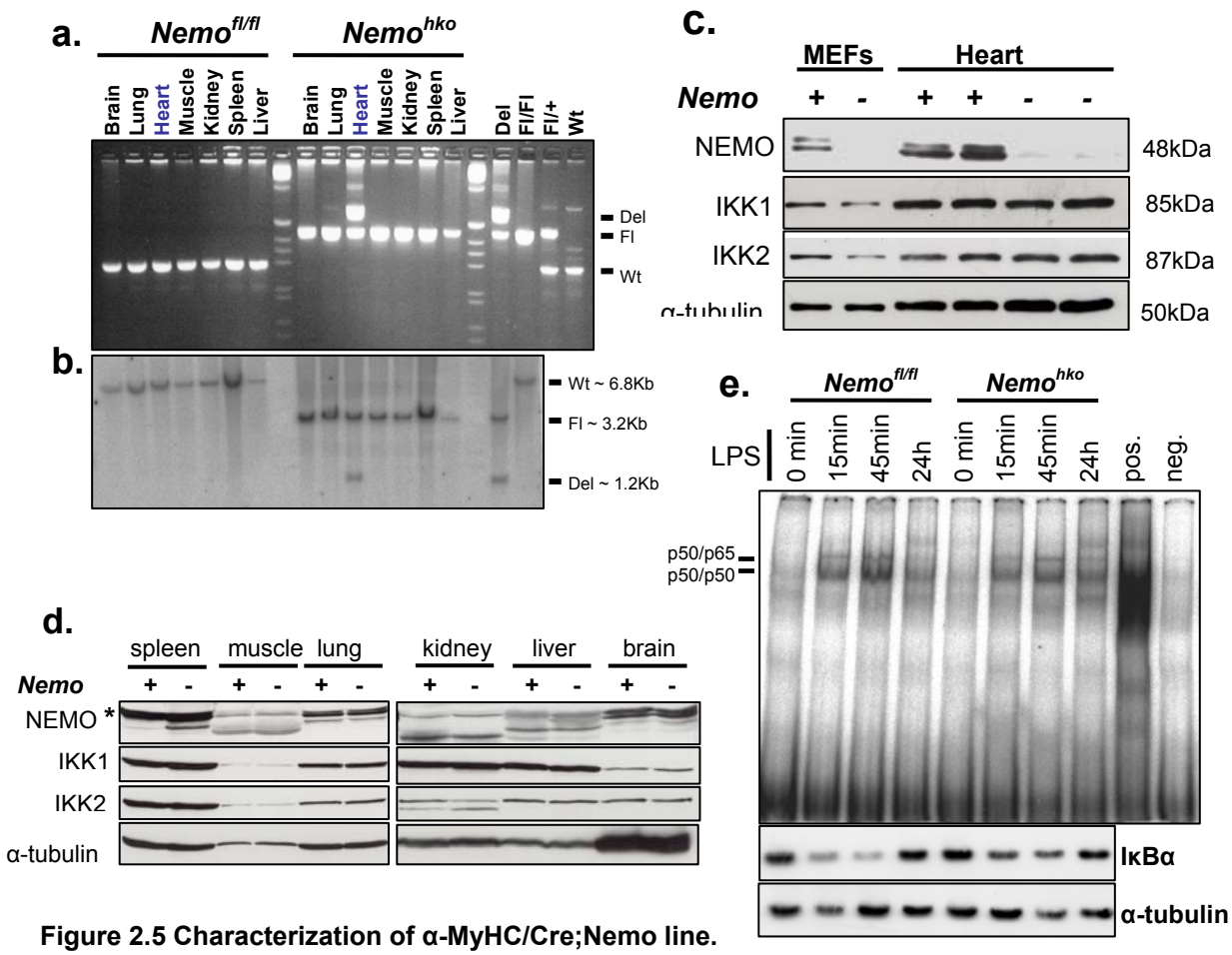

Figure 2.5 Characterization of α-MyHC/Cre;Nemo line.
PCR **(a)** and Southern blotting **(b)** on genomic DNA from brain, lung, heart, skeletal muscle, kidney, spleen and liver from *Nemo*$^{fl/fl}$ and *Nemo*^{hko} mice. The PCR product sizes for the *Wt*, *floxed (Fl)* and *deleted (Del)* alleles are ~200bp, 450bp and 600bp, respectively while the BamHI fragments are 6.8Kb for *WT*, 3.2Kb for *floxed (Fl)* and 1.2Kb for the *deleted (Del)* allele. Western Blotting **(c)** confirms the absence of NEMO protein in the heart of *Nemo*^{hko} mice. Blotting for IKK1 and IKK2 reveals that the expression levels of the catalytic subunits of the IKK complex remain unaltered. Mouse embryonic fibroblasts (MEFs) from wt and total *Nemo knock-out* animals were used as control. The expression levels of NEMO, IKK1 and IKK2 were similar in several organs (spleen, muscle, lung, kidney, liver, brain) of *wt* and *Nemo*^{hko} mice **(d).** Antibodies against α-tubulin were used for normalization. Electrophoretic mobility shift assay (EMSA) demonstrates moderately suppressed NFκB activity in the heart (nuclear extracts) of *Nemo*^{hko} mice after LPS stimulation **(e).** The NFκB dimer is present either as a homodimer p50/p50 or as a heterodimer p50/p65. Western blot analysis shows moderate degradation of the Inhibitor of NFκB alpha (IκBα) in *Nemo*^{hko} hearts after 15min and 45min LPS stimulation.

2.2.4 *Nemo*^{hko} mice develop dilated cardiomyopathy

2.2.4.1 Assessment of cardiac morphology

Comparative histological analysis on Nemo$^{fl/fl}$ and Nemo^{hko} mice revealed no obvious abnormalities in cardiac morphology till the age of six months (fig.2.6 a - c).

Surprisingly, the Nemo^{hko} animals demonstrated left atrium enlargement, ventricular dilation and thinning of the myocardial wall at eight months of age, which became even more evident at ten months. The majority of these animals died between eight and ten months of age, which reflects the establishment of a pathological phenotype (fig.2.6 d,e).

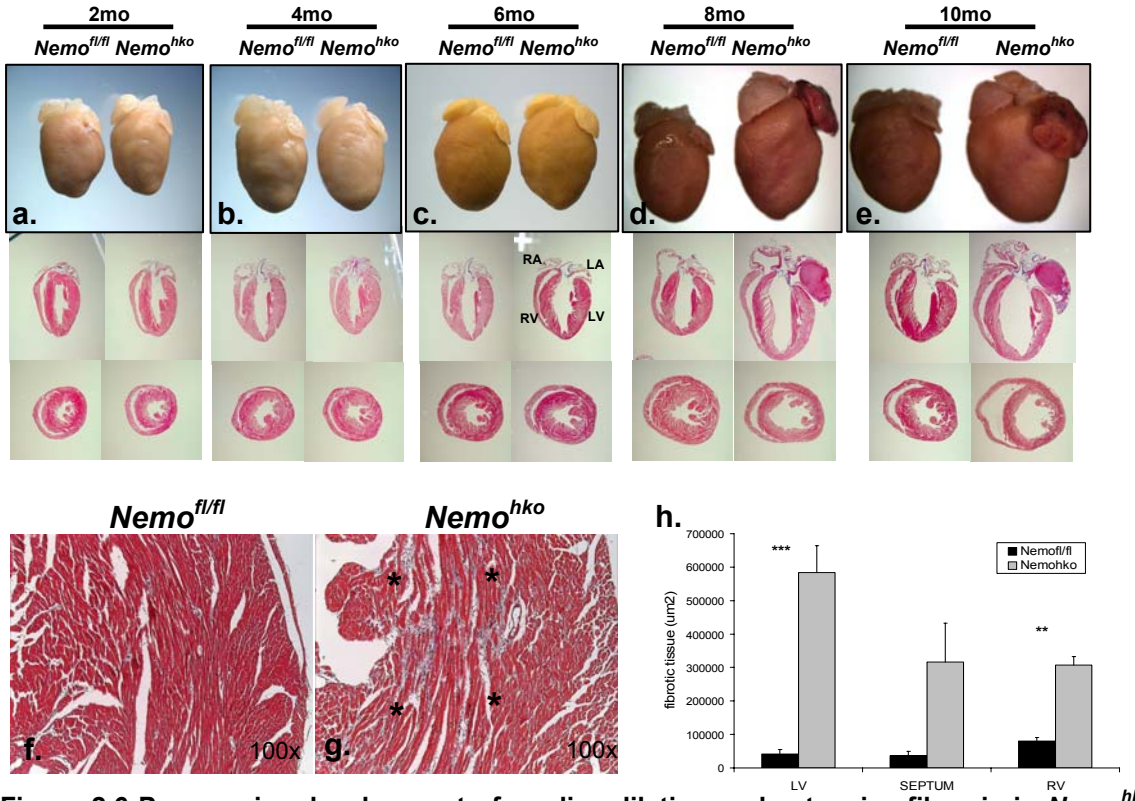

Figure 2.6 Progressive development of cardiac dilation and extensive fibrosis in *Nemo*^{hko} mice. The *Nemo*^{hko} hearts appear normal and indistinguishable from the WT (Nemo$^{fl/fl}$) till six months (6mo) of age at whole mount and histological level **(a-c)**. At the age of eight-ten months (8mo-10mo), the *Nemo*^{hko} hearts develop DCM accompanied with enlarged atrial and ventricular cavities and thinning of the ventricular wall **(d, e).** The middle and lower panels illustrate trichrome staining on longitudinal and cross-sections, respectively. Trichrome staining shows extensive collagen deposition (area between asterisks in **g.)** in *Nemo*^{hko} hearts at 8 months of age **(f, g).** Comparative quantification analysis on collagen deposition (μm2) reveals statistically significant differences at the left and right ventricle **(h).** (RA: right atrium, RV: right ventricle, LA: left atrium, LV: left ventricle), (t-test, * p<0.05, ** p<0.01, *** p<0.001)

The histological findings indicate the presence of a pathological phenotype in Nemo^{hko} animals, which is termed dilated cardiomyopathy (DCM). A prominent feature of DCM is extensive fibrosis of the cardiac muscle. Therefore, trichrome staining was performed on cross sections of 8-10month-old hearts and fibrotic tissue deposition was quantified by morphometry analysis. The Nemo^{hko} hearts clearly demonstrate extensive ventricular fibrosis when compared with control littermates (fig.2.6 f - h), which is reminiscent of DCM pathology.

2.2.4.2 Up-regulation of heart failure markers in *Nemo^{hko}* mice

In accordance with the histological findings, heart-to-body weight ratio measurements indicate the progressive development of pathological hypertrophy in Nemo^{hko} animals (fig.2.7 a). Previous studies have demonstrated that high expression of cardiac embryonic genes in the adult heart indicates the establishment of heart failure[59]. In order to test this possibility, we checked the expression of six well-studied heart failure markers [*myosin heavy chain-6 (Myh6), myosin heavy chain-7 (Myh7), atrial natriuretic peptide (Anp), brain natriuretic peptide (Bnp), glucose transporter-1 (Glut-1)* and *actin-alpha -1 skeletal muscle (Acta-1)]* in Nemo^{hko} hearts at various developmental stages.

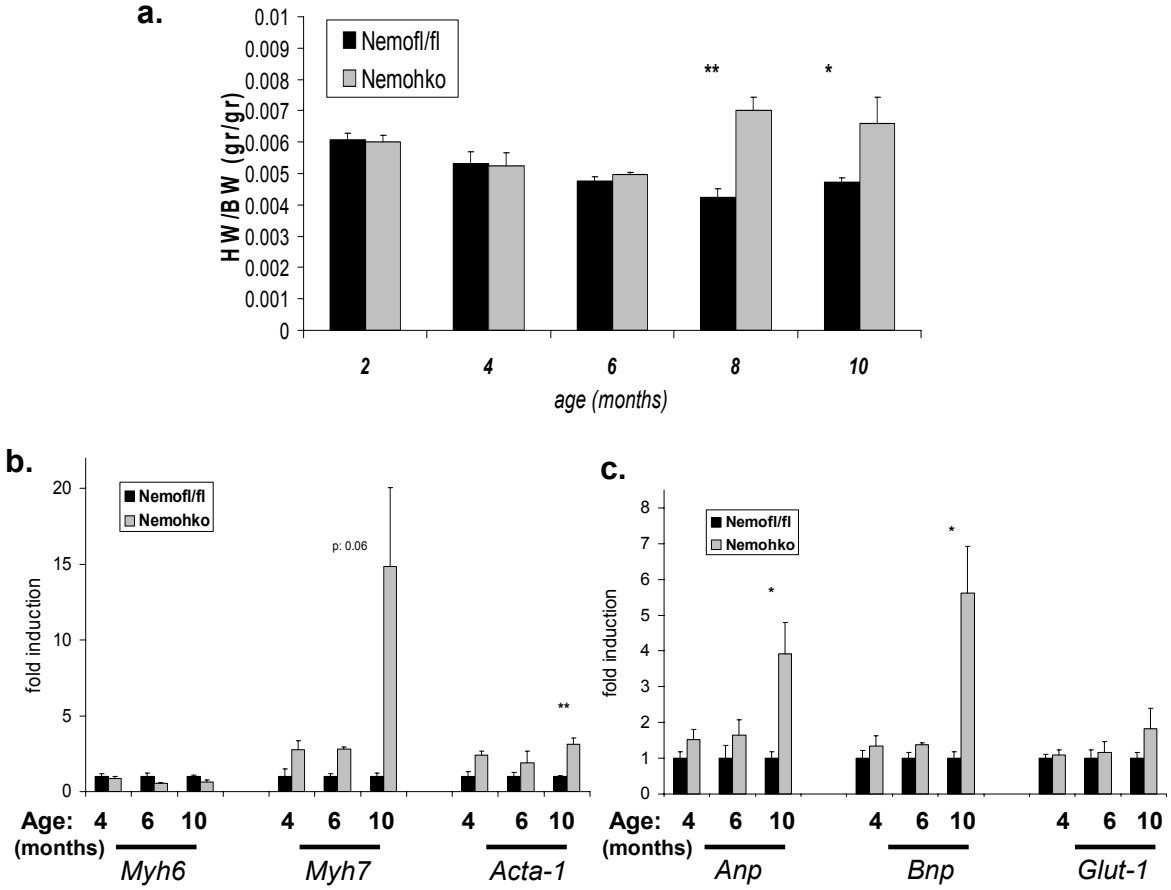

Figure 2.7 Up-regulation of heart failure markers in *Nemo^{hko}* mice. Heart-to-body weight ratio demonstrates progressive development of pathological hypertrophy in *Nemo^{hko}* mice **(a).** TaqMan Real-Time PCR analysis for *myosin heavy chain-6 (Myh6), myosin heavy chain-7 (Myh7), atrial natriuretic peptide (Anp), brain natriuretic peptide (Bnp), glucose transporter-1 (Glut-1)* and *actin-alpha -1 skeletal muscle (Acta-1)* genes confirms the establishment of heart failure in *Nemo^{hko}* mice **(b, c).** Taqman *glyceraldehyde 3-phosphate dehydrogenase (GAPDH)* probes were used for normalization. (t-test, * p<0.05, ** p<0.01, *** p<0.001), (n = at least 3 animals per genotype).

We clearly demonstrated a switch in the expression of the adult *Myh6* (low expression) and the embryonic *Myh7* (high expression) at 10 month-old *Nemo*^{hko} hearts (fig.2.7 b). Also, the heart failure markers *Anp, Bnp* and *Acta-1* were significantly up-regulated in the heart of 10 month-old *Nemo*^{hko} animals (fig.2.4 b, c) as revealed by TaqMan RT PCR. Taken together, these data prove the progressive development of dilated cardiomyopathy and heart failure in *Nemo*^{hko} mice.

2.2.5 Increased apoptosis in Nemo^{hko} hearts

Previously, it has been demonstrated that DCM is also accompanied with myocyte cell death[68]. Hence, we carried out TUNEL staining on eight to ten month-old hearts from *Nemo*$^{fl/fl}$ and *Nemo*^{hko} animals.

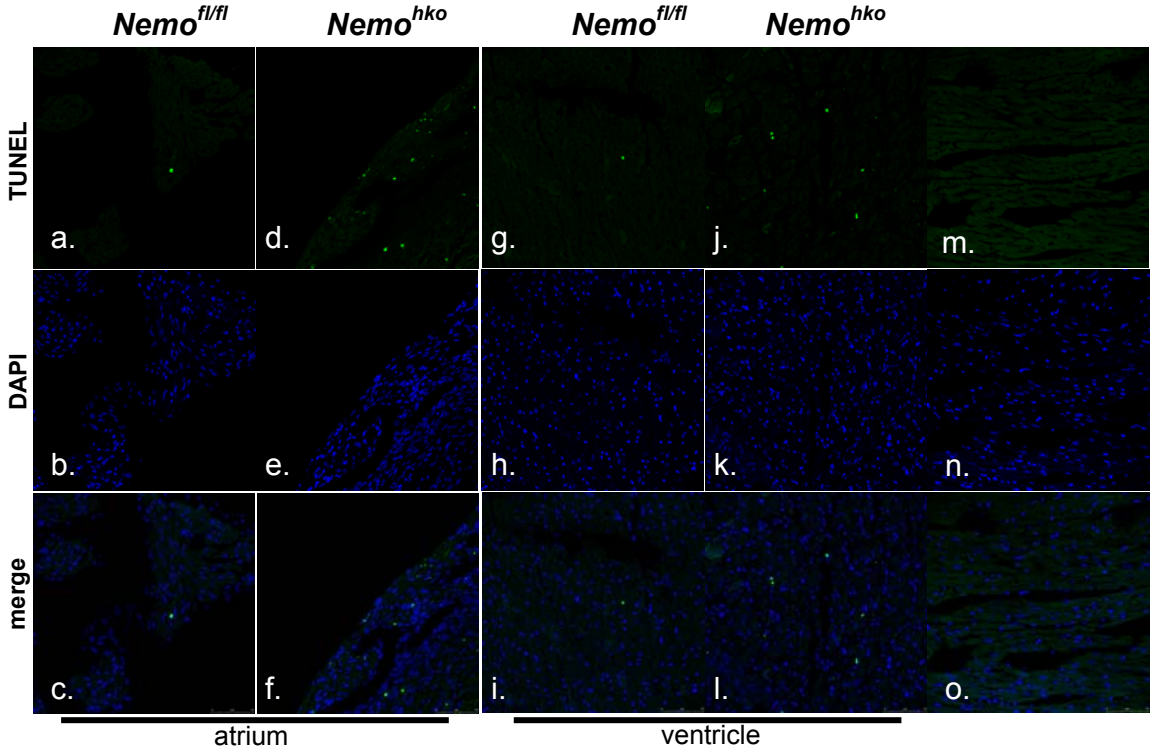

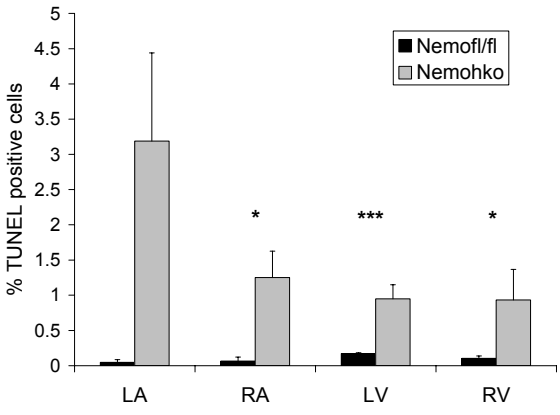

Figure 2.8 Increased apoptosis in the atria and ventricles of *Nemo*^{hko} hearts.
TUNEL staining in green indicates increased levels of apoptosis (TUNEL+ cells) in the atria **(a, d)** as well as in the ventricles **(g, j)** of *Nemo*^{hko} animals. The middle panel of images **(b, e, h, k, n)** shows DAPI staining and the lower panel **(c, f, i, l, o)** merged images. The negative control for TUNEL assay is shown in **m, n & o** images. Quantification of TUNEL positive cells reveals statistically significant differences in the right atrium (RA), right ventricle (RV) and left ventricle (LV). (t-test, * $p<0.05$, ** $p<0.01$, *** $p<0.001$), (n = at least 3 animals per genotype)

Carefully-controlled analysis of confocal images demonstrated higher apoptotic rate (percentage of TUNEL positive cells) in the atria (fig.2.8 a - f) and ventricles (fig.2.8 g - l) of old *Nemo*^{hko} hearts when compared with *Nemo*$^{fl/fl}$ hearts. Although the identity of the apoptotic cells is still unknown, these results provide one more indication in favor of the DCM phenotype in the *Nemo*^{hko} animals.

2.2.6 Advanced cardiac dysfunction in *Nemo*^{hko} mice

Assessment of cardiac function is also a well-documented indicator of heart failure used in clinics and laboratories[313, 314]. Carefully-designed echocardiography analysis was performed on *Nemo*^{hko} mice at various ages. Two-dimensional M-mode images confirmed ventricular dilation and further demonstrated compromised cardiac contraction in the *Nemo*^{hko} animals (fig.2.9 a). The cardiac function was assessed by left ventricular tracing on B-mode videos of the short axis and measurements for fractional shortening (FS), left ventricular transversal area in diastole (LVTA; d) and systole (LVTA; s) were extrapolated. Interestingly, there were no major differences in the cardiac function of *Nemo*$^{fl/fl}$ and *Nemo*^{hko} animals till the age of 5 months. Notably, the fractional shortening and the LVTA; s measurements were affected at six months of age in the *Nemo*^{hko} mice and deteriorated with aging (fig.2.9 b, c). The LVTA; d measurements revealed significant differences at 8 and 10 months of age and justify the absence of pathology in the *Nemo*^{hko} hearts at 6 months of age at the histological level (fig.2.9 d). Since differences exist in the timing that LVTA; s defects (6 months) and LVTA; d defects (8 months) occur, it is likely that problems in systole are present before problems in diastole in the *Nemo*^{hko} hearts. Taken together, these findings confirm the severe cardiac dysfunction that accompanies dilated cardiomyopathy in *Nemo*^{hko} mice.

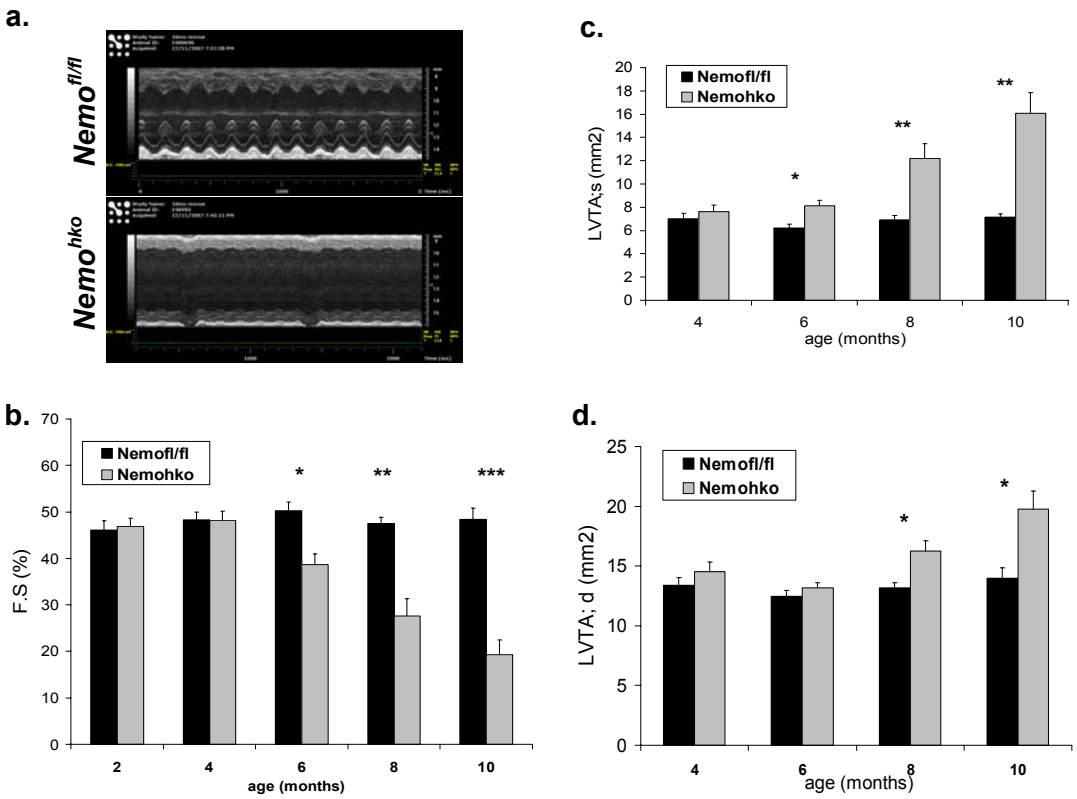

Figure 2.9 Echocardiography measurements on *Nemo*^{hko} animals. M-mode images on old (10 months) *Nemo*^{hko} animals represent left ventricular dilation, thin myocardial walls and compromised contraction **(a).** Using left ventricular trace on B-mode images, fractional shortening (F.S), left ventricular transversal area in systole (LVTA; s) and left ventricular transversal area in diastole (LVTA; d) were calculated at different stages. Fractional shortening **(b)** and LVTA; s **(c)** are affected at 6 months of age and deteriorate afterwards in *Nemo*^{hko} mice while LVTA; d **(d)** is significantly affected at 8 and 10 months of age. (t-test, * $p<0.05$, ** $p<0.01$, *** $p<0.001$), (n = at least 5 animals per genotype).

2.2.7 Recapitulation of the dilated cardiomyopathy phenotype in young *Nemo*^{hko} mice after transverse aortic banding

So far, we have demonstrated that cardiomyocyte-specific *Nemo* gene inactivation leads to dilated cardiomyopathy with aging. In order to test the hypothesis that *Nemo* gene inactivation also leads to heart failure in response to cardiac challenge, young (2-3 month-old) *Nemo*^{hko} mice were subjected to transverse aorting banding (TAB). TAB has been reported as a widely used model for pressure overload-induced cardiac hypertrophy that eventually leads to ventricular dysfunction and failure[430, 431].

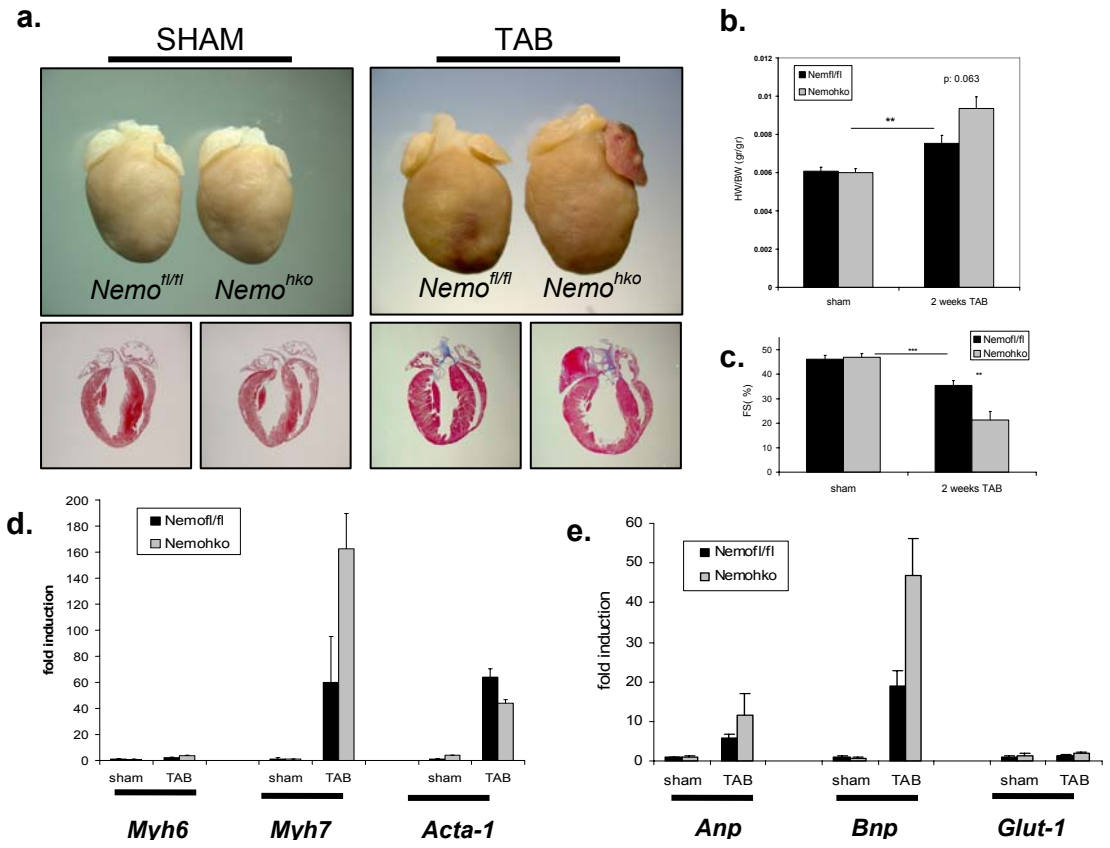

Figure 2.10 Transverse aortic banding (TAB) recapitulates the dilated cardiomyopathy phenotype in young *Nemo*^{hko} mice.
(a) Whole mount and histological (trichrome staining) comparison reveal no morphological differences between 3 month-old *Nemo*$^{fl/fl}$ and *Nemo*^{hko} hearts without TAB (sham). Two weeks after TAB, the *Nemo*^{hko} hearts demonstrate enlarged left atrium and left ventricular cavity. The heart-to-body weight ratio **(b)** is higher and the cardiac function (fractional shortening) significantly compromised **(c)** in *Nemo*^{hko} animals two weeks after TAB **(d, e).** TaqMan Real-Time PCR analysis for *myosin heavy chain-6 (Myh6), myosin heavy chain-7 (Myh7), atrial natriuretic peptide (Anp), brain natriuretic peptide (Bnp), glucose transporter-1 (Glut-1)* and *actin-alpha -1 skeletal muscle (Acta-1)* genes confirms the establishment of a pathological phenotype in *Nemo*^{hko} mice two weeks after TAB. Taqman *glyceraldehyde 3-phosphate dehydrogenase (GAPDH)* probes were used for normalization. (t-test, * p<0.05, ** p<0.01, *** p<0.001) , (n = 3 mice per genotype)

In contrast to wildtype controls, the *Nemo*^{hko} mice revealed signs of heart failure two weeks after the TAB operation, since histological examination demonstrated cardiac dilation (fig.2.10 a). In addition, the heart-to-body weight ratio was higher and the cardiac function significantly compromised (F.S < 20%) in the *Nemo*^{hko} mice two weeks after TAB (fig.2.10 b, c). Expression levels of heart failure markers [*myosin heavy chain-6 (Myh6), myosin heavy chain-7 (Myh7), atrial natriuretic peptide (Anp), brain natriuretic*

peptide (Bnp)] were elevated two weeks after the TAB operation, with no change in *glucose transporter-1 (Glut-1)* and *actin-alpha -1 skeletal muscle (Acta-1) mRNA levels* (fig. 2.10 d, e). The data obtained from this experiment are reminiscent of the features accompanying dilated cardiomyopathy in old *Nemo*^{hko} mice, and indicate that the *Nemo* deprivation in cardiomyocytes exacerbates both age- and stress-related decrements in cardiac function.

2.2.8 Antioxidant treatment ameliorates heart failure phenotype in old *Nemo*^{hko} hearts

The role of oxidative stress in myocardial remodeling after pressure-overload induced hypertrophy has been demonstrated by *in vivo* studies where mice deficient for antioxidant enzymes display ventricular dilation and increased apoptosis[432-435]. In order to test the possibility that ROS accumulation leads to increased cardiomyocyte apoptosis[436] in *Nemo*^{hko} mice, we followed a rescue approach by subjecting the mice to an antioxidant diet (butylated hydroxyaniole, BHA[355, 437]) at 3-4 months of age and onwards. Importantly, the antioxidant treatment resulted in partial rescue of the dilated cardiomyopathy phenotype. The *Nemo*^{hko} mice under antioxidant diet revealed moderate ventricular dilation when compared with *Nemo*^{hko} mice under control diet and the heart-to-body weight ratio was reversed to normal (fig.2.11 a, b). Moreover, improved cardiac function (higher fractional shortening) was observed in *Nemo*^{hko} mice under antioxidant diet at 8 and 10 months of age after careful monitoring by echocardiography (fig.2.11 c). These findings are in accordance with previous reports where NF-κB inhibits reactive oxygen species (ROS) accumulation and oxidative stress by regulating the expression of various antioxidant enzymes, including manganese-dependent superoxide dismutase (MnSOD) and ferritin heavy chain (FHC)[438] and indicate that NEMO/NF-κB inactivation in cardiomyocytes possibly results in ROS accumulation and myocyte apoptosis in *Nemo*^{hko} animals.

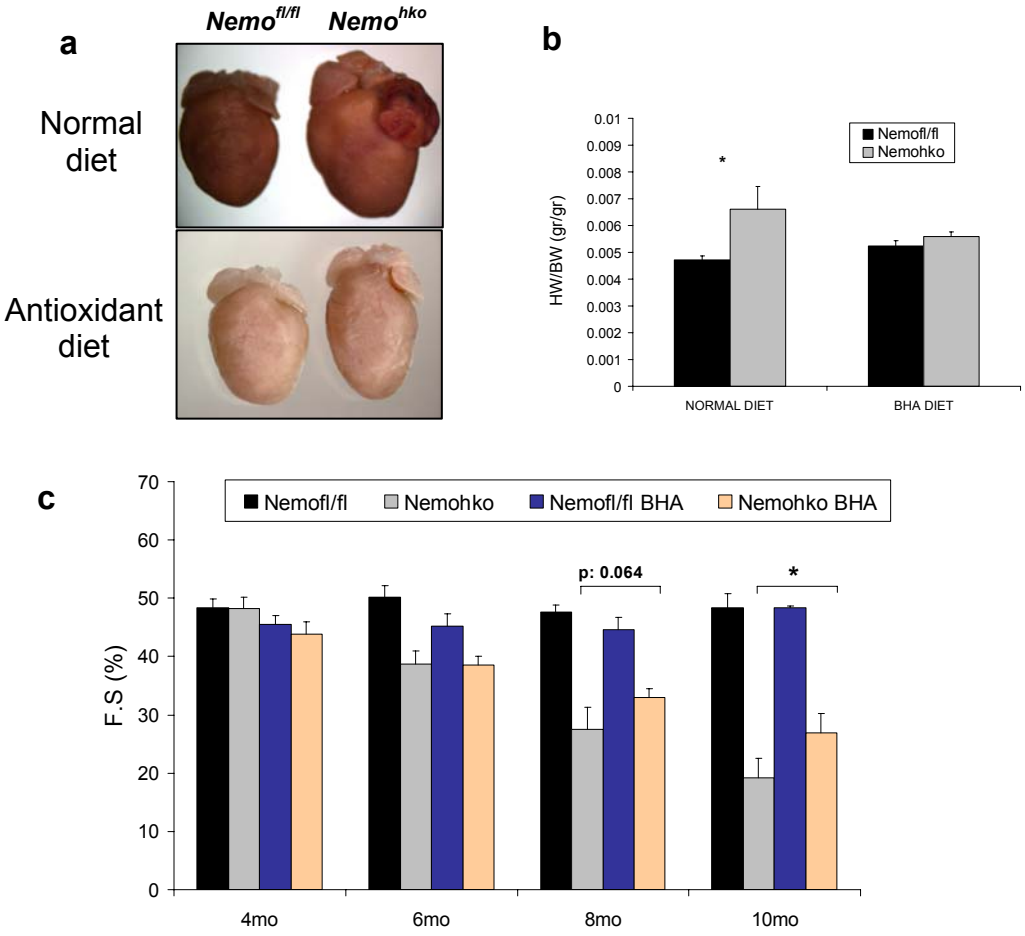

Figure 2.11 Antioxidant diet partially rescues cardiac dilation and dysfunction in *Nemo*^{hko} mice. Mice were subjected to antioxidant diet (BHA) starting at 3-4 months of age and onwards. **(a).** Whole mount comparison at 10 months of age reveals prominent cardiac dilation in the *Nemo*^{hko} mice under normal diet whereas *Nemo*^{hko} mice under antioxidant diet (BHA) demonstrate moderate ventricular dilation. **(b).** In addition, the heart-to-body (HW/BW) weight ratio is significantly higher in Nemohko mice under normal diet compared to control (*Nemo*$^{fl/fl}$) littermates, whereas the antioxidant diet reversed the HW/BW ratio to normal levels in 10 month-old *Nemo*^{hko} mice. **(c).** Monitoring of the cardiac function by echocardiography demonstrates partial rescue of the cardiac function in *Nemo*^{hko} mice under antioxidant diet (BHA) at 8 and 10 months of age when compared with control (*Nemo*$^{fl/fl}$) littermates under normal diet. (t-test, * p<0.05, ** p<0.01, *** p<0.001) (n= at least 5 mice per genotype)

2.3 DISCUSSION

2.3.1 Discussion

This study shows that lack of NF-κB activity leads to direct transition to DCM in a cardiomyocyte-autonomous manner. Taking advantage of Cre/loxP technology, we demonstrate that the canonical (NEMO-dependent) NF-κB pathway is not required for cardiac development since *Nemo*^{hko} mice are viable and fertile. However, *Nemo*^{hko} animals develop progressive DCM and die suddenly at 8 - 10 months of age, establishing a cardiac-specific requirement for NF-κB activity later in life. Landmarks of DCM, including left ventricular dilation, cardiomyocyte cell death and advanced cardiac dysfunction, are observed in ageing *Nemo*^{hko} animals and confirm the presence of a pathological cardiac phenotype[57]. Intriguingly, oxidative stress provides a mechanistic explanation for the DCM phenotype observed in *Nemo*^{hko} mice since antioxidant diet partially rescues the DCM-associated defects. Moreover, mechanical load (thoracic aortic banding) on young *Nemo*^{hko} mice recapitulates the DCM phenotype seen in old *Nemo*^{hko} animals, indicating that the *Nemo* deprivation in cardiomyocytes exacerbates both age- and stress-related decrements in cardiac function.

Our study demonstrates that *Nemo*^{hko} animals develop rapidly DCM without undergoing the stage of compensated hypertrophy and establishes NEMO/NF-κB pathway as a key regulator of the transition from normal to dilated heart. Consistent with this notion, the cardiac function is slightly affected at 6 months but the fractional shortening values are severely decreased later (8-10months) in *Nemo*^{hko} hearts. Moreover, morphological defects (ventricular dilation and fibrosis) and cardiomyocyte cell death are only present in the heart of old (8-10months) *Nemo*^{hko} mice and not earlier during development. One more indication for the rapid transition to heart failure is the late up-regulation of the well-documented hypertrophy markers[59] *Anp, Bnp, Myh7, Acta-1* in the heart of 10 month old *Nemo*^{hko} animals. Remarkably, rapid transition to cardiac dilation and failure was also observed in young *Nemo*^{hko} hearts when mechanical stress (thoracic aortic banding) was administered.

Our observations are in accordance with recent reports that attribute a pro-hypertrophic role to NF-κB signaling in the heart. Recently, it has been demonstrated that NF-κB activity is required for hypertrophic growth of primary cardiomyocytes[400, 439] and regulates the expression of the hypertrophy inhibitory molecule IEX-1[440]. Moreover, blockade of NF-κB using p50$^{-/-}$ mice[404, 405], IκBa super-suppressor[406] or pharmacological

inhibitors[399] ameliorates myocardial hypertrophy and improves cardiac function in models of TNFα- or angiotensin/isoprotenerol-induced hypertrophy. In our study, we demonstrate that in the absence of hypertrophic stimuli cardiac-restricted *Nemo* gene inactivation leads directly to dilated cardiomyopathy in adult mice without the intermediate stage of compensated hypertrophy. Moreover, when the pressure-overload model of cardiac hypertrophy (thoracic aortic banding) was employed on young *Nemo*^{hko} mice, the animals recapitulated the pathological phenotype of the old *Nemo*^{hko} mice and developed directly ventricular dilation, suggesting that the NEMO/ NF-κB actions in the cardiomyocyte compartment favor hypertrophic growth.

In line with our findings, cardiac-restricted TNFα over-expression[70, 71, 409] or cardiomyocyte-specific gp130-dependent survival pathway inactivation[69] lead to cardiac dilation accompanied with prominent myocyte cell death, establishing survival pathways as key mediators of the progression to heart failure. A growing body of data suggests that NF-κB signaling controls cell survival by regulating the expression of anti-apoptotic genes, including BcL-xL, X chromosome-linked inhibitor of apoptosis - XIAP, and cellular FLICE-inhibitory protein - c-FLIP[416]. Furthermore, NF-κB inhibits reactive oxygen species (ROS) accumulation and oxidative stress by regulating the expression of various antioxidant enzymes, including manganese-dependent superoxide dismutase (MnSOD) and ferritin heavy chain (FHC)[438] . The role of oxidative stress in myocardial remodeling after pressure-overload induced hypertrophy has been demonstrated by *in vivo* studies where mice deficient for antioxidant enzymes display ventricular dilation and increased apoptosis[432-435].

In support of the proposal that ROS accumulation leads to increased cardiomyocyte apoptosis[436] in *Nemo*^{hko} mice, we followed a rescue approach by subjecting the mice to an antioxidant diet (butylated hydroxyaniole, BHA)[355, 437] at 4-5 months of age and onwards. Improved cardiac function (higher fractional shortening) and moderate ventricular dilation was observed when compared with *Nemo*^{hko} mice under control diet up to 10 months, although the mutant animals were still compromised compared to *Nemo*$^{fl/fl}$ littermates. Moreover, the heart-to-body weight ratio in *Nemo*^{hko} mice under antioxidant diet reverted to wildtype at 10 months. These findings indicate that NEMO/NF-κB inactivation in cardiomyocytes possibly results in transcriptional dysregulation of anti-oxidant enzymes (MnSOD, FHC) and ROS accumulation, which could promote myocyte apoptosis in *Nemo*^{hko} animals. Moreover, the partial rescue of

the phenotype by antioxidant diet suggests that other mechanisms, including impaired transcription of the anti-apoptotic NF-κB target genes (BcL-xL, cFLIP, XIAP), could also be affected in *Nemo*^{hko} hearts. Importantly, oxidative stress (ROS accumulation) could partially explain the dilated cardiomyopathy phenotype both in aging and in young (after thoracic aortic banding) *Nemo*^{hko} mice since ROS accumulation has been reported in the aging[441-443]or mechanically-overloaded[444, 445] heart, respectively. Taken together, oxidative stress appears as an attractive mechanistic explanation for the cardiac pathology observed in *Nemo*^{hko} animals, although further research focusing on the NF-κB-dependent transcription of anti-oxidant and anti-apoptotic genes is required in order to elucidate the molecular mechanism responsible for DCM establishment.

The development of interstitial fibrosis is a prominent feature of cardiac remodeling in dilated cardiomyopathy and associated with alterations in matrix metalloproteinase (MMP) activity[446]. *In vitro* and *in vivo* studies associate activation of NF-κB pathway with increased MMP activity[405,411,415]. Interestingly, reactive oxygen species (ROS) accumulation is a key regulator of interstitial fibrosis since mice lacking the antioxidant enzyme Nox2 displayed decreased MMP activity and minimal fibrotic tissue deposition in models of aldosterone or angiotensin II induced hypertrophy[447, 448]. Since we have demonstrated that ROS accumulation is involved in the myocardial remodeling of *Nemo*^{hko} mice, oxidative stress could also partially explain the increased fibrotic tissue deposition observed in *Nemo*^{hko} hearts. In line with this notion, activation of NF-κB and increased MMP activity in a Nox2-dependent manner have been reported in models of *in vitro*[449] and *in vivo*[447] cardiomyocyte hypertrophy. Our present study raises the possibility that cardiomyocyte NEMO/NF-κB inactivation leads to oxidative stress and interstitial fibrosis possibly due to dysregulation of MMP activity, although this issue awaits also further investigation.

2.3.2 Future perspectives

Our present study demonstrates a cardiomyocyte requirement for the NEMO/ NF-κB canonical pathway in the regulation of cardiac hypertrophy. In the absence of hypertrophic stimuli, cardiac-restricted inactivation of the *Nemo* gene leads directly to DCM in old mice without the intermediate stage of compensated hypertrophy. Moreover, when the pressure-overload model of cardiac hypertrophy was employed on young *Nemo*^{hko} mice, the animals recapitulated the pathological phenotype of the old *Nemo*^{hko}

mice and developed directly ventricular dilation and severe cardiac dysfunction. However, the molecular mechanism that is triggered by the absence of NEMO in the cardiomyocytes and leads to the establishment of a DCM phenotype remains to be elucidated.

NF-κB is a pleiotropic transcription factor that also regulates anti-apoptotic and anti-oxidant gene expression, as previously discussed. Our apoptosis studies revealed that cardiomyocyte cell death could be the mechanism responsible for the rapid progression to DCM in old *Nemo*^{hko} animals. Moreover, antioxidant treatment partially rescued the DCM phenotype in old *Nemo*^{hko} mice, suggesting that lack of NF-κB activity in cardiomyocytes results in ROS accumulation (oxidative stress) and apoptosis. However, given the broad spectrum of NF-κB-dependent processes, future research employing comparative whole genome microarray analysis would increase our understanding regarding the role of NEMO/ NF-κB in cardiac pathophysiology.

Another possible avenue for future research is based on the remarkable recapitulation of the DCM phenotype in young *Nemo*^{hko} animals following the pressure-overload model of cardiac hypertrophy (thoracic aortic banding). Ventricular dilation and up-regulation of the heart failure markers (*Myh7, Anp, Bnp*) in young *Nemo*^{hko} mice strongly suggest the existence of a common molecular mechanism that leads to the recapitulation of the DCM phenotype in young *Nemo*^{hko} animals. Apoptosis studies and anti-oxidant treatment on young *Nemo*^{hko} mice following aortic banding, as well as comparative microarray analysis will prove whether the *Nemo* gene deprivation in cardiomyocytes exacerbates both age- and stress-related decrements in cardiac function.

2.3.3 Conclusions

Taken together, our findings demonstrate that cardiac-restricted *Nemo* gene inactivation leads to dilated cardiomyopathy. Intriguingly, the transition from normal to failing (dilated) heart occurs rapidly without the intermediate stage of compensated hypertrophy, suggesting a cardiomyocyte-autonomous requirement for the canonical (NEMO-dependent) NF-κB pathway in cardiac hypertrophy. Here, we propose that NEMO/NF-κB cardiomyocyte ablation results in increased apoptosis which eventually leads to cardiac dilation and dysfunction. The fact that mechanical load (aortic banding) recapitulates the direct transition to cardiac dilation/dysfunction in young *Nemo*^{hko} mice

demonstrates that the NEMO actions in cardiomyocytes are not solely ageing-dependent, but also essential in stress conditions. Several studies report ROS accumulation/apoptosis in the ageing or mechanically-overloaded heart and shed light in the explanation of the dilated cardiomyopathy phenotype in ageing or mechanically-overloaded *Nemo*^{hko} hearts. Following a rescue approach, we demonstrate that oxidative stress (ROS accumulation) could possibly lead to increased apoptosis and dilation in the *Nemo*^{hko} hearts, since antioxidant diet partially rescues defects in cardiac function and morphology. To summarize, our study associates the canonical (NEMO-dependent) NF-κB pathway with direct transition to cardiac dilation and failure, providing valuable insights in the pathogenesis of the commonest cardiomyopathy, the dilated cardiomyopathy.

2.4. MATERIALS & METHODS

Chapter 2

Cardiac-restricted *Nemo* gene inactivation leads to dilated cardiomyopathy

2.4 Materials & methods

2.4.1 Animals

2.4.1.1 Generation of *Nemo*^{hko} mice

Transgenic C57Bl6 mice expressing Cre recombinase under the control of the *alpha-Myosin Heavy Chain (α-MyHC)* gene promoter[290] were crossed with *NEMO* FLOXED (*Nemo*$^{fl/fl}$) C57Bl6 mice[378] in order to generate *Nemo* heart-specific knock-out (*Nemo*^{hko}) animals. Construct details are provided in Box 2.1.

BOX 2.1 Genetic strategy for *Nemo* gene inactivation in cardiomyocytes

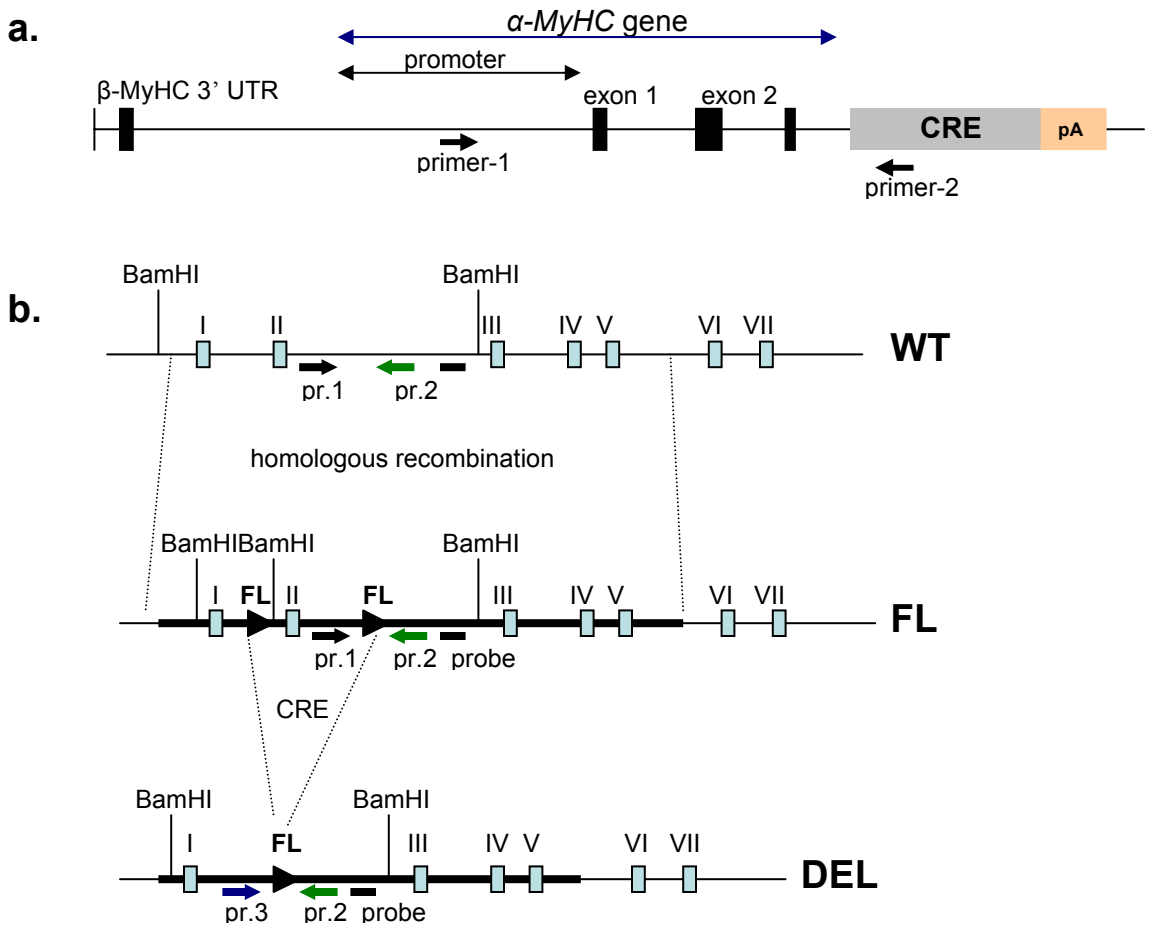

a). Construct structure of α-MyHC/Cre line; the regulatory region upstream of Cre recombinase is consisted of the 3'UTR of *β-Myosin heavy chain (β-MyHC) gene,* the entire promoter sequence and the first three exons of *α-myosin heavy chain (α-MyHC)* gene. Two primers (primer-1, primer-2) that bind to the α-MyHC gene promoter and the *Cre* recombinase gene, respectively, are used for genotyping the α-MyHC/Cre line and the expected PCR product is ~1kb. The poly-A (pA) tail has been used for enhancement of mRNA stability.

b). Targeting the second exon of the *Nemo* gene; the first seven exons of the *Nemo* gene are depicted and following homologous recombination loxP sites have been introduced upstream and downstream of the second exon. Cre-mediated excision of the second exon results in a frameshift followed

by a premature stop codon. The three arrows (black, blue, green) indicate the genomic location of the three primers used to genotype the offsprings of the α-MyHC/Cre; Nemofl/fl. The PCR product sizes for the WT, floxed (FL) and deleted (DEL) alleles are ~200bp, 450bp and 600bp respectively. The genomic location of the probe used for Southern blotting as well as the BamHI restriction sites are given and the expected sizes of the BamHI fragments are 6.8Kb for WT, 3.2Kb for floxed (FL) and 1.2Kb for the deleted (DEL) allele respectively the BamHI fragments are 6.8Kb for WT, 3.2Kb for floxed (FL) and 1.2Kb for the deleted (DEL) allele respectively.

2.4.1.2 Genotyping

Genotyping was performed by PCR using genomic DNA from tail biopsies. Briefly, tail samples underwent Proteinase K digestion over/night (o/n) at 56°C and centrifuged at 13.000 rpm. The supernatant was recovered and DNA was precipitated with isopropanol after centrifugation. Next, the DNA pellet was washed with 70% ethanol and air-dried for 20min at room temperature (RT). Finally, the DNA pellet was reconstituted in dH_2O and 2μl of each sample were used for the PCR reaction. The PCR products were analyzed by electrophoresis on 2% agarose gels; primer sequences (table 2.1) and PCR programs (table 2.2) are provided below.

Table 2.1 Primer sequences for genotyping of *αMyHC/CRE* & Nemo$^{fl/fl}$ mice

Gene or transgene	Primer sequence (5'- 3')
αMyHC/CRE	ATG ACA GAC AGA TCC CTC CTA TCT CC (sense) CTC ATC ACT CGT TGC ATC ATC GAC (anti-sense)
Nemo	primer-1: CGT GGA CCT GCT AAA TTG TCT primer-2: ATC ACC TCT GCA AAT CAC CAG primer-3: ATG TGC CCA AGA ACC ATC CAG

Table 2.2 PCR programs for genotyping of *αMyHC/CRE* & Nemo$^{fl/fl}$ mice

PCR program for *αMyHC/CRE* mice		PCR program for *Nemo$^{fl/fl}$* mice	
30 cycles	94°C for 1min 59°C for 1min 72°C for 45sec 72°c for 10min	34 cycles	94°C for 30sec 60°C for 30sec 72°C for 30sec 72°c for 10min

2.4.1.3 Husbandry

Animals were housed in a clean, temperature controlled (22^{o}C) mouse facility on a 12-hour light/dark cycle, and standard diet was provided. Mice were weaned at post-natal day 21 (p21) and housed in same-sex groups of 3-5 per cage with pellet food and water *ab libidum*. All mouse procedures were approved by European Molecular Biology Laboratory Monterotondo Ethical Committee (Monterotondo, Italy) and were in accordance with national and European regulations. Male mice were used in all experiments.

2.4.1.4 Aortic Banding

Transverse aortic banding was performed in 9-12-week-old male *Nemo*$^{fl/fl}$ and *Nemo*^{hko} mice (C57BL/6). Mice were anesthetized with 2% isoflurane and intubated in a Harvard Apparatus ventilator. A horizontal skin incision was made at the level of the 2 to 3 intercostals space; the aorta was isolated and a 6.0 silk suture was snared with wire and pulled back around the aorta. A bent 25-gauge needle was then placed next to the aorta, and the suture was tied snugly around the needle and the aorta. After ligation, the needle was quickly removed, the chest and skin were closed (using 6.0 silk suture), and the mice were allowed to recover for 2 weeks.

2.4.1.5 Echocardiography Analysis

Animals were anesthetized with 2% isoflurane and left hemithorax was shaved. The mice were placed on a temperature-controlled pad and heart rate was continuously monitored (400-550bpm). Ultrasound transmission gel (Parker Laboratories Inc.) was used and the heart was imaged in the parasternal short-axis view. Two-dimensional B-mode images were obtained at the papillary muscle level using the Vevo 770 Ultrasound system (VisualSonics). Fractional shortening (F.S), left ventricular transversal area in diastole and systole (LVTA;d and LVTA;s) were calculated using the Vevo 770 V2.2.3 software.

2.4.1.6 Antioxidant Treatment

Nemo^{hko} mice were fed with anti-oxidant food (Butylated HydroxyAnisole, BHA, SIgma) at 3 and 4 months of age and onwards. Detailed monitoring of the cardiac function by echocardiography analysis was performed before and during the BHA treatment (6, 8 and 10 months). Ten-month old mice were sacrificed and the hearts were examined at the histological (Trichrome staining) and molecular (TaqMan QRT-PCR) level (details provided below).

2.4.2 Histology

2.4.2.1 Morphological and morphometrical analysis

Hearts were excised at the indicated developmental stages and fixed over-night at 4% paraformaldehyde. Following progressive tissue dehydration with serial ethanol concentrations and xylene, the heart samples were embedded in paraffin. Eight micrometer (μm) thick longitudinal and cross-sections were subjected to Trichrome staining (Sigma-Aldrich) for nuclei, cytoplasm and collagen visualization. Images were collected using a Leica DMR microscope and a Leica DC 500 camera (Leica Microsystems). Quantification of collagen tissue deposition was performed with MetaMorph software (version 6.2r5; Universal Imaging Corporation).

2.4.2.2 TUNEL Assay

Eight μm longitudinal heart sections were deparaffinized in xylene and gradually dehydrated by immersion in ethanol solutions with different concentration (100%, 95%, 85%, 70%, 50%). Then, the slides were placed in 0.85% NaCl for 5min and later fixed in 4% paraformaldehyde at room temperature. The samples were permeabilized by proteinase K treatment for 30min and then fixed again in 4% paraformaldehyde. After an equilibration step, the 3´-OH end of DNA breaks was labeled with fluorescein-12-dUTP using a recombinant Terminal Deoxynucleotidyl Transferase (rTdT) enzyme (Promega) by incubating the slides at 37^{o}C for 1hour. The reaction was terminated in 2X SSC solution and after washing in PBS the slides were mounted in medium with DAPI (Vectashield). Images were obtained using the Leica TCS SP5 spectral confocal and multiphoton microscope system and the LAS AF software (Leica, Microsystems).

2.4.3 Molecular Biology

2.4.3.1 Quantitative RT-PCR

Total RNA was isolated from hearts using TRIzol (Invitrogen). The RNA was treated with DNaseI enzyme (Promega) for 1h at 37°C and cleaned by column purification (Qiagen). The RNA concentration was determined with a spectrophotometer (SmartSpec™ 3000, BioRad). RNA quality verification was performed on a 1% agarose gel (0.2M MOPS, 50mM NaOAc, 10mM EDTA). 1-2μg total RNA were used to prepare cDNA (Ready-To-Go, T-Primed First-Strand Kit, Amersham Bioscience). Inventoried FAM TaqMan probes (Applied Biosystems) were used for the relative quantification of the mRNA levels of *myosin heavy chain-6 (Myh6), myosin heavy chain-7 (Myh7), atrial natriuretic peptide (Anp), brain natriuretic peptide (Bnp), glucose transporter-1 (Glut-1)* and *actin-alpha -1skeletal muscle (Acta-1)* genes. Taqman VIC *Glyceraldehyde 3-phosphate dehydrogenase (GAPDH)* probes were used for normalization (table 2.3).

Table 2.3 TaqMAn assays

Gene	*TaqMan assay part number*
atrial natriuretic peptide (Anp)	Mm01255747_g1
brain natriuretic peptide (Bnp)	Mm00435304_g1
glucose transporter-1 (Glut-1)	Mm00441473_m1
actin-alpha -1skeletal muscle (Acta-1)	Mm00808218_g1
myosin heavy chain-6 (Myh6)	Mm00440354_m1
myosin heavy chain-7 (Myh7	Mm00600555_m1
Glyceraldehyde 3-phosphate dehydrogenase (GAPDH)	4352339E

2.4.3.2 Southern blot analysis

Mouse tissues (kidney, brain, spleen, lung, liver, heart and skeletal muscle) were homogenized in lysis buffer (20mM Tris-HCl pH 7.5, 200mM NaCl, 20mM EDTA, 2% SDS) and digested with Proteinase K for 1hour at 37°C. Genomic DNA was extracted with the addition of equilibrated phenol/chloroform solution and subsequent centrifugation at 13.000rpm for 2min. The supernatant was recovered and RNA fragments were eliminated by RnaseA treatment (10min, 37°C). Next, the phenol/chloroform step was repeated and DNA was precipitated with NaOAc (3M, pH 6.0) and ethanol. After centrifugation, the DNA pellet was washed with 70% ethanol, air-

dried and diluted in dH2O. DNA concentration was determined with a spectrophotometer (SmartSpec^{TM} 3000, BioRad). Twenty μgr of genomic DNA from various mouse tissues were digested over-night (o/n) with BamHI restriction enzyme at 37^{o}C. The BamHI genomic fragments were separated by electrophoresis in a 0.7% agarose gel (run at 20V for 8h), and transferred o/n to a positively charged nylon membrane (Amersham). Next, the membrane was neutralized with 2x SSPE and pre-hybridized with the hybridization buffer (Rapid-Hyb buffer, Amersham) for 2 hours at 65^{o}C. Then, the *Nemo* DNA probe was synthesized by PCR following the Nemo genotyping conditions (5"-3" primer sequences: CAG CCT ATC ACC AAC TCT TCC and TCT GCT GCT CCT ACT CTA TGC) and was labeled using Klenow polymerase with ^{32}P-dGTP. Next, the probe was purified through a Sephadex column and added to the hybridization buffer. After o/n incubation, the membrane was washed (2x SSPE) and radioactive signals were detected by phosphoimager.

2.4.3.3 Immunoblot Analysis

Protein extraction was performed in RIPA buffer (1% (w/w) Nonidet P40, 1% (w/w) Sodiumdeoxycate, 0.1% (w/v) SDS, 150mM NaCl, 50mM HEPES pH 7.0, 2mM EDTA pH 8.0, 100mM NaF, 10% glycerol, 1.5mM $MgCl_2$, 100mM PMSF in ETOH, 200mM sodium orthovanadate, 1 μgr/ml aprotin and one tablet of protease inhibitor cocktail (Roche) per 10ml of RIPA buffer. Protein determination was done using Brandford method (Biorad) and 40μgr of protein lysates were separated in 10% SDS polyacrylamide mini-gel (Biorad system) and transferred onto a hybond ECL nitrocellulose membrane (Amersham). Filters were blocked with 5% milk, blotted with specific antibodies o/n at 4^{o}C, washed with 3 times for 30min with washing buffer (TBS and 0,1% Tween-20) and blotted with specific secondary antibodies (horseradish peroxidase-conjugated, 1:5000, Amersham) with 5% milk for 1h at RT. The filter was incubated for 1 min using ECL kit (Amersham) before exposure. Primary antibodies were: anti-IKK1 and anti-IKK2 (1:250, IMGENEX), anti-NEMO (1:500, provided by Ralph Gareus, Manolis Pasparakis laboratory). Anti-α-tubulin (1:2000, SIGMA) was used for normalization.

2.4.3.4 Electromobility Assay

Animals were injected intraperitoneally with 1ml of 0.1mgr LPS (Sigma) and hearts were excised and snap-frozen at the indicated time points. Cytoplasmic proteins were collected after smashing the frozen heart samples in a porcelain mortar and

homogenizing them with a douncer in 300µl of buffer A (10mM Hepes pH 7,6, 10mM KCl, 2mM MgCl2, 1mM DTT and 0.1mM EDTA). A swelling step at 4^{o}C for 10min was required and after the addition of 3.5 µl of 10% Nonidet P-40, the samples were centrifuged at maximum speed (14.000rpm) for 1min at 4^{o}C. The cytoplasmic fraction (supernatant) was recovered, aliquoted and placed at -20^{o}C. After washing the pellet with 100µl of Buffer A, the samples were again centrifuged at maximum speed for 15sec and the supernatant was discarded. 100µl of Buffer C (50mM Hepes pH 7.8, 50mM KCl, 300mM NaCl, 0.1 mM EDTA, 1mM DTT and 10% glycerol) were then added into the samples and the nuclear extracts (supernatant) were obtained after 30min on ice incubation and subsequent centrifugation at maximum speed for 10min. Nuclear and cytoplasmic protein fractions were quantified with the Bradford method. Nuclear extracts (4µg) from heart tissue were incubated for 30min at room temperature with 2µg poly (dI-dC) (Pharmacia), 0.5ng of ^{32}P-labeled κB probe (prepared from H2-κB-b site primer: 5'CGG GCT GGG GAT TCC CCA TCT CGG TAC-3' and 5'-GTA CCG AGA TGG GGA ATC CCC AGC CCG-3') and 2.5µl of 10x Binding Reaction Buffer-BRB (100mM Tris pH 7.5, 1M NaCl, 50mM DTT, 10mM EDTA, 40% Glycerol, 1mg/ml BSA). Samples were fractionated on a 5% polyacrylamide gel for 3h and visualized by autoradiography.

2.5 Statistics

Statistical analysis was performed using the student's *t* test (tail 2, type 2). Values were expressed as mean ± SEM and differences with p value < 0.05 were considered significant (* $p < 0.05$, ** $p < 0.01$, *** $p < 0.001$).

3. BIBLIOGRAPHY

1. Olson, E. N. Gene regulatory networks in the evolution and development of the heart. Science 313, 1922-7 (2006).
2. Moorman, A. F. & Christoffels, V. M. Cardiac chamber formation: development, genes, and evolution. Physiol Rev 83, 1223-67 (2003).
3. Romer, A. S. Major steps in vertebrate evolution. Science 158, 1629-37 (1967).
4. Simoes-Costa, M. S. et al. The evolutionary origin of cardiac chambers. Dev Biol 277, 1-15 (2005).
5. Cripps, R. M. & Olson, E. N. Twist is required for muscle template splitting during adult Drosophila myogenesis. Dev Biol 203, 106-15 (1998).
6. S, O. O. & Saitou, N. Phylogenetic relationship of muscle tissues deduced from superimposition of gene trees. Mol Biol Evol 16, 856-67 (1999).
7. Grens, A., Gee, L., Fisher, D. A. & Bode, H. R. CnNK-2, an NK-2 homeobox gene, has a role in patterning the basal end of the axis in hydra. Dev Biol 180, 473-88 (1996).
8. Holland, N. D., Venkatesh, T. V., Holland, L. Z., Jacobs, D. K. & Bodmer, R. AmphiNk2-tin, an amphioxus homeobox gene expressed in myocardial progenitors: insights into evolution of the vertebrate heart. Dev Biol 255, 128-37 (2003).
9. Hoffman, J. I. & Kaplan, S. The incidence of congenital heart disease. J Am Coll Cardiol 39, 1890-900 (2002).
10. Dunwoodie, S. L. Combinatorial signaling in the heart orchestrates cardiac induction, lineage specification and chamber formation. Semin Cell Dev Biol 18, 54-66 (2007).
11. Mjaatvedt, C. H. et al. The outflow tract of the heart is recruited from a novel heart-forming field. Dev Biol 238, 97-109 (2001).
12. Waldo, K. L. et al. Conotruncal myocardium arises from a secondary heart field. Development 128, 3179-88 (2001).
13. Cai, C. L. et al. Isl1 identifies a cardiac progenitor population that proliferates prior to differentiation and contributes a majority of cells to the heart. Dev Cell 5, 877-89 (2003).
14. Kelly, R. G., Brown, N. A. & Buckingham, M. E. The arterial pole of the mouse heart forms from Fgf10-expressing cells in pharyngeal mesoderm. Dev Cell 1, 435-40 (2001).
15. Meilhac, S. M., Esner, M., Kelly, R. G., Nicolas, J. F. & Buckingham, M. E. The clonal origin of myocardial cells in different regions of the embryonic mouse heart. Dev Cell 6, 685-98 (2004).
16. Zaffran, S., Kelly, R. G., Meilhac, S. M., Buckingham, M. E. & Brown, N. A. Right ventricular myocardium derives from the anterior heart field. Circ Res 95, 261-8 (2004).
17. Bockman, D. E. & Kirby, M. L. Dependence of thymus development on derivatives of the neural crest. Science 223, 498-500 (1984).
18. Kirby, M. L., Gale, T. F. & Stewart, D. E. Neural crest cells contribute to normal aorticopulmonary septation. Science 220, 1059-61 (1983).
19. Garcia-Martinez, V. & Schoenwolf, G. C. Primitive-streak origin of the cardiovascular system in avian embryos. Dev Biol 159, 706-19 (1993).
20. Tam, P. P., Parameswaran, M., Kinder, S. J. & Weinberger, R. P. The allocation of epiblast cells to the embryonic heart and other mesodermal lineages: the role of ingression and tissue movement during gastrulation. Development 124, 1631-42 (1997).
21. Srivastava, D. Making or breaking the heart: from lineage determination to morphogenesis. Cell 126, 1037-48 (2006).
22. Buckingham, M., Meilhac, S. & Zaffran, S. Building the mammalian heart from two sources of myocardial cells. Nat Rev Genet 6, 826-35 (2005).
23. Abu-Issa, R., Waldo, K. & Kirby, M. L. Heart fields: one, two or more? Dev Biol 272, 281-5 (2004).
24. Stoller, J. Z. & Epstein, J. A. Cardiac neural crest. Semin Cell Dev Biol 16, 704-15 (2005).
25. Moorman, A. F., de Jong, F., Denyn, M. M. & Lamers, W. H. Development of the cardiac conduction system. Circ Res 82, 629-44 (1998).
26. Tomanek, R. J. Formation of the coronary vasculature during development. Angiogenesis 8, 273-84 (2005).
27. McFadden, D. G. et al. The Hand1 and Hand2 transcription factors regulate expansion of the embryonic cardiac ventricles in a gene dosage-dependent manner. Development 132, 189-201 (2005).
28. Riley, P., Anson-Cartwright, L. & Cross, J. C. The Hand1 bHLH transcription factor is essential for placentation and cardiac morphogenesis. Nat Genet 18, 271-5 (1998).
29. Lyons, I. et al. Myogenic and morphogenetic defects in the heart tubes of murine embryos lacking the homeo box gene Nkx2-5. Genes Dev 9, 1654-66 (1995).

30. Tanaka, M. et al. Complex modular cis-acting elements regulate expression of the cardiac specifying homeobox gene Csx/Nkx2.5. Development 126, 1439-50 (1999).
31. Bruneau, B. G. et al. A murine model of Holt-Oram syndrome defines roles of the T-box transcription factor Tbx5 in cardiogenesis and disease. Cell 106, 709-21 (2001).
32. von Both, I. et al. Foxh1 is essential for development of the anterior heart field. Dev Cell 7, 331-45 (2004).
33. Lin, Q., Schwarz, J., Bucana, C. & Olson, E. N. Control of mouse cardiac morphogenesis and myogenesis by transcription factor MEF2C. Science 276, 1404-7 (1997).
34. Srivastava, D., Cserjesi, P. & Olson, E. N. A subclass of bHLH proteins required for cardiac morphogenesis. Science 270, 1995-9 (1995).
35. Srivastava, D. et al. Regulation of cardiac mesodermal and neural crest development by the bHLH transcription factor, dHAND. Nat Genet 16, 154-60 (1997).
36. Singh, M. K. et al. Tbx20 is essential for cardiac chamber differentiation and repression of Tbx2. Development 132, 2697-707 (2005).
37. Stennard, F. A. et al. Murine T-box transcription factor Tbx20 acts as a repressor during heart development, and is essential for adult heart integrity, function and adaptation. Development 132, 2451-62 (2005).
38. Takeuchi, J. K. et al. Tbx20 dose-dependently regulates transcription factor networks required for mouse heart and motoneuron development. Development 132, 2463-74 (2005).
39. Abu-Issa, R., Smyth, G., Smoak, I., Yamamura, K. & Meyers, E. N. Fgf8 is required for pharyngeal arch and cardiovascular development in the mouse. Development 129, 4613-25 (2002).
40. Frank, D. U. et al. An Fgf8 mouse mutant phenocopies human 22q11 deletion syndrome. Development 129, 4591-603 (2002).
41. Garg, V. et al. Tbx1, a DiGeorge syndrome candidate gene, is regulated by sonic hedgehog during pharyngeal arch development. Dev Biol 235, 62-73 (2001).
42. Jerome, L. A. & Papaioannou, V. E. DiGeorge syndrome phenotype in mice mutant for the T-box gene, Tbx1. Nat Genet 27, 286-91 (2001).
43. Lindsay, E. A. et al. Tbx1 haploinsufficieny in the DiGeorge syndrome region causes aortic arch defects in mice. Nature 410, 97-101 (2001).
44. Merscher, S. et al. TBX1 is responsible for cardiovascular defects in velo-cardio-facial/DiGeorge syndrome. Cell 104, 619-29 (2001).
45. Li, L. et al. Alagille syndrome is caused by mutations in human Jagged1, which encodes a ligand for Notch1. Nat Genet 16, 243-51 (1997).
46. Oda, T. et al. Mutations in the human Jagged1 gene are responsible for Alagille syndrome. Nat Genet 16, 235-42 (1997).
47. McCright, B., Lozier, J. & Gridley, T. A mouse model of Alagille syndrome: Notch2 as a genetic modifier of Jag1 haploinsufficiency. Development 129, 1075-82 (2002).
48. Donovan, J., Kordylewska, A., Jan, Y. N. & Utset, M. F. Tetralogy of fallot and other congenital heart defects in Hey2 mutant mice. Curr Biol 12, 1605-10 (2002).
49. Sakata, Y. et al. Ventricular septal defect and cardiomyopathy in mice lacking the transcription factor CHF1/Hey2. Proc Natl Acad Sci U S A 99, 16197-202 (2002).
50. Soonpaa, M. H., Kim, K. K., Pajak, L., Franklin, M. & Field, L. J. Cardiomyocyte DNA synthesis and binucleation during murine development. Am J Physiol 271, H2183-9 (1996).
51. MacLellan, W. R. & Schneider, M. D. Genetic dissection of cardiac growth control pathways. Annu Rev Physiol 62, 289-319 (2000).
52. Anversa, P. & Kajstura, J. Ventricular myocytes are not terminally differentiated in the adult mammalian heart. Circ Res 83, 1-14 (1998).
53. Nakagawa, M., Hamaoka, K., Hattori, T. & Sawada, T. Postnatal DNA synthesis in hearts of mice: autoradiographic and cytofluorometric investigations. Cardiovasc Res 22, 575-83 (1988).
54. Soonpaa, M. H. & Field, L. J. Assessment of cardiomyocyte DNA synthesis in normal and injured adult mouse hearts. Am J Physiol 272, H220-6 (1997).
55. Zhu, X., Sasse, J., McAllister, D. & Lough, J. Evidence that fibroblast growth factors 1 and 4 participate in regulation of cardiogenesis. Dev Dyn 207, 429-38 (1996).
56. Kuhn, B. et al. Periostin induces proliferation of differentiated cardiomyocytes and promotes cardiac repair. Nat Med 13, 962-9 (2007).
57. Heineke, J. & Molkentin, J. D. Regulation of cardiac hypertrophy by intracellular signalling pathways. Nat Rev Mol Cell Biol 7, 589-600 (2006).
58. Olson, E. N. & Schneider, M. D. Sizing up the heart: development redux in disease. Genes Dev 17, 1937-56 (2003).
59. Hunter, J. J. & Chien, K. R. Signaling pathways for cardiac hypertrophy and failure. N Engl J Med 341, 1276-83 (1999).

60. Oka, T. et al. Cardiac-specific deletion of Gata4 reveals its requirement for hypertrophy, compensation, and myocyte viability. Circ Res 98, 837-45 (2006).
61. Nadruz, W., Jr., Corat, M. A., Marin, T. M., Guimaraes Pereira, G. A. & Franchini, K. G. Focal adhesion kinase mediates MEF2 and c-Jun activation by stretch: role in the activation of the cardiac hypertrophic genetic program. Cardiovasc Res 68, 87-97 (2005).
62. Xu, J. et al. Myocyte enhancer factors 2A and 2C induce dilated cardiomyopathy in transgenic mice. J Biol Chem 281, 9152-62 (2006).
63. Lee, Y. et al. The cardiac tissue-restricted homeobox protein Csx/Nkx2.5 physically associates with the zinc finger protein GATA4 and cooperatively activates atrial natriuretic factor gene expression. Mol Cell Biol 18, 3120-9 (1998).
64. Takimoto, E. et al. Up-regulation of natriuretic peptides in the ventricle of Csx/Nkx2-5 transgenic mice. Biochem Biophys Res Commun 270, 1074-9 (2000).
65. Chien, K. R. et al. Transcriptional regulation during cardiac growth and development. Annu Rev Physiol 55, 77-95 (1993).
66. MacLellan, W. R. & Schneider, M. D. Death by design. Programmed cell death in cardiovascular biology and disease. Circ Res 81, 137-44 (1997).
67. Deschamps, A. M. & Spinale, F. G. Pathways of matrix metalloproteinase induction in heart failure: bioactive molecules and transcriptional regulation. Cardiovasc Res 69, 666-76 (2006).
68. Kang, P. M. & Izumo, S. Apoptosis in heart: basic mechanisms and implications in cardiovascular diseases. Trends Mol Med 9, 177-82 (2003).
69. Hirota, H. et al. Loss of a gp130 cardiac muscle cell survival pathway is a critical event in the onset of heart failure during biomechanical stress. Cell 97, 189-98 (1999).
70. Sivasubramanian, N. et al. Left ventricular remodeling in transgenic mice with cardiac restricted overexpression of tumor necrosis factor. Circulation 104, 826-31 (2001).
71. Kubota, T., McTiernan, C. F., Frye, C. S., Demetris, A. J. & Feldman, A. M. Cardiac-specific overexpression of tumor necrosis factor-alpha causes lethal myocarditis in transgenic mice. J Card Fail 3, 117-24 (1997).
72. Chien, K. R. Stress pathways and heart failure. Cell 98, 555-8 (1999).
73. Levy, D. et al. Long-term trends in the incidence of and survival with heart failure. N Engl J Med 347, 1397-402 (2002).
74. Redfield, M. M. Heart failure--an epidemic of uncertain proportions. N Engl J Med 347, 1442-4 (2002).
75. Bruneau, B. G. The developmental genetics of congenital heart disease. Nature 451, 943-8 (2008).
76. Cleland, J. G., Khand, A. & Clark, A. The heart failure epidemic: exactly how big is it? Eur Heart J 22, 623-6 (2001).
77. Zannad, F. et al. Incidence, clinical and etiologic features, and outcomes of advanced chronic heart failure: the EPICAL Study. Epidemiologie de l'Insuffisance Cardiaque Avancee en Lorraine. J Am Coll Cardiol 33, 734-42 (1999).
78. Lips, D. J., deWindt, L. J., van Kraaij, D. J. & Doevendans, P. A. Molecular determinants of myocardial hypertrophy and failure: alternative pathways for beneficial and maladaptive hypertrophy. Eur Heart J 24, 883-96 (2003).
79. Kerkela, R. et al. Cardiotoxicity of the cancer therapeutic agent imatinib mesylate. Nat Med 12, 908-16 (2006).
80. Berenji, K., Drazner, M. H., Rothermel, B. A. & Hill, J. A. Does load-induced ventricular hypertrophy progress to systolic heart failure? Am J Physiol Heart Circ Physiol 289, H8-H16 (2005).
81. Pedrazzini, T. Control of cardiogenesis by the notch pathway. Trends Cardiovasc Med 17, 83-90 (2007).
82. Reinecke, H., Zhang, M., Bartosek, T. & Murry, C. E. Survival, integration, and differentiation of cardiomyocyte grafts: a study in normal and injured rat hearts. Circulation 100, 193-202 (1999).
83. Taylor, D. A. et al. Regenerating functional myocardium: improved performance after skeletal myoblast transplantation. Nat Med 4, 929-33 (1998).
84. Reinecke, H., Poppa, V. & Murry, C. E. Skeletal muscle stem cells do not transdifferentiate into cardiomyocytes after cardiac grafting. J Mol Cell Cardiol 34, 241-9 (2002).
85. Menasche, P. et al. Autologous skeletal myoblast transplantation for severe postinfarction left ventricular dysfunction. J Am Coll Cardiol 41, 1078-83 (2003).
86. Orlic, D. et al. Bone marrow cells regenerate infarcted myocardium. Nature 410, 701-5 (2001).
87. Orlic, D. et al. Mobilized bone marrow cells repair the infarcted heart, improving function and survival. Proc Natl Acad Sci U S A 98, 10344-9 (2001).
88. Pittenger, M. F. et al. Multilineage potential of adult human mesenchymal stem cells. Science 284, 143-7 (1999).
89. Shake, J. G. et al. Mesenchymal stem cell implantation in a swine myocardial infarct model: engraftment and functional effects. Ann Thorac Surg 73, 1919-25; discussion 1926 (2002).

90. Badorff, C. et al. Transdifferentiation of blood-derived human adult endothelial progenitor cells into functionally active cardiomyocytes. Circulation 107, 1024-32 (2003).
91. Condorelli, G. et al. Cardiomyocytes induce endothelial cells to trans-differentiate into cardiac muscle: implications for myocardium regeneration. Proc Natl Acad Sci U S A 98, 10733-8 (2001).
92. Assmus, B. et al. Transplantation of Progenitor Cells and Regeneration Enhancement in Acute Myocardial Infarction (TOPCARE-AMI). Circulation 106, 3009-17 (2002).
93. Stamm, C. et al. Autologous bone-marrow stem-cell transplantation for myocardial regeneration. Lancet 361, 45-6 (2003).
94. Oh, H. et al. Telomerase reverse transcriptase promotes cardiac muscle cell proliferation, hypertrophy, and survival. Proc Natl Acad Sci U S A 98, 10308-13 (2001).
95. Leri, A. et al. Ablation of telomerase and telomere loss leads to cardiac dilatation and heart failure associated with p53 upregulation. Embo J 22, 131-9 (2003).
96. Cheng, R. K. et al. Cyclin A2 induces cardiac regeneration after myocardial infarction and prevents heart failure. Circ Res 100, 1741-8 (2007).
97. Rybkin, II et al. Conditional expression of SV40 T-antigen in mouse cardiomyocytes facilitates an inducible switch from proliferation to differentiation. J Biol Chem 278, 15927-34 (2003).
98. Asakura, A. & Rudnicki, M. A. Side population cells from diverse adult tissues are capable of in vitro hematopoietic differentiation. Exp Hematol 30, 1339-45 (2002).
99. Hierlihy, A. M., Seale, P., Lobe, C. G., Rudnicki, M. A. & Megeney, L. A. The post-natal heart contains a myocardial stem cell population. FEBS Lett 530, 239-43 (2002).
100. Beltrami, A. P. et al. Adult cardiac stem cells are multipotent and support myocardial regeneration. Cell 114, 763-76 (2003).
101. Oh, H. et al. Cardiac progenitor cells from adult myocardium: homing, differentiation, and fusion after infarction. Proc Natl Acad Sci U S A 100, 12313-8 (2003).
102. Bock-Marquette, I., Saxena, A., White, M. D., Dimaio, J. M. & Srivastava, D. Thymosin beta4 activates integrin-linked kinase and promotes cardiac cell migration, survival and cardiac repair. Nature 432, 466-72 (2004).
103. Kusano, K. F. et al. Sonic hedgehog myocardial gene therapy: tissue repair through transient reconstitution of embryonic signaling. Nat Med 11, 1197-204 (2005).
104. Leri, A., Kajstura, J. & Anversa, P. Cardiac stem cells and mechanisms of myocardial regeneration. Physiol Rev 85, 1373-416 (2005).
105. Smart, N. et al. Thymosin beta4 induces adult epicardial progenitor mobilization and neovascularization. Nature 445, 177-82 (2007).
106. Mitchell, L. E. et al. Spina bifida. Lancet 364, 1885-95 (2004).
107. High, F. A. & Epstein, J. A. The multifaceted role of Notch in cardiac development and disease. Nat Rev Genet 9, 49-61 (2008).
108. Artavanis-Tsakonas, S., Rand, M. D. & Lake, R. J. Notch signaling: cell fate control and signal integration in development. Science 284, 770-6 (1999).
109. Bray, S. J. Notch signalling: a simple pathway becomes complex. Nat Rev Mol Cell Biol 7, 678-89 (2006).
110. Yoshida, K. et al. Targeted disruption of gp130, a common signal transducer for the interleukin 6 family of cytokines, leads to myocardial and hematological disorders. Proc Natl Acad Sci U S A 93, 407-11 (1996).
111. Ehebauer, M., Hayward, P. & Arias, A. M. Notch, a universal arbiter of cell fate decisions. Science 314, 1414-5 (2006).
112. Simpson, P. Lateral inhibition and the development of the sensory bristles of the adult peripheral nervous system of Drosophila. Development 109, 509-19 (1990).
113. Schweisguth, F. Regulation of notch signaling activity. Curr Biol 14, R129-38 (2004).
114. Kidd, S., Kelley, M. R. & Young, M. W. Sequence of the notch locus of Drosophila melanogaster: relationship of the encoded protein to mammalian clotting and growth factors. Mol Cell Biol 6, 3094-108 (1986).
115. Wharton, K. A., Johansen, K. M., Xu, T. & Artavanis-Tsakonas, S. Nucleotide sequence from the neurogenic locus notch implies a gene product that shares homology with proteins containing EGF-like repeats. Cell 43, 567-81 (1985).
116. Kadesch, T. Notch signaling: the demise of elegant simplicity. Curr Opin Genet Dev 14, 506-12 (2004).
117. Aulehla, A. & Herrmann, B. G. Segmentation in vertebrates: clock and gradient finally joined. Genes Dev 18, 2060-7 (2004).
118. Shi, S. & Stanley, P. Evolutionary origins of Notch signaling in early development. Cell Cycle 5, 274-8 (2006).
119. Good, K. et al. The T-box transcription factors TBX-37 and TBX-38 link GLP-1/Notch signaling to mesoderm induction in C. elegans embryos. Development 131, 1967-78 (2004).

120. Kikuchi, Y. et al. Notch signaling can regulate endoderm formation in zebrafish. Dev Dyn 229, 756-62 (2004).
121. Contakos, S. P., Gaydos, C. M., Pfeil, E. C. & McLaughlin, K. A. Subdividing the embryo: a role for Notch signaling during germ layer patterning in Xenopus laevis. Dev Biol 288, 294-307 (2005).
122. Donoviel, D. B. et al. Mice lacking both presenilin genes exhibit early embryonic patterning defects. Genes Dev 13, 2801-10 (1999).
123. Oka, C. et al. Disruption of the mouse RBP-J kappa gene results in early embryonic death. Development 121, 3291-301 (1995).
124. Swiatek, P. J., Lindsell, C. E., del Amo, F. F., Weinmaster, G. & Gridley, T. Notch1 is essential for postimplantation development in mice. Genes Dev 8, 707-19 (1994).
125. Brennan, K., Tateson, R., Lewis, K. & Arias, A. M. A functional analysis of Notch mutations in Drosophila. Genetics 147, 177-88 (1997).
126. Sanchez-Irizarry, C. et al. Notch subunit heterodimerization and prevention of ligand-independent proteolytic activation depend, respectively, on a novel domain and the LNR repeats. Mol Cell Biol 24, 9265-73 (2004).
127. Kurooka, H. & Honjo, T. Functional interaction between the mouse notch1 intracellular region and histone acetyltransferases PCAF and GCN5. J Biol Chem 275, 17211-20 (2000).
128. Schroeter, E. H., Kisslinger, J. A. & Kopan, R. Notch-1 signalling requires ligand-induced proteolytic release of intracellular domain. Nature 393, 382-6 (1998).
129. Struhl, G. & Adachi, A. Nuclear access and action of notch in vivo. Cell 93, 649-60 (1998).
130. Fortini, M. E. Gamma-secretase-mediated proteolysis in cell-surface-receptor signalling. Nat Rev Mol Cell Biol 3, 673-84 (2002).
131. Chitnis, A. Why is delta endocytosis required for effective activation of notch? Dev Dyn 235, 886-94 (2006).
132. Overstreet, E., Fitch, E. & Fischer, J. A. Fat facets and Liquid facets promote Delta endocytosis and Delta signaling in the signaling cells. Development 131, 5355-66 (2004).
133. Pitsouli, C. & Delidakis, C. The interplay between DSL proteins and ubiquitin ligases in Notch signaling. Development 132, 4041-50 (2005).
134. Wang, W. & Struhl, G. Distinct roles for Mind bomb, Neuralized and Epsin in mediating DSL endocytosis and signaling in Drosophila. Development 132, 2883-94 (2005).
135. Lawrence, N., Klein, T., Brennan, K. & Martinez Arias, A. Structural requirements for notch signalling with delta and serrate during the development and patterning of the wing disc of Drosophila. Development 127, 3185-95 (2000).
136. Rebay, I. et al. Specific EGF repeats of Notch mediate interactions with Delta and Serrate: implications for Notch as a multifunctional receptor. Cell 67, 687-99 (1991).
137. Sisodia, S. S. & St George-Hyslop, P. H. gamma-Secretase, Notch, Abeta and Alzheimer's disease: where do the presenilins fit in? Nat Rev Neurosci 3, 281-90 (2002).
138. Strooper, B. D. & Annaert, W. Presenilins and the intramembrane proteolysis of proteins: facts and fiction. Nat Cell Biol 3, E221-5 (2001).
139. Levitan, D., Yu, G., St George Hyslop, P. & Goutte, C. APH-2/nicastrin functions in LIN-12/Notch signaling in the Caenorhabditis elegans somatic gonad. Dev Biol 240, 654-61 (2001).
140. L'Hernault, S. W. & Arduengo, P. M. Mutation of a putative sperm membrane protein in Caenorhabditis elegans prevents sperm differentiation but not its associated meiotic divisions. J Cell Biol 119, 55-68 (1992).
141. Wolfe, M. S., De Los Angeles, J., Miller, D. D., Xia, W. & Selkoe, D. J. Are presenilins intramembrane-cleaving proteases? Implications for the molecular mechanism of Alzheimer's disease. Biochemistry 38, 11223-30 (1999).
142. Wolfe, M. S. et al. Two transmembrane aspartates in presenilin-1 required for presenilin endoproteolysis and gamma-secretase activity. Nature 398, 513-7 (1999).
143. Ray, W. J. et al. Cell surface presenilin-1 participates in the gamma-secretase-like proteolysis of Notch. J Biol Chem 274, 36801-7 (1999).
144. Ye, Y. & Fortini, M. E. Characterization of Drosophila Presenilin and its colocalization with Notch during development. Mech Dev 79, 199-211 (1998).
145. Goutte, C., Tsunozaki, M., Hale, V. A. & Priess, J. R. APH-1 is a multipass membrane protein essential for the Notch signaling pathway in Caenorhabditis elegans embryos. Proc Natl Acad Sci U S A 99, 775-9 (2002).
146. Hu, Y., Ye, Y. & Fortini, M. E. Nicastrin is required for gamma-secretase cleavage of the Drosophila Notch receptor. Dev Cell 2, 69-78 (2002).
147. Chung, H. M. & Struhl, G. Nicastrin is required for Presenilin-mediated transmembrane cleavage in Drosophila. Nat Cell Biol 3, 1129-32 (2001).
148. Lopez-Schier, H. & St Johnston, D. Drosophila nicastrin is essential for the intramembranous cleavage of notch. Dev Cell 2, 79-89 (2002).

149. Francis, R. et al. aph-1 and pen-2 are required for Notch pathway signaling, gamma-secretase cleavage of betaAPP, and presenilin protein accumulation. Dev Cell 3, 85-97 (2002).
150. Kao, H. Y. et al. A histone deacetylase corepressor complex regulates the Notch signal transduction pathway. Genes Dev 12, 2269-77 (1998).
151. Hsieh, J. J., Zhou, S., Chen, L., Young, D. B. & Hayward, S. D. CIR, a corepressor linking the DNA binding factor CBF1 to the histone deacetylase complex. Proc Natl Acad Sci U S A 96, 23-8 (1999).
152. Oswald, F. et al. SHARP is a novel component of the Notch/RBP-Jkappa signalling pathway. Embo J 21, 5417-26 (2002).
153. Fortini, M. E. & Artavanis-Tsakonas, S. The suppressor of hairless protein participates in notch receptor signaling. Cell 79, 273-82 (1994).
154. Kato, H. et al. Involvement of RBP-J in biological functions of mouse Notch1 and its derivatives. Development 124, 4133-41 (1997).
155. Tamura, K. et al. Physical interaction between a novel domain of the receptor Notch and the transcription factor RBP-J kappa/Su(H). Curr Biol 5, 1416-23 (1995).
156. Tani, S., Kurooka, H., Aoki, T., Hashimoto, N. & Honjo, T. The N- and C-terminal regions of RBP-J interact with the ankyrin repeats of Notch1 RAMIC to activate transcription. Nucleic Acids Res 29, 1373-80 (2001).
157. Wu, L. et al. MAML1, a human homologue of Drosophila mastermind, is a transcriptional co-activator for NOTCH receptors. Nat Genet 26, 484-9 (2000).
158. Kitagawa, M. et al. A human protein with sequence similarity to Drosophila mastermind coordinates the nuclear form of notch and a CSL protein to build a transcriptional activator complex on target promoters. Mol Cell Biol 21, 4337-46 (2001).
159. Nam, Y., Weng, A. P., Aster, J. C. & Blacklow, S. C. Structural requirements for assembly of the CSL.intracellular Notch1.Mastermind-like 1 transcriptional activation complex. J Biol Chem 278, 21232-9 (2003).
160. Wu, L., Sun, T., Kobayashi, K., Gao, P. & Griffin, J. D. Identification of a family of mastermind-like transcriptional coactivators for mammalian notch receptors. Mol Cell Biol 22, 7688-700 (2002).
161. Fryer, C. J., Lamar, E., Turbachova, I., Kintner, C. & Jones, K. A. Mastermind mediates chromatin-specific transcription and turnover of the Notch enhancer complex. Genes Dev 16, 1397-411 (2002).
162. Fryer, C. J., White, J. B. & Jones, K. A. Mastermind recruits CycC:CDK8 to phosphorylate the Notch ICD and coordinate activation with turnover. Mol Cell 16, 509-20 (2004).
163. Mumm, J. S. & Kopan, R. Notch signaling: from the outside in. Dev Biol 228, 151-65 (2000).
164. Mumm, J. S. et al. A ligand-induced extracellular cleavage regulates gamma-secretase-like proteolytic activation of Notch1. Mol Cell 5, 197-206 (2000).
165. Fischer, A. & Gessler, M. Hey genes in cardiovascular development. Trends Cardiovasc Med 13, 221-6 (2003).
166. Bae, S., Bessho, Y., Hojo, M. & Kageyama, R. The bHLH gene Hes6, an inhibitor of Hes1, promotes neuronal differentiation. Development 127, 2933-43 (2000).
167. Bessho, Y., Miyoshi, G., Sakata, R. & Kageyama, R. Hes7: a bHLH-type repressor gene regulated by Notch and expressed in the presomitic mesoderm. Genes Cells 6, 175-85 (2001).
168. Pissarra, L., Henrique, D. & Duarte, A. Expression of hes6, a new member of the Hairy/Enhancer-of-split family, in mouse development. Mech Dev 95, 275-8 (2000).
169. Sasai, Y., Kageyama, R., Tagawa, Y., Shigemoto, R. & Nakanishi, S. Two mammalian helix-loop-helix factors structurally related to Drosophila hairy and Enhancer of split. Genes Dev 6, 2620-34 (1992).
170. Chin, M. T. et al. Cardiovascular basic helix loop helix factor 1, a novel transcriptional repressor expressed preferentially in the developing and adult cardiovascular system. J Biol Chem 275, 6381-7 (2000).
171. Iso, T. et al. HERP, a new primary target of Notch regulated by ligand binding. Mol Cell Biol 21, 6071-9 (2001).
172. Leimeister, C., Schumacher, N., Steidl, C. & Gessler, M. Analysis of HeyL expression in wild-type and Notch pathway mutant mouse embryos. Mech Dev 98, 175-8 (2000).
173. Nakagawa, O. et al. Members of the HRT family of basic helix-loop-helix proteins act as transcriptional repressors downstream of Notch signaling. Proc Natl Acad Sci U S A 97, 13655-60 (2000).
174. Nakagawa, O., Nakagawa, M., Richardson, J. A., Olson, E. N. & Srivastava, D. HRT1, HRT2, and HRT3: a new subclass of bHLH transcription factors marking specific cardiac, somitic, and pharyngeal arch segments. Dev Biol 216, 72-84 (1999).
175. Iso, T., Hamamori, Y. & Kedes, L. Notch signaling in vascular development. Arterioscler Thromb Vasc Biol 23, 543-53 (2003).

176. Iso, T., Kedes, L. & Hamamori, Y. HES and HERP families: multiple effectors of the Notch signaling pathway. J Cell Physiol 194, 237-55 (2003).
177. Maier, M. M. & Gessler, M. Comparative analysis of the human and mouse Hey1 promoter: Hey genes are new Notch target genes. Biochem Biophys Res Commun 275, 652-60 (2000).
178. Jarriault, S. & Greenwald, I. Evidence for functional redundancy between C. elegans ADAM proteins SUP-17/Kuzbanian and ADM-4/TACE. Dev Biol 287, 1-10 (2005).
179. Ohtsuka, T. et al. Hes1 and Hes5 as notch effectors in mammalian neuronal differentiation. Embo J 18, 2196-207 (1999).
180. Koyano-Nakagawa, N., Kim, J., Anderson, D. & Kintner, C. Hes6 acts in a positive feedback loop with the neurogenins to promote neuronal differentiation. Development 127, 4203-16 (2000).
181. Nishimura, M. et al. Structure, chromosomal locus, and promoter of mouse Hes2 gene, a homologue of Drosophila hairy and Enhancer of split. Genomics 49, 69-75 (1998).
182. Fischer, A. & Gessler, M. Delta-Notch--and then? Protein interactions and proposed modes of repression by Hes and Hey bHLH factors. Nucleic Acids Res 35, 4583-96 (2007).
183. Okajima, T. & Irvine, K. D. Regulation of notch signaling by o-linked fucose. Cell 111, 893-904 (2002).
184. Shi, S. & Stanley, P. Protein O-fucosyltransferase 1 is an essential component of Notch signaling pathways. Proc Natl Acad Sci U S A 100, 5234-9 (2003).
185. Logeat, F. et al. The Notch1 receptor is cleaved constitutively by a furin-like convertase. Proc Natl Acad Sci U S A 95, 8108-12 (1998).
186. Haines, N. & Irvine, K. D. Glycosylation regulates Notch signalling. Nat Rev Mol Cell Biol 4, 786-97 (2003).
187. Kidd, S. & Lieber, T. Furin cleavage is not a requirement for Drosophila Notch function. Mech Dev 115, 41-51 (2002).
188. Matsuno, K., Diederich, R. J., Go, M. J., Blaumueller, C. M. & Artavanis-Tsakonas, S. Deltex acts as a positive regulator of Notch signaling through interactions with the Notch ankyrin repeats. Development 121, 2633-44 (1995).
189. Lai, E. C. Protein degradation: four E3s for the notch pathway. Curr Biol 12, R74-8 (2002).
190. Shirayoshi, Y. et al. Proto-oncogene of int-3, a mouse Notch homologue, is expressed in endothelial cells during early embryogenesis. Genes Cells 2, 213-24 (1997).
191. Timmerman, L. A. et al. Notch promotes epithelial-mesenchymal transition during cardiac development and oncogenic transformation. Genes Dev 18, 99-115 (2004).
192. Williams, R., Lendahl, U. & Lardelli, M. Complementary and combinatorial patterns of Notch gene family expression during early mouse development. Mech Dev 53, 357-68 (1995).
193. Loomes, K. M. et al. Characterization of Notch receptor expression in the developing mammalian heart and liver. Am J Med Genet 112, 181-9 (2002).
194. Hamada, Y. et al. Mutation in ankyrin repeats of the mouse Notch2 gene induces early embryonic lethality. Development 126, 3415-24 (1999).
195. Loomes, K. M. et al. The expression of Jagged1 in the developing mammalian heart correlates with cardiovascular disease in Alagille syndrome. Hum Mol Genet 8, 2443-9 (1999).
196. Kokubo, H., Miyagawa-Tomita, S. & Johnson, R. L. Hesr, a mediator of the Notch signaling, functions in heart and vessel development. Trends Cardiovasc Med 15, 190-4 (2005).
197. Kokubo, H., Miyagawa-Tomita, S., Nakazawa, M., Saga, Y. & Johnson, R. L. Mouse hesr1 and hesr2 genes are redundantly required to mediate Notch signaling in the developing cardiovascular system. Dev Biol 278, 301-9 (2005).
198. Watanabe, Y. et al. Activation of Notch1 signaling in cardiogenic mesoderm induces abnormal heart morphogenesis in mouse. Development 133, 1625-34 (2006).
199. Xin, M. et al. Essential roles of the bHLH transcription factor Hrt2 in repression of atrial gene expression and maintenance of postnatal cardiac function. Proc Natl Acad Sci U S A 104, 7975-80 (2007).
200. Nemir, M., Croquelois, A., Pedrazzini, T. & Radtke, F. Induction of cardiogenesis in embryonic stem cells via downregulation of Notch1 signaling. Circ Res 98, 1471-8 (2006).
201. Schroeder, T. et al. Recombination signal sequence-binding protein Jkappa alters mesodermal cell fate decisions by suppressing cardiomyogenesis. Proc Natl Acad Sci U S A 100, 4018-23 (2003).
202. Schroeder, T. et al. Activated Notch1 alters differentiation of embryonic stem cells into mesodermal cell lineages at multiple stages of development. Mech Dev 123, 570-9 (2006).
203. Chau, M. D., Tuft, R., Fogarty, K. & Bao, Z. Z. Notch signaling plays a key role in cardiac cell differentiation. Mech Dev 123, 626-40 (2006).
204. Han, Z. & Bodmer, R. Myogenic cells fates are antagonized by Notch only in asymmetric lineages of the Drosophila heart, with or without cell division. Development 130, 3039-51 (2003).
205. Park, M., Yaich, L. E. & Bodmer, R. Mesodermal cell fate decisions in Drosophila are under the control of the lineage genes numb, Notch, and sanpodo. Mech Dev 75, 117-26 (1998).

206. Rones, M. S., McLaughlin, K. A., Raffin, M. & Mercola, M. Serrate and Notch specify cell fates in the heart field by suppressing cardiomyogenesis. Development 127, 3865-76 (2000).
207. Grego-Bessa, J. et al. Notch signaling is essential for ventricular chamber development. Dev Cell 12, 415-29 (2007).
208. Kokubo, H., Tomita-Miyagawa, S., Hamada, Y. & Saga, Y. Hesr1 and Hesr2 regulate atrioventricular boundary formation in the developing heart through the repression of Tbx2. Development 134, 747-55 (2007).
209. Rutenberg, J. B. et al. Developmental patterning of the cardiac atrioventricular canal by Notch and Hairy-related transcription factors. Development 133, 4381-90 (2006).
210. Eisenberg, L. M. & Markwald, R. R. Molecular regulation of atrioventricular valvuloseptal morphogenesis. Circ Res 77, 1-6 (1995).
211. Noseda, M. et al. Notch activation results in phenotypic and functional changes consistent with endothelial-to-mesenchymal transformation. Circ Res 94, 910-7 (2004).
212. Garg, V. et al. Mutations in NOTCH1 cause aortic valve disease. Nature 437, 270-4 (2005).
213. Mohamed, S. A. et al. Novel missense mutations (p.T596M and p.P1797H) in NOTCH1 in patients with bicuspid aortic valve. Biochem Biophys Res Commun 345, 1460-5 (2006).
214. McDaniell, R. et al. NOTCH2 mutations cause Alagille syndrome, a heterogeneous disorder of the notch signaling pathway. Am J Hum Genet 79, 169-73 (2006).
215. Eldadah, Z. A. et al. Familial Tetralogy of Fallot caused by mutation in the jagged1 gene. Hum Mol Genet 10, 163-9 (2001).
216. McElhinney, D. B. et al. Analysis of cardiovascular phenotype and genotype-phenotype correlation in individuals with a JAG1 mutation and/or Alagille syndrome. Circulation 106, 2567-74 (2002).
217. Nakajima, M., Moriizumi, E., Koseki, H. & Shirasawa, T. Presenilin 1 is essential for cardiac morphogenesis. Dev Dyn 230, 795-9 (2004).
218. High, F. A. et al. An essential role for Notch in neural crest during cardiovascular development and smooth muscle differentiation. J Clin Invest 117, 353-63 (2007).
219. Roca, C. & Adams, R. H. Regulation of vascular morphogenesis by Notch signaling. Genes Dev 21, 2511-24 (2007).
220. Leslie, J. D. et al. Endothelial signalling by the Notch ligand Delta-like 4 restricts angiogenesis. Development 134, 839-44 (2007).
221. Mailhos, C. et al. Delta4, an endothelial specific notch ligand expressed at sites of physiological and tumor angiogenesis. Differentiation 69, 135-44 (2001).
222. Shutter, J. R. et al. Dll4, a novel Notch ligand expressed in arterial endothelium. Genes Dev 14, 1313-8 (2000).
223. Siekmann, A. F. & Lawson, N. D. Notch signalling limits angiogenic cell behaviour in developing zebrafish arteries. Nature 445, 781-4 (2007).
224. Lawson, N. D. et al. Notch signaling is required for arterial-venous differentiation during embryonic vascular development. Development 128, 3675-83 (2001).
225. Zhong, T. P., Rosenberg, M., Mohideen, M. A., Weinstein, B. & Fishman, M. C. gridlock, an HLH gene required for assembly of the aorta in zebrafish. Science 287, 1820-4 (2000).
226. Fischer, A. et al. Phenotypic variability in Hey2 -/- mice and absence of HEY2 mutations in patients with congenital heart defects or Alagille syndrome. Mamm Genome 15, 711-6 (2004).
227. Fischer, A., Schumacher, N., Maier, M., Sendtner, M. & Gessler, M. The Notch target genes Hey1 and Hey2 are required for embryonic vascular development. Genes Dev 18, 901-11 (2004).
228. Gale, N. W. et al. Haploinsufficiency of delta-like 4 ligand results in embryonic lethality due to major defects in arterial and vascular development. Proc Natl Acad Sci U S A 101, 15949-54 (2004).
229. Koo, B. K. et al. Mind bomb 1 is essential for generating functional Notch ligands to activate Notch. Development 132, 3459-70 (2005).
230. Krebs, L. T. et al. Haploinsufficient lethality and formation of arteriovenous malformations in Notch pathway mutants. Genes Dev 18, 2469-73 (2004).
231. Krebs, L. T. et al. Notch signaling is essential for vascular morphogenesis in mice. Genes Dev 14, 1343-52 (2000).
232. Xue, Y. et al. Embryonic lethality and vascular defects in mice lacking the Notch ligand Jagged1. Hum Mol Genet 8, 723-30 (1999).
233. Heil, M., Eitenmuller, I., Schmitz-Rixen, T. & Schaper, W. Arteriogenesis versus angiogenesis: similarities and differences. J Cell Mol Med 10, 45-55 (2006).
234. Beckers, J., Clark, A., Wunsch, K., Hrabe De Angelis, M. & Gossler, A. Expression of the mouse Delta1 gene during organogenesis and fetal development. Mech Dev 84, 165-8 (1999).
235. Limbourg, A. et al. Notch ligand Delta-like 1 is essential for postnatal arteriogenesis. Circ Res 100, 363-71 (2007).
236. Hrabe de Angelis, M., McIntyre, J., 2nd & Gossler, A. Maintenance of somite borders in mice requires the Delta homologue DII1. Nature 386, 717-21 (1997).

237. Takeshita, K. et al. Critical role of endothelial Notch1 signaling in postnatal angiogenesis. Circ Res 100, 70-8 (2007).
238. Joutel, A. et al. Strong clustering and stereotyped nature of Notch3 mutations in CADASIL patients. Lancet 350, 1511-5 (1997).
239. Kalaria, R. N., Viitanen, M., Kalimo, H., Dichgans, M. & Tabira, T. The pathogenesis of CADASIL: an update. J Neurol Sci 226, 35-9 (2004).
240. Haritunians, T. et al. CADASIL Notch3 mutant proteins localize to the cell surface and bind ligand. Circ Res 90, 506-8 (2002).
241. Karlstrom, H. et al. A CADASIL-mutated Notch 3 receptor exhibits impaired intracellular trafficking and maturation but normal ligand-induced signaling. Proc Natl Acad Sci U S A 99, 17119-24 (2002).
242. Domenga, V. et al. Notch3 is required for arterial identity and maturation of vascular smooth muscle cells. Genes Dev 18, 2730-5 (2004).
243. Ruchoux, M. M. et al. Transgenic mice expressing mutant Notch3 develop vascular alterations characteristic of cerebral autosomal dominant arteriopathy with subcortical infarcts and leukoencephalopathy. Am J Pathol 162, 329-42 (2003).
244. Jouve, C. et al. Notch signalling is required for cyclic expression of the hairy-like gene HES1 in the presomitic mesoderm. Development 127, 1421-9 (2000).
245. Tomita, K. et al. The bHLH gene Hes1 is essential for expansion of early T cell precursors. Genes Dev 13, 1203-10 (1999).
246. Leimeister, C., Externbrink, A., Klamt, B. & Gessler, M. Hey genes: a novel subfamily of hairy- and Enhancer of split related genes specifically expressed during mouse embryogenesis. Mech Dev 85, 173-7 (1999).
247. Gessler, M. et al. Mouse gridlock: no aortic coarctation or deficiency, but fatal cardiac defects in Hey2 -/- mice. Curr Biol 12, 1601-4 (2002).
248. Kokubo, H. et al. Targeted disruption of hesr2 results in atrioventricular valve anomalies that lead to heart dysfunction. Circ Res 95, 540-7 (2004).
249. Sakata, Y. et al. The spectrum of cardiovascular anomalies in CHF1/Hey2 deficient mice reveals roles in endocardial cushion, myocardial and vascular maturation. J Mol Cell Cardiol 40, 267-73 (2006).
250. Fischer, A. et al. Combined loss of Hey1 and HeyL causes congenital heart defects because of impaired epithelial to mesenchymal transition. Circ Res 100, 856-63 (2007).
251. Dahlqvist, C. et al. Functional Notch signaling is required for BMP4-induced inhibition of myogenic differentiation. Development 130, 6089-99 (2003).
252. Itoh, F. et al. Synergy and antagonism between Notch and BMP receptor signaling pathways in endothelial cells. Embo J 23, 541-51 (2004).
253. Noseda, M. et al. Smooth Muscle alpha-actin is a direct target of Notch/CSL. Circ Res 98, 1468-70 (2006).
254. Hurlbut, G. D., Kankel, M. W., Lake, R. J. & Artavanis-Tsakonas, S. Crossing paths with Notch in the hyper-network. Curr Opin Cell Biol 19, 166-75 (2007).
255. Parmacek, M. S. & Epstein, J. A. Pursuing cardiac progenitors: regeneration redux. Cell 120, 295-8 (2005).
256. Chiba, S. Notch signaling in stem cell systems. Stem Cells 24, 2437-47 (2006).
257. Conboy, I. M. & Rando, T. A. The regulation of Notch signaling controls satellite cell activation and cell fate determination in postnatal myogenesis. Dev Cell 3, 397-409 (2002).
258. Schuster-Gossler, K., Cordes, R. & Gossler, A. Premature myogenic differentiation and depletion of progenitor cells cause severe muscle hypotrophy in Delta1 mutants. Proc Natl Acad Sci U S A 104, 537-42 (2007).
259. Vasyutina, E. et al. RBP-J (Rbpsuh) is essential to maintain muscle progenitor cells and to generate satellite cells. Proc Natl Acad Sci U S A 104, 4443-8 (2007).
260. Poss, K. D., Wilson, L. G. & Keating, M. T. Heart regeneration in zebrafish. Science 298, 2188-90 (2002).
261. Raya, A. et al. Activation of Notch signaling pathway precedes heart regeneration in zebrafish. Proc Natl Acad Sci U S A 100 Suppl 1, 11889-95 (2003).
262. Slack, J. M., Beck, C. W., Gargioli, C. & Christen, B. Cellular and molecular mechanisms of regeneration in Xenopus. Philos Trans R Soc Lond B Biol Sci 359, 745-51 (2004).
263. Katogi, R. et al. Large-scale analysis of the genes involved in fin regeneration and blastema formation in the medaka, Oryzias latipes. Mech Dev 121, 861-72 (2004).
264. Maxwell, P. H. The HIF pathway in cancer. Semin Cell Dev Biol 16, 523-30 (2005).
265. Lee, S. H. et al. Early expression of angiogenesis factors in acute myocardial ischemia and infarction. N Engl J Med 342, 626-33 (2000).

266. Gustafsson, M. V. et al. Hypoxia requires notch signaling to maintain the undifferentiated cell state. Dev Cell 9, 617-28 (2005).
267. Androutsellis-Theotokis, A. et al. Notch signalling regulates stem cell numbers in vitro and in vivo. Nature 442, 823-6 (2006).
268. Arumugam, T. V. et al. Gamma secretase-mediated Notch signaling worsens brain damage and functional outcome in ischemic stroke. Nat Med 12, 621-3 (2006).
269. Gridley, T. Notch signaling in vascular development and physiology. Development 134, 2709-18 (2007).
270. Conboy, I. M., Conboy, M. J., Smythe, G. M. & Rando, T. A. Notch-mediated restoration of regenerative potential to aged muscle. Science 302, 1575-7 (2003).
271. Krebs, L. T. et al. Notch signaling regulates left-right asymmetry determination by inducing Nodal expression. Genes Dev 17, 1207-12 (2003).
272. Przemeck, G. K., Heinzmann, U., Beckers, J. & Hrabe de Angelis, M. Node and midline defects are associated with left-right development in Delta1 mutant embryos. Development 130, 3-13 (2003).
273. McCright, B. et al. Defects in development of the kidney, heart and eye vasculature in mice homozygous for a hypomorphic Notch2 mutation. Development 128, 491-502 (2001).
274. Del Monte, G., Grego-Bessa, J., Gonzalez-Rajal, A., Bolos, V. & De La Pompa, J. L. Monitoring Notch1 activity in development: evidence for a feedback regulatory loop. Dev Dyn 236, 2594-614 (2007).
275. Kim, J. S., Viragh, S., Moorman, A. F., Anderson, R. H. & Lamers, W. H. Development of the myocardium of the atrioventricular canal and the vestibular spine in the human heart. Circ Res 88, 395-402 (2001).
276. Kim, R. Y., Robertson, E. J. & Solloway, M. J. Bmp6 and Bmp7 are required for cushion formation and septation in the developing mouse heart. Dev Biol 235, 449-66 (2001).
277. Guentchev, M. & McKay, R. D. Notch controls proliferation and differentiation of stem cells in a dose-dependent manner. Eur J Neurosci 24, 1504 (2006).
278. Hitoshi, S., Tropepe, V., Ekker, M. & van der Kooy, D. Neural stem cell lineages are regionally specified, but not committed, within distinct compartments of the developing brain. Development 129, 233-44 (2002).
279. Gallahan, D. & Callahan, R. Mammary tumorigenesis in feral mice: identification of a new int locus in mouse mammary tumor virus (Czech II)-induced mammary tumors. J Virol 61, 66-74 (1987).
280. Gallahan, D. et al. Expression of a truncated Int3 gene in developing secretory mammary epithelium specifically retards lobular differentiation resulting in tumorigenesis. Cancer Res 56, 1775-85 (1996).
281. Jhappan, C. et al. Expression of an activated Notch-related int-3 transgene interferes with cell differentiation and induces neoplastic transformation in mammary and salivary glands. Genes Dev 6, 345-55 (1992).
282. Ellisen, L. W. et al. TAN-1, the human homolog of the Drosophila notch gene, is broken by chromosomal translocations in T lymphoblastic neoplasms. Cell 66, 649-61 (1991).
283. Reynolds, T. C., Smith, S. D. & Sklar, J. Analysis of DNA surrounding the breakpoints of chromosomal translocations involving the beta T cell receptor gene in human lymphoblastic neoplasms. Cell 50, 107-17 (1987).
284. Urbanek, K. et al. Stem cell niches in the adult mouse heart. Proc Natl Acad Sci U S A 103, 9226-31 (2006).
285. Koibuchi, N. & Chin, M. T. CHF1/Hey2 plays a pivotal role in left ventricular maturation through suppression of ectopic atrial gene expression. Circ Res 100, 850-5 (2007).
286. Kraman, M. & McCright, B. Functional conservation of Notch1 and Notch2 intracellular domains. Faseb J 19, 1311-3 (2005).
287. Grego-Bessa, J., Diez, J., Timmerman, L. & de la Pompa, J. L. Notch and epithelial-mesenchyme transition in development and tumor progression: another turn of the screw. Cell Cycle 3, 718-21 (2004).
288. Kwon, C., Han, Z., Olson, E. N. & Srivastava, D. MicroRNA1 influences cardiac differentiation in Drosophila and regulates Notch signaling. Proc Natl Acad Sci U S A 102, 18986-91 (2005).
289. Moses, K. A., DeMayo, F., Braun, R. M., Reecy, J. L. & Schwartz, R. J. Embryonic expression of an Nkx2-5/Cre gene using ROSA26 reporter mice. Genesis 31, 176-80 (2001).
290. Agah, R. et al. Gene recombination in postmitotic cells. Targeted expression of Cre recombinase provokes cardiac-restricted, site-specific rearrangement in adult ventricular muscle in vivo. J Clin Invest 100, 169-79 (1997).
291. Tu, L. et al. Notch signaling is an important regulator of type 2 immunity. J Exp Med 202, 1037-42 (2005).
292. Laugwitz, K. L. et al. Postnatal isl1+ cardioblasts enter fully differentiated cardiomyocyte lineages. Nature 433, 647-53 (2005).

293. Moretti, A. et al. Multipotent embryonic isl1+ progenitor cells lead to cardiac, smooth muscle, and endothelial cell diversification. Cell 127, 1151-65 (2006).
294. Scorsin, M. et al. Comparison of the effects of fetal cardiomyocyte and skeletal myoblast transplantation on postinfarction left ventricular function. J Thorac Cardiovasc Surg 119, 1169-75 (2000).
295. Soonpaa, M. H., Koh, G. Y., Klug, M. G. & Field, L. J. Formation of nascent intercalated disks between grafted fetal cardiomyocytes and host myocardium. Science 264, 98-101 (1994).
296. Toma, C., Pittenger, M. F., Cahill, K. S., Byrne, B. J. & Kessler, P. D. Human mesenchymal stem cells differentiate to a cardiomyocyte phenotype in the adult murine heart. Circulation 105, 93-8 (2002).
297. Yoo, K. J. et al. Autologous smooth muscle cell transplantation improved heart function in dilated cardiomyopathy. Ann Thorac Surg 70, 859-65 (2000).
298. Huppert, S. S. et al. Embryonic lethality in mice homozygous for a processing-deficient allele of Notch1. Nature 405, 966-70 (2000).
299. Villa, N. et al. Vascular expression of Notch pathway receptors and ligands is restricted to arterial vessels. Mech Dev 108, 161-4 (2001).
300. Kohler, C. et al. Expression of Notch-1 and its ligand Jagged-1 in rat liver during liver regeneration. Hepatology 39, 1056-65 (2004).
301. Nijjar, S. S., Wallace, L., Crosby, H. A., Hubscher, S. G. & Strain, A. J. Altered Notch ligand expression in human liver disease: further evidence for a role of the Notch signaling pathway in hepatic neovascularization and biliary ductular defects. Am J Pathol 160, 1695-703 (2002).
302. Campos, A. H., Wang, W., Pollman, M. J. & Gibbons, G. H. Determinants of Notch-3 receptor expression and signaling in vascular smooth muscle cells: implications in cell-cycle regulation. Circ Res 91, 999-1006 (2002).
303. Lindner, V. et al. Members of the Jagged/Notch gene families are expressed in injured arteries and regulate cell phenotype via alterations in cell matrix and cell-cell interaction. Am J Pathol 159, 875-83 (2001).
304. Li, D. et al. Mutations of presenilin genes in dilated cardiomyopathy and heart failure. Am J Hum Genet 79, 1030-9 (2006).
305. Lien, C. L., Schebesta, M., Makino, S., Weber, G. J. & Keating, M. T. Gene expression analysis of zebrafish heart regeneration. PLoS Biol 4, e260 (2006).
306. Limbourg, F. P. et al. Essential role of endothelial Notch1 in angiogenesis. Circulation 111, 1826-32 (2005).
307. Germani, A. et al. Vascular endothelial growth factor modulates skeletal myoblast function. Am J Pathol 163, 1417-28 (2003).
308. Lawson, N. D., Vogel, A. M. & Weinstein, B. M. sonic hedgehog and vascular endothelial growth factor act upstream of the Notch pathway during arterial endothelial differentiation. Dev Cell 3, 127-36 (2002).
309. Liu, Z. J. et al. Regulation of Notch1 and Dll4 by vascular endothelial growth factor in arterial endothelial cells: implications for modulating arteriogenesis and angiogenesis. Mol Cell Biol 23, 14-25 (2003).
310. Rissanen, T. T. et al. Expression of vascular endothelial growth factor and vascular endothelial growth factor receptor-2 (KDR/Flk-1) in ischemic skeletal muscle and its regeneration. Am J Pathol 160, 1393-403 (2002).
311. Steventon, B., Carmona-Fontaine, C. & Mayor, R. Genetic network during neural crest induction: from cell specification to cell survival. Semin Cell Dev Biol 16, 647-54 (2005).
312. Sohal, D. S. et al. Temporally regulated and tissue-specific gene manipulations in the adult and embryonic heart using a tamoxifen-inducible Cre protein. Circ Res 89, 20-5 (2001).
313. Jessup, M. & Brozena, S. Heart failure. N Engl J Med 348, 2007-18 (2003).
314. Richardson, P. et al. Report of the 1995 World Health Organization/International Society and Federation of Cardiology Task Force on the Definition and Classification of cardiomyopathies. Circulation 93, 841-2 (1996).
315. Codd, M. B., Sugrue, D. D., Gersh, B. J. & Melton, L. J., 3rd. Epidemiology of idiopathic dilated and hypertrophic cardiomyopathy. A population-based study in Olmsted County, Minnesota, 1975-1984. Circulation 80, 564-72 (1989).
316. Gillum, R. F. Idiopathic dilated cardiomyopathy. Epidemiology 5, 383-5 (1994).
317. Bowles, N. E., Bowles, K. R. & Towbin, J. A. The "final common pathway" hypothesis and inherited cardiovascular disease. The role of cytoskeletal proteins in dilated cardiomyopathy. Herz 25, 168-75 (2000).
318. Sinagra, G. et al. Current perspective new insights into the molecular basis of familial dilated cardiomyopathy. Ital Heart J 2, 280-6 (2001).

319. Hart, K. A. et al. DNA deletions in mild and severe Becker muscular dystrophy. Hum Genet 75, 281-5 (1987).
320. Koenig, M. et al. Complete cloning of the Duchenne muscular dystrophy (DMD) cDNA and preliminary genomic organization of the DMD gene in normal and affected individuals. Cell 50, 509-17 (1987).
321. Milasin, J. et al. A point mutation in the 5' splice site of the dystrophin gene first intron responsible for X-linked dilated cardiomyopathy. Hum Mol Genet 5, 73-9 (1996).
322. Muntoni, F., Melis, M. A., Ganau, A. & Dubowitz, V. Transcription of the dystrophin gene in normal tissues and in skeletal muscle of a family with X-linked dilated cardiomyopathy. Am J Hum Genet 56, 151-7 (1995).
323. Yoshida, K., Nakamura, A., Yazaki, M., Ikeda, S. & Takeda, S. Insertional mutation by transposable element, L1, in the DMD gene results in X-linked dilated cardiomyopathy. Hum Mol Genet 7, 1129-32 (1998).
324. Hoffman, E. P., Brown, R. H., Jr. & Kunkel, L. M. Dystrophin: the protein product of the Duchenne muscular dystrophy locus. Cell 51, 919-28 (1987).
325. Towbin, J. A. et al. X-linked dilated cardiomyopathy. Molecular genetic evidence of linkage to the Duchenne muscular dystrophy (dystrophin) gene at the Xp21 locus. Circulation 87, 1854-65 (1993).
326. Berko, B. A. & Swift, M. X-linked dilated cardiomyopathy. N Engl J Med 316, 1186-91 (1987).
327. Coral-Vazquez, R. et al. Disruption of the sarcoglycan-sarcospan complex in vascular smooth muscle: a novel mechanism for cardiomyopathy and muscular dystrophy. Cell 98, 465-74 (1999).
328. Nigro, V. et al. Autosomal recessive limb-girdle muscular dystrophy, LGMD2F, is caused by a mutation in the delta-sarcoglycan gene. Nat Genet 14, 195-8 (1996).
329. Knoll, R. et al. The cardiac mechanical stretch sensor machinery involves a Z disc complex that is defective in a subset of human dilated cardiomyopathy. Cell 111, 943-55 (2002).
330. Mohapatra, B. et al. Mutations in the muscle LIM protein and alpha-actinin-2 genes in dilated cardiomyopathy and endocardial fibroelastosis. Mol Genet Metab 80, 207-15 (2003).
331. Arber, S. et al. MLP-deficient mice exhibit a disruption of cardiac cytoarchitectural organization, dilated cardiomyopathy, and heart failure. Cell 88, 393-403 (1997).
332. Nikolova, V. et al. Defects in nuclear structure and function promote dilated cardiomyopathy in lamin A/C-deficient mice. J Clin Invest 113, 357-69 (2004).
333. Bonne, G. et al. Mutations in the gene encoding lamin A/C cause autosomal dominant Emery-Dreifuss muscular dystrophy. Nat Genet 21, 285-8 (1999).
334. Olson, T. M., Michels, V. V., Thibodeau, S. N., Tai, Y. S. & Keating, M. T. Actin mutations in dilated cardiomyopathy, a heritable form of heart failure. Science 280, 750-2 (1998).
335. Kamisago, M. et al. Mutations in sarcomere protein genes as a cause of dilated cardiomyopathy. N Engl J Med 343, 1688-96 (2000).
336. Li, Z. et al. Desmin is essential for the tensile strength and integrity of myofibrils but not for myogenic commitment, differentiation, and fusion of skeletal muscle. J Cell Biol 139, 129-44 (1997).
337. Gerull, B. et al. Mutations of TTN, encoding the giant muscle filament titin, cause familial dilated cardiomyopathy. Nat Genet 30, 201-4 (2002).
338. Chen, J. & Chien, K. R. Complexity in simplicity: monogenic disorders and complex cardiomyopathies. J Clin Invest 103, 1483-5 (1999).
339. Kadambi, V. J. & Kranias, E. G. Genetically engineered mice: model systems for left ventricular failure. J Card Fail 4, 349-61 (1998).
340. Nigro, V. et al. Identification of the Syrian hamster cardiomyopathy gene. Hum Mol Genet 6, 601-7 (1997).
341. Milano, C. A. et al. Enhanced myocardial function in transgenic mice overexpressing the beta 2-adrenergic receptor. Science 264, 582-6 (1994).
342. Koch, W. J. et al. Cardiac function in mice overexpressing the beta-adrenergic receptor kinase or a beta ARK inhibitor. Science 268, 1350-3 (1995).
343. Hawkins, H. K. et al. Acute inflammatory reaction after myocardial ischemic injury and reperfusion. Development and use of a neutrophil-specific antibody. Am J Pathol 148, 1957-69 (1996).
344. Adams, J. W. et al. Cardiomyocyte apoptosis induced by Galphaq signaling is mediated by permeability transition pore formation and activation of the mitochondrial death pathway. Circ Res 87, 1180-7 (2000).
345. Sakata, Y., Hoit, B. D., Liggett, S. B., Walsh, R. A. & Dorn, G. W., 2nd. Decompensation of pressure-overload hypertrophy in G alpha q-overexpressing mice. Circulation 97, 1488-95 (1998).
346. Mende, U. et al. Transient cardiac expression of constitutively active Galphaq leads to hypertrophy and dilated cardiomyopathy by calcineurin-dependent and independent pathways. Proc Natl Acad Sci U S A 95, 13893-8 (1998).

347. Kapadia, S. et al. Tumor necrosis factor-alpha gene and protein expression in adult feline myocardium after endotoxin administration. J Clin Invest 96, 1042-52 (1995).
348. Sheng, Z. et al. Cardiotrophin 1 (CT-1) inhibition of cardiac myocyte apoptosis via a mitogen-activated protein kinase-dependent pathway. Divergence from downstream CT-1 signals for myocardial cell hypertrophy. J Biol Chem 272, 5783-91 (1997).
349. Sen, R. & Baltimore, D. Multiple nuclear factors interact with the immunoglobulin enhancer sequences. Cell 46, 705-16 (1986).
350. Karin, M. Nuclear factor-kappaB in cancer development and progression. Nature 441, 431-6 (2006).
351. Li, Q. & Verma, I. M. NF-kappaB regulation in the immune system. Nat Rev Immunol 2, 725-34 (2002).
352. Courtois, G. & Gilmore, T. D. Mutations in the NF-kappaB signaling pathway: implications for human disease. Oncogene 25, 6831-43 (2006).
353. Mourkioti, F. et al. Targeted ablation of IKK2 improves skeletal muscle strength, maintains mass, and promotes regeneration. J Clin Invest 116, 2945-54 (2006).
354. Herrmann, O. et al. IKK mediates ischemia-induced neuronal death. Nat Med 11, 1322-9 (2005).
355. Luedde, T. et al. Deletion of NEMO/IKKgamma in liver parenchymal cells causes steatohepatitis and hepatocellular carcinoma. Cancer Cell 11, 119-32 (2007).
356. Nenci, A. et al. Epithelial NEMO links innate immunity to chronic intestinal inflammation. Nature 446, 557-61 (2007).
357. Ghosh, S., May, M. J. & Kopp, E. B. NF-kappa B and Rel proteins: evolutionarily conserved mediators of immune responses. Annu Rev Immunol 16, 225-60 (1998).
358. Hoffmann, A., Natoli, G. & Ghosh, G. Transcriptional regulation via the NF-kappaB signaling module. Oncogene 25, 6706-16 (2006).
359. Silverman, N. & Maniatis, T. NF-kappaB signaling pathways in mammalian and insect innate immunity. Genes Dev 15, 2321-42 (2001).
360. Verma, I. M., Stevenson, J. K., Schwarz, E. M., Van Antwerp, D. & Miyamoto, S. Rel/NF-kappa B/I kappa B family: intimate tales of association and dissociation. Genes Dev 9, 2723-35 (1995).
361. Dechend, R. et al. The Bcl-3 oncoprotein acts as a bridging factor between NF-kappaB/Rel and nuclear co-regulators. Oncogene 18, 3316-23 (1999).
362. Li, Q., Estepa, G., Memet, S., Israel, A. & Verma, I. M. Complete lack of NF-kappaB activity in IKK1 and IKK2 double-deficient mice: additional defect in neurulation. Genes Dev 14, 1729-33 (2000).
363. May, M. J., Marienfeld, R. B. & Ghosh, S. Characterization of the Ikappa B-kinase NEMO binding domain. J Biol Chem 277, 45992-6000 (2002).
364. Li, Q., Van Antwerp, D., Mercurio, F., Lee, K. F. & Verma, I. M. Severe liver degeneration in mice lacking the IkappaB kinase 2 gene. Science 284, 321-5 (1999).
365. Hu, Y. et al. IKKalpha controls formation of the epidermis independently of NF-kappaB. Nature 410, 710-4 (2001).
366. Sizemore, N., Lerner, N., Dombrowski, N., Sakurai, H. & Stark, G. R. Distinct roles of the Ikappa B kinase alpha and beta subunits in liberating nuclear factor kappa B (NF-kappa B) from Ikappa B and in phosphorylating the p65 subunit of NF-kappa B. J Biol Chem 277, 3863-9 (2002).
367. Senftleben, U. et al. Activation by IKKalpha of a second, evolutionary conserved, NF-kappa B signaling pathway. Science 293, 1495-9 (2001).
368. Claudio, E., Brown, K., Park, S., Wang, H. & Siebenlist, U. BAFF-induced NEMO-independent processing of NF-kappa B2 in maturing B cells. Nat Immunol 3, 958-65 (2002).
369. Dejardin, E. et al. The lymphotoxin-beta receptor induces different patterns of gene expression via two NF-kappaB pathways. Immunity 17, 525-35 (2002).
370. Bonizzi, G. & Karin, M. The two NF-kappaB activation pathways and their role in innate and adaptive immunity. Trends Immunol 25, 280-8 (2004).
371. Yamaoka, S. et al. Complementation cloning of NEMO, a component of the IkappaB kinase complex essential for NF-kappaB activation. Cell 93, 1231-40 (1998).
372. Rothwarf, D. M., Zandi, E., Natoli, G. & Karin, M. IKK-gamma is an essential regulatory subunit of the IkappaB kinase complex. Nature 395, 297-300 (1998).
373. Tegethoff, S., Behlke, J. & Scheidereit, C. Tetrameric oligomerization of IkappaB kinase gamma (IKKgamma) is obligatory for IKK complex activity and NF-kappaB activation. Mol Cell Biol 23, 2029-41 (2003).
374. Devin, A. et al. The alpha and beta subunits of IkappaB kinase (IKK) mediate TRAF2-dependent IKK recruitment to tumor necrosis factor (TNF) receptor 1 in response to TNF. Mol Cell Biol 21, 3986-94 (2001).
375. Rudolph, D. et al. Severe liver degeneration and lack of NF-kappaB activation in NEMO/IKKgamma-deficient mice. Genes Dev 14, 854-62 (2000).

376. Smahi, A. et al. Genomic rearrangement in NEMO impairs NF-kappaB activation and is a cause of incontinentia pigmenti. The International Incontinentia Pigmenti (IP) Consortium. Nature 405, 466-72 (2000).
377. Doffinger, R. et al. X-linked anhidrotic ectodermal dysplasia with immunodeficiency is caused by impaired NF-kappaB signaling. Nat Genet 27, 277-85 (2001).
378. Schmidt-Supprian, M. et al. NEMO/IKK gamma-deficient mice model incontinentia pigmenti. Mol Cell 5, 981-92 (2000).
379. Makris, C. et al. Female mice heterozygous for IKK gamma/NEMO deficiencies develop a dermatopathy similar to the human X-linked disorder incontinentia pigmenti. Mol Cell 5, 969-79 (2000).
380. Huang, T. T., Wuerzberger-Davis, S. M., Wu, Z. H. & Miyamoto, S. Sequential modification of NEMO/IKKgamma by SUMO-1 and ubiquitin mediates NF-kappaB activation by genotoxic stress. Cell 115, 565-76 (2003).
381. Akira, S., Takeda, K. & Kaisho, T. Toll-like receptors: critical proteins linking innate and acquired immunity. Nat Immunol 2, 675-80 (2001).
382. Wang, C. et al. TAK1 is a ubiquitin-dependent kinase of MKK and IKK. Nature 412, 346-51 (2001).
383. Yang, J. et al. The essential role of MEKK3 in TNF-induced NF-kappaB activation. Nat Immunol 2, 620-4 (2001).
384. Kelliher, M. A. et al. The death domain kinase RIP mediates the TNF-induced NF-kappaB signal. Immunity 8, 297-303 (1998).
385. Newton, K., Sun, X. & Dixit, V. M. Kinase RIP3 is dispensable for normal NF-kappa Bs, signaling by the B-cell and T-cell receptors, tumor necrosis factor receptor 1, and Toll-like receptors 2 and 4. Mol Cell Biol 24, 1464-9 (2004).
386. Lee, T. H., Shank, J., Cusson, N. & Kelliher, M. A. The kinase activity of Rip1 is not required for tumor necrosis factor-alpha-induced IkappaB kinase or p38 MAP kinase activation or for the ubiquitination of Rip1 by Traf2. J Biol Chem 279, 33185-91 (2004).
387. Martin, M. U. & Wesche, H. Summary and comparison of the signaling mechanisms of the Toll/interleukin-1 receptor family. Biochim Biophys Acta 1592, 265-80 (2002).
388. Arendt, C. W., Albrecht, B., Soos, T. J. & Littman, D. R. Protein kinase C-theta: signaling from the center of the T-cell synapse. Curr Opin Immunol 14, 323-30 (2002).
389. Ruland, J. et al. Bcl10 is a positive regulator of antigen receptor-induced activation of NF-kappaB and neural tube closure. Cell 104, 33-42 (2001).
390. McAllister-Lucas, L. M. et al. Bimp1, a MAGUK family member linking protein kinase C activation to Bcl10-mediated NF-kappaB induction. J Biol Chem 276, 30589-97 (2001).
391. Sun, Z. et al. PKC-theta is required for TCR-induced NF-kappaB activation in mature but not immature T lymphocytes. Nature 404, 402-7 (2000).
392. Shinohara, H. et al. PKC beta regulates BCR-mediated IKK activation by facilitating the interaction between TAK1 and CARMA1. J Exp Med 202, 1423-31 (2005).
393. Beg, A. A., Sha, W. C., Bronson, R. T., Ghosh, S. & Baltimore, D. Embryonic lethality and liver degeneration in mice lacking the RelA component of NF-kappa B. Nature 376, 167-70 (1995).
394. Sha, W. C., Liou, H. C., Tuomanen, E. I. & Baltimore, D. Targeted disruption of the p50 subunit of NF-kappa B leads to multifocal defects in immune responses. Cell 80, 321-30 (1995).
395. Weih, F. et al. p50-NF-kappaB complexes partially compensate for the absence of RelB: severely increased pathology in p50(-/-)relB(-/-) double-knockout mice. J Exp Med 185, 1359-70 (1997).
396. Yeh, W. C. et al. FADD: essential for embryo development and signaling from some, but not all, inducers of apoptosis. Science 279, 1954-8 (1998).
397. Herron, B. J. et al. A mutation in NFkB interacting protein 1 results in cardiomyopathy and abnormal skin development in wa3 mice. Hum Mol Genet 14, 667-77 (2005).
398. Frantz, S. et al. Sustained activation of nuclear factor kappa B and activator protein 1 in chronic heart failure. Cardiovasc Res 57, 749-56 (2003).
399. Li, Y. et al. NF-kappaB activation is required for the development of cardiac hypertrophy in vivo. Am J Physiol Heart Circ Physiol 287, H1712-20 (2004).
400. Purcell, N. H. et al. Activation of NF-kappa B is required for hypertrophic growth of primary rat neonatal ventricular cardiomyocytes. Proc Natl Acad Sci U S A 98, 6668-73 (2001).
401. Torre-Amione, G. et al. Tumor necrosis factor-alpha and tumor necrosis factor receptors in the failing human heart. Circulation 93, 704-11 (1996).
402. Beg, A. A., Sha, W. C., Bronson, R. T. & Baltimore, D. Constitutive NF-kappa B activation, enhanced granulopoiesis, and neonatal lethality in I kappa B alpha-deficient mice. Genes Dev 9, 2736-46 (1995).
403. Kontgen, F. et al. Mice lacking the c-rel proto-oncogene exhibit defects in lymphocyte proliferation, humoral immunity, and interleukin-2 expression. Genes Dev 9, 1965-77 (1995).

404. Kawano, S. et al. Blockade of NF-kappaB ameliorates myocardial hypertrophy in response to chronic infusion of angiotensin II. Cardiovasc Res 67, 689-98 (2005).
405. Kawamura, N. et al. Blockade of NF-kappaB improves cardiac function and survival without affecting inflammation in TNF-alpha-induced cardiomyopathy. Cardiovasc Res 66, 520-9 (2005).
406. Freund, C. et al. Requirement of nuclear factor-kappaB in angiotensin II- and isoproterenol-induced cardiac hypertrophy in vivo. Circulation 111, 2319-25 (2005).
407. Sun, M. et al. Tumor necrosis factor-alpha mediates cardiac remodeling and ventricular dysfunction after pressure overload state. Circulation 115, 1398-407 (2007).
408. Haudek, S. B., Taffet, G. E., Schneider, M. D. & Mann, D. L. TNF provokes cardiomyocyte apoptosis and cardiac remodeling through activation of multiple cell death pathways. J Clin Invest 117, 2692-701 (2007).
409. Bryant, D. et al. Cardiac failure in transgenic mice with myocardial expression of tumor necrosis factor-alpha. Circulation 97, 1375-81 (1998).
410. Engel, D., Peshock, R., Armstong, R. C., Sivasubramanian, N. & Mann, D. L. Cardiac myocyte apoptosis provokes adverse cardiac remodeling in transgenic mice with targeted TNF overexpression. Am J Physiol Heart Circ Physiol 287, H1303-11 (2004).
411. Siwik, D. A., Chang, D. L. & Colucci, W. S. Interleukin-1beta and tumor necrosis factor-alpha decrease collagen synthesis and increase matrix metalloproteinase activity in cardiac fibroblasts in vitro. Circ Res 86, 1259-65 (2000).
412. Thomas, C. V. et al. Increased matrix metalloproteinase activity and selective upregulation in LV myocardium from patients with end-stage dilated cardiomyopathy. Circulation 97, 1708-15 (1998).
413. Tyagi, S. C., Campbell, S. E., Reddy, H. K., Tjahja, E. & Voelker, D. J. Matrix metalloproteinase activity expression in infarcted, noninfarcted and dilated cardiomyopathic human hearts. Mol Cell Biochem 155, 13-21 (1996).
414. Roten, L. et al. Effects of gene deletion of the tissue inhibitor of the matrix metalloproteinase-type 1 (TIMP-1) on left ventricular geometry and function in mice. J Mol Cell Cardiol 32, 109-20 (2000).
415. Spinale, F. G. et al. A matrix metalloproteinase induction/activation system exists in the human left ventricular myocardium and is upregulated in heart failure. Circulation 102, 1944-9 (2000).
416. Karin, M. & Lin, A. NF-kappaB at the crossroads of life and death. Nat Immunol 3, 221-7 (2002).
417. Dawn, B. et al. Cardiac-specific abrogation of NF- kappa B activation in mice by transdominant expression of a mutant I kappa B alpha. J Mol Cell Cardiol 33, 161-73 (2001).
418. Morgan, E. N. et al. An essential role for NF-kappaB in the cardioadaptive response to ischemia. Ann Thorac Surg 68, 377-82 (1999).
419. Xuan, Y. T. et al. Nuclear factor-kappaB plays an essential role in the late phase of ischemic preconditioning in conscious rabbits. Circ Res 84, 1095-109 (1999).
420. Cook, S. A., Novikov, M. S., Ahn, Y., Matsui, T. & Rosenzweig, A. A20 is dynamically regulated in the heart and inhibits the hypertrophic response. Circulation 108, 664-7 (2003).
421. Sano, M. et al. Interleukin-6 family of cytokines mediate angiotensin II-induced cardiac hypertrophy in rodent cardiomyocytes. J Biol Chem 275, 29717-23 (2000).
422. Frantz, S. et al. Toll4 (TLR4) expression in cardiac myocytes in normal and failing myocardium. J Clin Invest 104, 271-80 (1999).
423. Ha, T. et al. Reduced cardiac hypertrophy in toll-like receptor 4-deficient mice following pressure overload. Cardiovasc Res 68, 224-34 (2005).
424. Han, R. O., Ray, P. E., Baughman, K. L. & Feldman, A. M. Detection of interleukin and interleukin-receptor mRNA in human heart by polymerase chain reaction. Biochem Biophys Res Commun 181, 520-3 (1991).
425. Habib, F. M. et al. Tumour necrosis factor and inducible nitric oxide synthase in dilated cardiomyopathy. Lancet 347, 1151-5 (1996).
426. Pohl, T. et al. The combined absence of NF-kappa B1 and c-Rel reveals that overlapping roles for these transcription factors in the B cell lineage are restricted to the activation and function of mature cells. Proc Natl Acad Sci U S A 99, 4514-9 (2002).
427. Horwitz, B. H. et al. The p65 subunit of NF-kappa B is redundant with p50 during B cell proliferative responses, and is required for germline CH transcription and class switching to IgG3. J Immunol 162, 1941-6 (1999).
428. Frantz, S. et al. Absence of NF-kappaB subunit p50 improves heart failure after myocardial infarction. Faseb J 20, 1918-20 (2006).
429. Valen, G. Signal transduction through nuclear factor kappa B in ischemia-reperfusion and heart failure. Basic Res Cardiol 99, 1-7 (2004).
430. Hill, J. A. et al. Cardiac hypertrophy is not a required compensatory response to short-term pressure overload. Circulation 101, 2863-9 (2000).
431. van Rooij, E. et al. Control of stress-dependent cardiac growth and gene expression by a microRNA. Science 316, 575-9 (2007).

432. van Empel, V. P. et al. Downregulation of apoptosis-inducing factor in harlequin mutant mice sensitizes the myocardium to oxidative stress-related cell death and pressure overload-induced decompensation. Circ Res 96, e92-e101 (2005).
433. Minhas, K. M. et al. Xanthine oxidoreductase inhibition causes reverse remodeling in rats with dilated cardiomyopathy. Circ Res 98, 271-9 (2006).
434. Ruetten, H., Dimmeler, S., Gehring, D., Ihling, C. & Zeiher, A. M. Concentric left ventricular remodeling in endothelial nitric oxide synthase knockout mice by chronic pressure overload. Cardiovasc Res 66, 444-53 (2005).
435. Takimoto, E. et al. Oxidant stress from nitric oxide synthase-3 uncoupling stimulates cardiac pathologic remodeling from chronic pressure load. J Clin Invest 115, 1221-31 (2005).
436. Kwon, S. H., Pimentel, D. R., Remondino, A., Sawyer, D. B. & Colucci, W. S. H(2)O(2) regulates cardiac myocyte phenotype via concentration-dependent activation of distinct kinase pathways. J Mol Cell Cardiol 35, 615-21 (2003).
437. Maher, J. M. et al. Oxidative and electrophilic stress induces multidrug resistance-associated protein transporters via the nuclear factor-E2-related factor-2 transcriptional pathway. Hepatology 46, 1597-610 (2007).
438. Nakano, H. et al. Reactive oxygen species mediate crosstalk between NF-kappaB and JNK. Cell Death Differ 13, 730-7 (2006).
439. Hirotani, S. et al. Involvement of nuclear factor-kappaB and apoptosis signal-regulating kinase 1 in G-protein-coupled receptor agonist-induced cardiomyocyte hypertrophy. Circulation 105, 509-15 (2002).
440. De Keulenaer, G. W. et al. Identification of IEX-1 as a biomechanically controlled nuclear factor-kappaB target gene that inhibits cardiomyocyte hypertrophy. Circ Res 90, 690-6 (2002).
441. Marin-Garcia, J., Pi, Y. & Goldenthal, M. J. Mitochondrial-nuclear cross-talk in the aging and failing heart. Cardiovasc Drugs Ther 20, 477-91 (2006).
442. Terzioglu, M. & Larsson, N. G. Mitochondrial dysfunction in mammalian ageing. Novartis Found Symp 287, 197-208; discussion 208-13 (2007).
443. O'Rourke, B., Cortassa, S., Akar, F. & Aon, M. Mitochondrial ion channels in cardiac function and dysfunction. Novartis Found Symp 287, 140-51; discussion 152-6 (2007).
444. Yamamoto, K. et al. Induction of tenascin-C in cardiac myocytes by mechanical deformation. Role of reactive oxygen species. J Biol Chem 274, 21840-6 (1999).
445. Cheng, W. et al. Stretch-induced programmed myocyte cell death. J Clin Invest 96, 2247-59 (1995).
446. Zhang, M. & Shah, A. M. Role of reactive oxygen species in myocardial remodeling. Curr Heart Fail Rep 4, 26-30 (2007).
447. Johar, S., Cave, A. C., Narayanapanicker, A., Grieve, D. J. & Shah, A. M. Aldosterone mediates angiotensin II-induced interstitial cardiac fibrosis via a Nox2-containing NADPH oxidase. Faseb J 20, 1546-8 (2006).
448. Cox, M. J., Hawkins, U. A., Hoit, B. D. & Tyagi, S. C. Attenuation of oxidative stress and remodeling by cardiac inhibitor of metalloproteinase protein transfer. Circulation 109, 2123-8 (2004).
449. Zhang, M. et al. Glycated proteins stimulate reactive oxygen species production in cardiac myocytes: involvement of Nox2 (gp91phox)-containing NADPH oxidase. Circulation 113, 1235-43 (2006).

4. Publications

1. Platsoucas CD, Lu S, Nwaneshiudu I, Solomides C, Agelan A, Ntaoula N, Purev E, Li LP, **Kratsios P**, Mylonas E, Jung WJ, Evans K, Roberts S, Lu Y, Layvi R, Lin WL, Zhang X, Gaughan J, Monos DS, Oleszak EL, White JV. Abdominal aortic aneurysm is a specific antigen-driven T cell disease. *Ann N Y Acad Sci*. 2006 Nov;1085:224-35.

2. Mourkioti F, **Kratsios P**, Luedde T, Song YH, Delafontaine P, Adami R, Parente V, Bottinelli R, Pasparakis M, Rosenthal N. Targeted ablation of IKK2 improves skeletal muscle strength, maintains mass, and promotes regeneration. *J Clin Invest*. 2006 Nov;116(11):2945-54.